

LEAD DETERMINATION BY FLAME ATOMIC ABSORPTION SPECTROMETRY
USING A SLOTTED QUARTZ TUBE ATOM TRAP AND METAL COATINGS

A THESIS SUBMITTED TO
THE GRADUATE SCHOOL OF NATURAL AND APPLIED SCIENCES
OF
MIDDLE EAST TECHNICAL UNIVERSITY

BY

İLKNUR DEMİRTAŞ

IN PARTIAL FULFILLMENT OF THE REQUIREMENTS
FOR
THE DEGREE OF MASTER OF SCIENCE
IN
CHEMISTRY

JULY 2009

Approval of the Thesis;

**LEAD DETERMINATION BY FLAME ATOMIC ABSORPTION
SPECTROMETRY USING A SLOTTED QUARTZ TUBE ATOM TRAP AND
METAL COATINGS**

submitted by **İLKNUR DEMİRTAŞ** in a partial fulfillment of the requirements for the degree of **Master of Science in Chemistry Department, Middle East Technical University** by

Prof. Dr. Canan Özgen
Dean, Graduate School of **Natural and Applied Sciences** _____

Prof. Dr. Ahmet M. Önal
Head of Department, **Chemistry** _____

Prof Dr. O. Yavuz Ataman
Supervisor, **Chemistry Department, METU** _____

Examining Committee Members:

Prof. Dr. E. Hale Göktürk
Chemistry Department, METU _____

Prof. Dr. O. Yavuz Ataman
Chemistry Department, METU _____

Prof. Dr. Mürvet Volkan
Chemistry Department, METU _____

Assoc. Prof. Dr. Nusret Ertaş
Faculty of Pharmacy, Gazi University _____

Assoc. Prof. Dr. Uğur Tamer
Faculty of Pharmacy, Gazi University _____

Date: 14.07.2009

I hereby declare that all information in this document has been obtained and presented in accordance with academic rules and ethical conduct. I also declare that, as required by these rules and conduct, I have fully cited and referenced all material and results that are not original to this work.

Name, Last name: İlknur Demirtaş

Signature

ABSTRACT

LEAD DETERMINATION BY FLAME ATOMIC ABSORPTION SPECTROMETRY USING A SLOTTED QUARTZ TUBE ATOM TRAP AND METAL COATINGS

Demirtaş, İlknur

M.S., Department of Chemistry

Supervisor: Prof. Dr. O. Yavuz Ataman

July 2009, 98 pages

Flame Atomic Absorption Spectrometry (FAAS) still keeps its importance despite the relatively low sensitivity; because it is a simple and economical technique for determination of metals. In recent years atom traps have been developed to increase the sensitivity of FAAS. Although the detection limit of FAAS is only at the level of mg/L, with the use of atom traps it can reach to ng/mL. Slotted quartz tube (SQT) is one of these atom traps, it is applied for determination of volatile elements; it is economical, commercially available and easy to use. In this study, a sensitive analytical method has been developed for the determination of lead with the help of SQT. Regarding the angle between the two slots of SQT, 120° and 180° configurations were used and the results were compared. There were three modes of SQT used. The first application was for providing longer residence time of analyte atoms in the measurement zone; 3 fold sensitivity enhancement was observed. The second mode was the usage of SQT for preconcentration of lead atoms. In the presence of a lean air-acetylene flame, analyte atoms were trapped in the inner surface of SQT for a few minutes. Then, by the help of a

small volume (10-50 μL) of Methyl isobutyl ketone (MIBK), analyte atoms were revolatilized and a rapid atomization took place. Using this mode, a sensitivity enhancement of 574 was obtained at a rather low (3.9 mL/min) suction rate; 1320 fold improvement was reached at higher sample suction rate (7.4 mL/min) for 5.0 min collection. The last mode involves coating of the inner surface of SQT with several kinds of transition metals. The best sensitivity enhancement, 1650 fold, was obtained by the Ta coated SQT. In addition, effects of some elements and anions on Pb signal in Ta-coated-SQT-AT-FAAS were examined. Final step consists of surface analysis; chemical nature of Pb trapped on quartz and Ta surface, and the chemical nature of Ta on quartz surface were investigated by X-ray Photoelectron Spectroscopy (XPS) and Raman Spectroscopy.

Keywords: Flame atomic absorption spectrometry, slotted quartz tube, tantalum, lead, preconcentration, sensitivity enhancement.

ÖZ

ALEVLİ ATOMİK ABSORPRİYON SPEKTROMETRESİ İLE YARIKLI KUVARS TÜP ATOM TUZAĞI KULLANARAK KURŞUN TAYİNİ

Demirtaş, İlknur

Yüksek Lisans, Kimya Bölümü

Tez Yöneticisi: Prof. Dr. O. Yavuz Ataman

Temmuz 2009, 98 sayfa

Alevli Atomik Absorpsiyon Spektrometri (FAAS) göreceli düşük duyarlılığına rağmen önemini hala korumaktadır; çünkü bu teknik metal tayini için kolay ve ekonomiktir. Son yıllarda FAAS tekniğinin duyarlılığını artırmak için atom tuzakları geliştirilmiştir. FAAS tekniğinin gözlenebilme sınırı mg/L düzeyindeyken atom tuzakları kullanıldığında bu değer ng/mL düzeyine ulaşmaktadır. Yarıklı kuvars tüp (YKT), bu atom tuzaklarından biridir; uçucu element tayininde kullanılır, ekonomiktir, ticari olarak mevcuttur ve basit bir kullanıma sahiptir. Bu çalışmada, kurşunun FAAS yöntemi ile tayininde YKT kullanarak duyarlı bir analitik metot geliştirilmiştir. Yarıklar arasındaki açının 120° ve 180° olduğu durumlarda YKT sonuçları kıyaslanmıştır. YKT'nin üç farklı modu kullanılmıştır; bunlardan ilki analit atomlarının ölçüm bölgesindeki kalma süresini artırma amaçlıdır; 3 kat duyarlılık artışı gözlemlenmiştir. İkincisi, YKT'nin kurşunun özenleştirilmesinde kullanılmasıdır. Düşük asetilen akış hızındaki aleve gönderilen analit YKT'nin iç yüzeyinde birkaç dakika içinde toplanır. Daha sonra aleve düşük hacimde (10-50 µL) Metil izobutil keton (MIBK) püskürtülmesi ile tuzaklanmış

analit atomları buharlaşır ve hızla atomlaşır. Bu çeşit tuzaklama yöntemi ile AAS ye göre, 5 dakikalık toplama süresi ve düşük örnek çekiş hızında (3.9 mL/min) 574 kat, yüksek örnek çekiş hızında (7.4 mL/min) 1320 kat duyarlılık artışı elde edilmiştir. Son uygulamada ise YKT'nin iç yüzeyi bazı metallerle kaplanmıştır. En fazla duyarlılık artışı, 1650 kat olarak, Ta kaplı YKT ile elde edilmiştir. Ayrıca, bazı elementlerin ve anyonların Ta kaplı-YKT-AT-FAAS metodu kullanıldığında Pb sinyali üzerine etkileri araştırılmıştır. Çalışmanın son basamağı yüzey çalışmalarını içermektedir. Kuvars ve Ta yüzeyinde tuzaklanan kurşunun yükseltgenme basamağı ve Ta elementinin kuvars yüzey üzerindeki yükseltgenme basamağı X ışınları fotoelektron spektroskopisi (XPS) ve Raman spektroskopisinden yararlanılarak bulunmuştur.

Anahtar Kelimeler: Alevli Atomik Absorpsiyon Spektrometri, yarıklı kuvars tüp, tantalum, kurşun, özenleştirme, duyarlılık artışı.

To My Family

ACKNOWLEDGEMENTS

I wish to express my gratitude to my supervisor Prof. Dr. O. Yavuz Ataman for his guidance, understanding and suggestions throughout this research.

I would like to thank Sezgin Bakırdere for his endless patience, guidance and contribution in each part of this study.

I would like to thank to Yasin Arslan for his encourage and guidance.

I am deeply grateful to Pınar Akay, Emrah Yıldırım and Selin Bora for their help, support and friendship.

I want to thank Necati Koç for his help, all AtaMAN Research and C-50 group members for their understanding and friendship.

I would like to thank Dr. Selda Keskin from METU, Central Laboratory for her help in XPS studies.

I also would like to thank to Murat Kaya for his help in Raman Study.

Finally, my special thanks to my mother, father, sisters and brother for their trust, patience, support and love.

TABLE OF CONTENTS

ABSTRACT	iv
ÖZ	vi
ACKNOWLEDGEMENTS	ix
TABLE OF CONTENTS	x
LIST OF TABLES	xiv
LIST OF FIGURES	xvi
LIST OF ABBREVIATIONS	xxi
CHAPTERS	1
CHAPTER 1	1
INTRODUCTION	1
1.1 Lead and Lead Sources	2
1.2 Lead and Health	3
1.3 Determination of Lead	4
1.3.1 Determination of Lead by Plasma Techniques	4
1.3.2 Determination of Lead by Atomic Absorption Spectrometry	5
1.3.2.1 Electrothermal Atomic Absorption Spectrometry	6
1.3.2.2 Hydride Generation Atomic Absorption Spectrometry	6
1.3.2.3 Flame Atomic Absorption Spectrometry	7
1.4 Atom Trapping Techniques in Atomic Absorption Spectrometry	8
1.4.1 Atom Traps for Hydride Generation Techniques	8
1.4.1.1 Graphite Furnace Atom Trap for Hydride Generation Techniques	8
1.4.1.2 Quartz Atom Traps for Hydride Generation Techniques	9

1.4.1.3 Metal Atom Traps for Vapor Generation Techniques	10
1.4.2 Atom Traps for Flame Atomic Absorption Spectrometry	11
1.4.2.1 Long-Path Absorption Tube Method	11
1.4.2.2 Delves' Microsampling Cup Method.....	12
1.4.2.3 Slotted Quartz Tube FAAS Method.....	13
1.4.2.4 Water-Cooled Silica Atom Trap Method.....	15
1.4.2.5 Integrated Atom Trap Method	16
1.4.2.6 Slotted Quartz Tube Atom Trap Method	17
1.5 Atomization in FAAS-SQT-AT	19
1.5.1 Flame Alteration Technique.....	19
1.5.2 Organic Solvent Aspiration Technique.....	19
1.6 Surface Studies	20
1.7 Aim of the Study.....	21
CHAPTER 2	22
EXPERIMENTAL	22
2.1 Apparatus and Materials	22
2.2 Chemicals and Reagents	22
2.3 Atomic Absorption Spectrometer	24
2.4 Coating Procedure for Slotted Quartz Tube	25
2.5 Surface Studies	26
CHAPTER 3	28
RESULTS AND DISCUSSION	28
3.1 FAAS Study.....	29
3.1.1 Optimization of Fuel Flow Rate.....	30
3.1.2 Optimization of Suction Rate of Sample Solution.....	30
3.1.3 Calibration Plot for FAAS Method.....	31

3.2 Optimizations of Slotted Quartz Tube Flame AAS Method.....	33
3.2.1 Optimization of Fuel Flow Rate.....	33
3.2.2 Optimization of Sample Suction Rate.....	35
3.2.3 Optimization of Height of the SQT from the Burner Head	36
3.2.4 Calibration Plots for SQT-FAAS Method	38
3.3 Optimizations of Slotted Quartz Tube Atom Trap Flame AAS Method (SQT-AT-FAAS) Conditions for Determination of Lead.....	41
3.3.1 Effect of Organic Solvent.....	42
3.3.2 Optimization of Volume of Organic Solvent.....	44
3.3.3 Optimization of Sample Suction Rate.....	46
3.3.4 Optimization of Fuel Flow Rate.....	48
3.3.5 Optimization of Height of the SQT from the Burner Head	49
3.3.6 Investigation of Trapping Period	51
3.3.7 Calibration Plots for SQT-AT-FAAS Method.....	53
3.3.8 Analytical Figures of Merit of SQT-AT-FAAS.....	60
3.3.9 Accuracy Check for SQT-AT-FAAS Method	62
3.4 SQT-AT-FAAS Study with Different Inner and Outer Diameters Tubes	62
3.5 Optimizations of Coated Slotted Quartz Tube Atom Trap Flame AAS (Coated-SQT-AT-FAAS) and Conditions for Determination of Lead.....	64
3.5.1 Investigation of Coating Material on SQT-AT-FAAS Method	65
3.5.2 Effect of Organic Solvent.....	66
3.5.3 Optimization of Volume of Organic Solvent.....	67
3.5.4 Optimization of Sample Suction Rate.....	67
3.5.5 Optimization of Fuel Flow Rate.....	68
3.5.6 Optimization of Height of the SQT from the Burner Head	69
3.5.7 Investigation of Trapping Period	70
3.5.8 Calibration Plots for SQT-FAAS Method	72
3.5.9 Analytical Figures of Merit of Ta coated-SQT-AT-FAAS.....	73

3.5.10 Accuracy Check for Ta coated-SQT-AT-FAAS Method	74
3.6 Evaluation of System Performance	75
3.7 Interference Studies for Ta Coated-SQT-AT-FAAS Method.....	78
3.8 Surface Studies	83
3.8.1 Chemical State of Pb on Quartz Surface.....	84
3.8.2 Chemical State of Pb on Ta Surface	86
3.8.3 Chemical State of Ta on Quartz Surface.....	88
CHAPTER 4.....	92
CONCLUSIONS	92
REFERENCES.....	94

LIST OF TABLES

TABLES

Table 2.1 Certified Values for SCP SCIENCE EnviroMAT Waste Water, Low (EU-L-2).....	24
Table 2.2 Operating Conditions for FAAS.....	25
Table 3.1 Analytical Performance of FAAS.....	33
Table 3.2 Analytical Performance of 120° and 180° Angled SQT-FAAS Method.....	41
Table 3.3 Effect of Organic Solvents on Pb Signals for SQT-AT-FAAS Method.....	43
Table 3.4 Molecular Formulas and Flash Points of Organics Used for Revolatilization Step of Pb.....	44
Table 3.5 Conditions for SQT-AT-FAAS Method.....	53
Table 3.6 Analytical Performance of SQT-AT-FAAS Method, 5.0 min Collection.....	61
Table 3.7 The Result of the Accuracy Test for 180° Angled SQT-AT-FAAS Method.....	62
Table 3.8 Effect of Diameter of SQT on 10.0 ng/mL Pb Signal for SQT-AT-FAAS Method.....	63
Table 3.9 Effect of Wall Thickness on 10.0 ng/mL Pb Signal for SQT-AT-FAAS Method.....	64
Table 3.10 Effect of Coating Material on 10.0 ng/mL Pb Signal for SQT-AT-FAAS Method.....	65
Table 3.10 (continued).....	66
Table 3.11 Effect of Organic Solvents on 5.0 ng/mL Pb Signal for Ta-coated-SQT-AT-FAAS Method	66

Table 3.12 Optimized Conditions for Ta-Coated-SQT-AT-FAAS Method.....	72
Table 3.13 Analytical Performance of Pb using Ta-Coated-SQT-AT-FAAS Method.....	74
Table 3.14 Result of the Accuracy Test for Ta-Coated-SQT-AT-FAAS Method.....	75
Table 3.15 Comparison of Methods in Terms of E, Et and Ev Values.....	77
Table 3.16 Comparison of Developed Methods with Other Techniques.....	78
Table 3.17 Percentages and Orbitals of Elements on SQT Trapped with Pb.....	85
Table 3.18 Percentages and Orbitals of Elements on Ta Coated SQT Trapped with Pb.....	87
Table 3.18 (Continued).....	88
Table 3.19 Percentages and Orbitals of Elements on Ta Coated SQT.....	90

LIST OF FIGURES

FIGURES

Figure 1.1 Schematic representation of a long-tube absorption cell	11
Figure 1.2 Schematic representation of Delves' microsampling cup system.....	12
Figure 1.3 Schematic representation of 180° angled slotted quartz tube, SQT.....	14
Figure 1.4 Schematic representation of water-cooled U-tube atom trap.....	15
Figure 1.5 Schematic representation of integrated atom trap system.....	16
Figure 3.1 Optimization of fuel flow rate with use of 5.0 mg/L Pb in FAAS.....	30
Figure 3.2 Optimization of suction rate with use of 5.0 mg/L Pb in FAAS.....	31
Figure 3.3 Calibration plot for FAAS method.....	32
Figure 3.4 Linear calibration plot for FAAS method.....	32
Figure 3.5 Optimization of fuel flow rate using 5.0 mg/L Pb in 120° angled SQT-FAAS.....	34
Figure 3.6 Optimization of fuel flow rate using 5 mg/L Pb in 180° angled SQT-FAAS.....	34
Figure 3.7 Optimization of sample suction rate using 5.0 mg/L Pb in 120°angled SQT-FAAS.....	35
Figure 3.8 Optimization of sample suction rate using 5 mg/L Pb in 180° angled SQT-FAAS.....	36

Figure 3.9 Optimization of height of SQT from the burner using 5 mg/L Pb in 120° angled SQT-FAAS.....	37
Figure 3.10 Optimization of height SQT from the burner using 5 mg/L Pb in 180° angled SQT-FAAS.....	37
Figure 3.11 Calibration plot for 120° angled SQT-FAAS method.....	38
Figure 3.12 Linear calibration plot for 120° angled SQT-FAAS method....	39
Figure 3.13 Calibration plot for 180° angled SQT-FAAS method.....	40
Figure 3.14 Linear calibration plot for 180° angled SQT-FAAS method....	40
Figure 3.15 Optimization of the volume of organic solvent using 5.0 ng/mL Pb in 120° angled SQT-AT-FAAS.....	45
Figure 3.16 Optimization of the volume of organic solvent using 5.0 ng/mL Pb in 180° angled SQT-AT-FAAS.....	45
Figure 3.17 Optimization of suction rate of 5.0 ng/mL 30.0 mL Pb in 120° angled SQT-AT-FAAS.....	47
Figure 3.18 Optimization of suction rate of 5.0 ng/mL 30.0 mL Pb in 180° angled SQT-AT-FAAS.....	47
Figure 3.19 Optimization of the flow rate of acetylene using 5.0 ng/L Pb in 120° angled SQT-AT-FAAS.....	48
Figure 3.20 Optimization of the flow rate of acetylene using 5.0 ng/L Pb in 180° angled SQT-AT-FAAS.....	49
Figure 3.21 Optimization of the height SQT from the burner using 5.0 ng/L Pb in 120° angled SQT-AT-FAAS.....	50
Figure 3.22 Optimization of the height SQT from the burner using 5.0 ng/mL Pb in 180° angled SQT-AT-FAAS.....	50
Figure 3.23 Effect of trapping period using 5.0 ng/mL Pb in 120°angled SQT-AT-FAAS.....	51
Figure 3.24 Effect of trapping period using 5.0 ng/mL Pb in 180°angled SQT-AT-FAAS.....	52

Figure 3.25 The signal of SQT-AT-FAAS for 5.0 ng/mL Pb solution.....	52
Figure 3.26 Calibration plot for SQT-AT-FAAS 120° angled SQT-AT-FAAS method at 8.1 mL/min flow rate.....	54
Figure 3.27 Linear calibration plot for 120° angled SQT-AT-FAAS method at 8.1 mL/min flow rate.....	54
Figure 3.28 Calibration plot for SQT-AT-FAAS 120° angled SQT-AT-FAAS method at 3.9 mL/min flow rate.....	55
Figure 3.29 Linear calibration plot for 120° angled SQT-AT-FAAS method at 3.9 mL/min flow rate.....	55
Figure 3.30 Linear calibration plot for 120° angled SQT-AT-FAAS method at different sample suction rates.....	56
Figure 3.31 Calibration plot for SQT-AT-FAAS 180° angled SQT-AT-FAAS method at 7.4 mL/min flow rate.....	57
Figure 3.32 Linear calibration plot for 180° angled SQT-AT-FAAS method at 7.4 mL/min flow rate.....	57
Figure 3.33 Calibration plot for SQT-AT-FAAS 180° angled SQT-AT-FAAS method at 3.9 mL/min flow rate.....	58
Figure 3.34 Linear calibration plot for 180° angled SQT-AT-FAAS method at 3.9 mL/min flow rate.....	58
Figure 3.35 Linear calibration plot for 180° angled SQT-AT-FAAS method at different sample suction rates.....	59
Figure 3.36 Linear calibration plot for SQT-AT-FAAS method with different types of tubes.....	60
Figure 3.37 Optimization of amount of organic solvent using 5.0 ng/mL Pb in Ta Coated-SQT-AT-FAAS.....	67
Figure 3.38 Optimization of sample suction rate using 2.5 ng/mL Pb in Ta Coated-SQT-AT-FAAS.....	68
Figure 3.39 Optimization of acetylene flow rate using 2.5 ng/mL Pb in Ta Coated-SQT-AT-FAAS.....	69

Figure 3.40 Optimization of height of SQT from burner head using 2.5 ng/mL Pb in Ta Coated-SQT-AT-FAAS.....	70
Figure 3.41 Effect of trapping period on Pb signal using 2.5 ng/mL Pb in Ta Coated-SQT-AT-FAAS.....	71
Figure 3.42 The signal of Ta- Coated-SQT-AT-FAAS for 2.5 ng/mL Pb solution.....	71
Figure 3.43 Calibration plot for Ta-Coated-SQT-AT-FAAS method.....	73
Figure 3.44 Linear calibration plot for Ta-Coated-SQT-AT-FAAS method.....	73
Figure 3.45 Interference effects of Na, K, Mg, Ca 2.0 ng/mL Pb signal in Ta-Coated-SQT-AT-FAAS.....	79
Figure 3.46 Interference effects of Fe, Mn, Cr 2.0 ng/mL Pb signal in Ta-Coated-SQT-AT-FAAS.....	80
Figure 3.47 Interference effects of Co, Ni, Cu 2.0 ng/mL Pb signal in Ta-Coated-SQT-AT-FAAS.....	81
Figure 3.48 Interference effects of Cd, Se, Sb 2.0 ng/mL Pb signal in Ta-Coated-SQT-AT-FAAS.....	81
Figure 3.49 Interference effects of Zn, Sn, Al 2.0 ng/mL Pb signal in Ta-Coated-SQT-AT-FAAS.....	82
Figure 3.50 Interference effects of SO_4^{2-} , F^- , PO_4^{3-} on 2.0 ng/mL Pb signal in Ta-Coated-SQT-AT-FAAS.....	83
Figure 3.51 XPS spectrum of Pb on quartz surface.....	84
Figure 3.52 XPS spectrum of C in presence of Pb.....	84
Figure 3.53 XPS spectrum of Pb_{4f} on quartz surface.....	85
Figure 3.54 XPS spectrum of Pb on Ta surface.....	86
Figure 3.55 XPS spectrum of C in presence of Pb and Ta.....	86

Figure 3.56 XPS spectrum of Pb _{4f} on Ta surface.....	87
Figure 3.57 XPS spectrum of Ta on quartz surface.....	88
Figure 3.58 XPS spectrum of C in presence of Ta.....	89
Figure 3.59 XPS spectrum of Ta _{4f} on quartz surface.....	89
Figure 3.60 Raman Spectrum of Ta ₂ O ₅	90
Figure 3.61 Raman Spectrum of Ta coated SQT.....	91

LIST OF ABBREVIATIONS

ABBREVIATIONS

AAS	Atomic Absorption Spectrometry
CRM	Certified Reference Material
ETAAS	Electrothermal Atomic Absorption Spectrometry
FAAS	Flame Atomic Absorption Spectrometry
GFAAS	Graphite Furnace Atomic Absorption Spectrometry
HGAAS	Hydride Generation Atomic Absorption Spectrometry
ICPMS	Inductively Coupled Plasma Mass Spectrometry
ICPOES	Inductively Coupled Plasma Optical Emission Spectrometry
MEK	Methyl Ethyl Ketone
MIBK	Methyl Isobutyl Ketone
Ta-Coated-SQT-AT-FAAS	Tantalum-Coated-Slotted Quartz Tube Atom Trap Flame Absorption Spectrometry
SQT	Slotted Quartz Tube
SQT-AT	Slotted Quartz Tube Atom Trap
SQT-AT-FAAS	Slotted Quartz Tube Atom Trap Flame Atomic Absorption Spectrometry
SQT-FAAS	Slotted Quartz Tube Flame Atomic Absorption Spectrometry
XPS	X-Ray Photon Spectroscopy

CHAPTER 1

INTRODUCTION

Heavy metals such as Pb, Hg, Cd, As, Tl and Cu have important effects on human health, plants and animals even at very low concentrations. So it is very important to have powerful methods for detection of these metals in environmental, biological and metallurgical samples. However, detection limit of these determinations must be very low; therefore, the techniques which are highly sensitive and precise are strongly needed. In the last two decades, Inductively Coupled Plasma Optical Emission Spectrometry (ICPOES) and Inductively Coupled Plasma Mass Spectrometry (ICPMS) have been very popular; because these techniques give precise results, low detection limits and they are rapid. However, both the purchase and running costs of these techniques are usually very high. So, Atomic Absorption Spectrometry (AAS) as an older analytical technique keeps its importance, especially in developing countries; because it is simple, has low cost and it is readily available in most analytical chemistry laboratories.

In this study, an AAS technique for sensitive determination of lead was developed and presented. Simple flame AAS and slotted quartz tube-atom trap (SQT-AT) device were used.

1.1 Lead and Lead Sources

Lead is one of the most abundant heavy elements on earth [1], its atomic number is 82 and atomic mass is 207.2 amu. The word *lead* is taken from the Anglo-Saxon *leadan*, and the symbol Pb has origin in the Latin word, *Plumbum*. Lead has lustrous bluish-white color, is very soft, highly malleable, ductile and a poor conductor, also it has high resistivity to corrosion but when exposure to air it tarnishes [2].

Lead is rarely found as a pure element in nature, it is generally found as Pb(II) in mineral deposits with elements such as sulphur and oxygen. Galena (PbS) is the most important natural source of lead, other important sources are cerussite (PbCO₃), anglesite (PbSO₄), litharge massicot (PbO) and minium (Pb₃O₄) [3].

Lead and inorganic lead compounds are found in a variety of commercial products and industrial materials, including paints, plastics, storage batteries, bearing alloys, insecticides and ceramics [4].

Lead predominantly gets into the environment as a result of anthropogenic activities such as industrial emissions from mining, smelting, recycling or waste incineration [5].

Lead is present in ambient air mostly as a result of vehicle exhaust; PbBrCl, PbBrCl.2NH₄Cl and α -2PbBrCl.NH₄Cl were the forms of lead found in vehicle exhaust. In addition, PbBrCl.(NH₄)₂BrCl, PbSO₄, and PbSO₄.(NH₄)₂SO₄ are the predominant forms of lead in ambient air [6]. In water; lead tends to form compounds that have low solubility with major anions. Level of lead in water depends on the type of water, in water with pH near to 7, concentration of lead is lower than 10 mg/L, because of the combination with sulfates, carbonates and hydroxides to form insoluble compounds [3]. In soil; lead is present as a result of dry and wet deposition of atmospheric lead; contamination from industrial activities and stable organo-metal complexes [7].

The use of tetraethyl- and tetramethyllead as antiknock additives in gasoline is largely responsible for the presence of lead in the urban atmosphere [1]. Knowing the adverse effects of lead on health, lead in gasoline was started to be phased out in US, in 1974. Then usage of the leaded gasoline was totally banned in 1996 in US. In EU, phasing out of lead was later than US, in 2000. World Health Organization (WHO) called total ban in 2001. Turkey completely banned the use of leaded gasoline in 2006. However; the use of leaded gasoline is still going on some countries in South America, Asia and Middle East [8].

1.2 Lead and Health

Lead, which produces several diseases, is one of the most important and widely distributed pollutants in the environment [9]. Effects of lead are both toxicological and neurotoxic in nature, including irreversible brain damage [10].

Lead is taken into the human body by swallowing lead dust, or by eating lead containing soil or paint chips. Lead is toxic for brain, kidney and reproductive system, also cause impairment in intellectual functioning, infertility, miscarriage and hypertension [11]. According to Environmental Protection Agency, in children lead causes damage to brain and nervous system, headache and also behavior, learning and hearing problems [12].

The risk of lead poisoning is common in children between the age of 2 and 5, who has the habit of chewing objects around. There are restrictions on use of lead in materials readily available to children like toys, but especially in old houses painted surfaces may contain lead-pigmented paints. So chewing of lead-containing materials can cause severe effects to children, depending on the level of poisoning it can cause anemia, encephalitis (brain damage) and even death [13].

In biological samples amount of lead is very low, in the level of ng/kg or ng/mL. According to World Health Organization (WHO) provisional tolerable weekly intake of lead is 0.025 mg/kg body weight [14].

Lead has also negative affects to plants and animals. Most of the studies done on lichens show this affect clearly; these studies indicate that lead inhibits photosynthesis in lichens. Also these studies indicate that lead in lichens was derived from tetramethyl and tetraethyl lead which were used as antiknock agent in gasoline [15].

1.3 Determination of Lead

Reliable determinations of lead in substances that may cause lead introduction to humans are needed [16]. Therefore, high sensitivity analytical techniques are required for quantification of this element.

The mostly used methods for lead determination are plasma techniques such as inductively coupled plasma emission spectrometry (ICPOES) and inductively coupled plasma mass spectrometry (ICPMS), and atomic absorption spectrometric techniques such as electrothermal (ETAAS), hydride generation (HGAAS) and flame (FAAS) atomic absorption spectrometry.

1.3.1 Determination of Lead by Plasma Techniques

In ICPOES technique, components of sample are converted into atoms and also excited to higher electronic states. Then relaxation of the excited species results in production of ultraviolet and visible line spectra that are used for qualitative and quantitative elemental analysis [17].

Although ICPOES quite sensitive, in some samples level of lead lies below the detection limit; in addition, there are some spectral interferences like Aluminum (Al, 220.4 nm) and background shift due to iron (Fe). Therefore, some preconcentration and separation techniques are needed for determination of lead by this technique [2].

ICPMS is other kind of plasma technique which is used for trace element determination. Atomic mass spectrometric analysis consists of these steps; first, atomization of analyte with a plasma source, conversion of atoms into ions, separation of ions on the basis of their mass to charge ratio and counting of the ions of each type. It has some advantages; the detection limits are two orders of magnitude better than those obtained by ICPOES, mass spectra are simple and easily interpreted, and it is also possible to obtain atomic isotopic ratios [17].

Plasma spectrometry has several advantages over AAS. ICPMS has lower interelement interference because of high temperature of plasma, high dynamic range; it is rapid, multielement analysis and determination of low concentration of elements is possible with this technique [18].

1.3.2 Determination of Lead by Atomic Absorption Spectrometry

AAS is based on the absorption of radiation by free atoms, in their ground state. Every element has its specific wavelength for absorption by the ground state atoms. Absorbance is proportional to the amount of atoms in ground state, and so to the concentration of element.

An atomic absorption spectrometer consists of a radiation source, atomizer, a monochromator, a detector and electronics for data acquisition, processing and editing [17].

Hollow cathode lamps (HCL) and electrodeless discharge lamps (EDL) are the sources used in AAS. Atomizer is a place in which analyte is atomized such as flame, graphite tube or heated quartz tube. It is located in the light path between radiation source and monochromator. An ideal atomizer produces the complete sample atomization. The most sensitive analytical line of Pb is 217.0, but there is excessive background absorption effect at this line. Although 283.3 nm has lower sensitivity background absorption effect is low at this line; therefore this line is often preferred [19].

There are three types of atomic absorption techniques used for the determination of Pb; electrothermal atomic absorption spectrometry (ETAAS), hydride generation atomic absorption spectrometry (HGAAS) and flame atomic absorption spectrometry (FAAS). ETAAS and HGAAS techniques provide sensitivity improvement of 100-1000 fold over FAAS [20].

1.3.2.1 Electrothermal Atomic Absorption Spectrometry

ETAAS consists of electrothermal or graphite furnace atomizer which is heated electrically. Sample solution (10-50 μL) is deposited into atomizer; temperature is increased stepwise for removal of solvent and matrix before atomization. Then temperature is brought to atomization temperature and a rapid (generally 1 s) atomization occurs. A peak-shaped, time dependent signal is obtained and the area under this peak is proportional to mass of analyte in sample solution [19].

1.3.2.2 Hydride Generation Atomic Absorption Spectrometry

HGAAS is the second kind of atomic absorption technique used for Pb determination. In this procedure, analyte is first converted into its hydride obtained by addition of an

acidified aqueous solution of sample to a small volume of aqueous solution of NaBH_4 or metal/acid mixture such as Zn/HCl . For atomization, an externally heated quartz tube by flame or electrical means is used. The atomizer is kept at $800\text{-}900^\circ\text{C}$, where decomposition of hydride takes place leading to formation of analyte atoms [17, 19].

1.3.2.3 Flame Atomic Absorption Spectrometry

In this technique, a flame is used for atomization; the device which converts the sample solution into aerosol and sprays into flame consists of a nebulizer and a spray chamber. There are many kinds of nebulizers; most common one is the concentric tube. For the concentric tube nebulizer, liquid sample is aspirated through a capillary tube by the high pressure stream of gas flowing around the tip of tube. Liquid sample is broken up into fine droplets and transported to the flame [18].

There are several types of flames in FAAS. Air-acetylene and nitrous oxide-acetylene are the ones generally used. Former has the temperature in between $2100\text{-}2400^\circ\text{C}$, and commonly used for the determination of elements whose oxides are not refractory such as Ca, Cr, Cu, Co, Fe, Ni, Mg, Sr. Temperature of latter ranges in between $2600\text{-}2800^\circ\text{C}$ and it is used for elements such as Al, Si, Ta, Ti, V, Zr [17]. Determination of lead by FAAS requires an air-acetylene flame.

There are three important disadvantages of FAAS. The first one is low nebulization efficiency of the system, only 1-10% of sample solution reaches to the flame. Therefore, most of the sample is not transported to the atomizer. The second one is dilution of sample with flame gases. The third one is the short residence time of analyte atoms in the measurement zone, it is in the order of few milliseconds. Therefore, sensitivity of FAAS is limited by these negative aspects [20].

1.4 Atom Trapping Techniques in Atomic Absorption Spectrometry

To increase the residence time of analyte atoms in measurement zone and for on-line preconcentration, atom traps have been developed [21]. Metal and quartz metal traps and graphite furnace are used for preconcentration in HGAAS. For FAAS, long-path absorption tube, Delves' microsampling cup [13] and slotted quartz tube are used for increasing of retention time of analyte atoms in measurement zone; integrated atom trap and slotted quartz tube atom trap are used for preconcentration.

1.4.1 Atom Traps for Hydride Generation Techniques

Hydride generation (HG) provides very effective sample introduction for hydride forming elements such as As, Sb, Bi, Se, Sn, Ge, Pb, Tl, Te and In, because of the efficient transportation and atomization of gaseous hydride [22]. Atom traps have been developed for sensitivity improvement in hydride generation technique. There are three kinds of atom traps used with hydride generation; graphite furnace, quartz and metal atom traps.

1.4.1.1 Graphite Furnace Atom Trap for Hydride Generation Techniques

Graphite furnace (GF) is also used as an atom trap when coupled with hydride generation for ultratrace determination of metal hydrides. Metal hydrides are transported to GF, which is preheated, usually in between 200-800°C. In GF, volatile hydrides are decomposed and analyte species are trapped on the graphite tube surface; trapping causes clean, rapid separation from matrix. After trapping period is completed, trapped analyte is atomized by cycling the temperature programming and the analyte signal is obtained [23].

The inner surface of GF can be coated with platinum group elements for sensitivity improvement. The presence of these types of elements with GF reduces the temperatures at which analyte trapping occurs [22]. For this aim, inner surface of GF was coated with Zr for Pb determination by HGAAS. The method gave 6 fold enhancement of sensitivity with respect to that obtained by using the uncoated tube. In this study, while the sorption temperature of Pb on surface of uncoated GF was higher than 600°C, it was only 100°C on Zr surface [24].

1.4.1.2 Quartz Atom Traps for Hydride Generation Techniques

Quartz atom trap has been first introduced for determination of Pb [25]. A quartz atom trap uses quartz particles that are obtained by crushing and placing in the inlet arm of quartz T-tube atomizer, near the connection point to the horizontal arm; then this trap is heated externally by a resistively heated wire. Stages of technique are described by Ataman [20] as follows;

- i) By the reaction of analyte in HCl solution with NaBH₄ in a continuous flow system lead hydride (PbH₄) is formed.
- ii) By a gas-liquid separator analyte vapor is separated from the liquid stream then is transported to the quartz that is held at an optimized *collection temperature*; some of the analyte hydride molecules are trapped here.
- iii) After the collection stage analyte introduction is stopped.
- iv) The trap is rapidly heated to its *revolatilization temperature*; in the presence of hydrogen gas analyte species are released, and transported using a proper carrier gas to quartz atomizer where the transient signal is formed.

1.4.1.3 Metal Atom Traps for Vapor Generation Techniques

In recent years, metal traps have been used as alternative atomizers; metal atom trap is resistively heated by passage of electricity through the device. There are some kinds of metal traps for this usage. W coil is one of the most popular traps used first as an on-line preconcentration of Bi in Ataman research group [26] and for Se determination [27], and then it was used for Sb determination again in Ataman research group [28].

Procedure in determination of Sb with W trap HGAAS involves the following stages [28];

- i) Generation of SbH_3 in an acidic medium with NaBH_4
- ii) Volatile analyte species are preconcentrated on W-coil, previously heated to an optimized *collection temperature*.
- iii) Collected analyte species are re-volatilized by heating the trap to a higher temperature under an optimized argon and hydrogen gases
- iv) Analyte species are transported to an externally heated quartz atomizer and a transient signal is obtained.

W-coil coated with Rh has been used as both preconcentration and atomizer for determination of Se [27]. Gold wire placed in the inlet arm of quartz T-tube as a trapping medium was also used for Se hydrides [29].

1.4.2 Atom Traps for Flame Atomic Absorption Spectrometry

Flame AAS is a simple, robust and low cost technique. However, this technique was not sensitive enough for trace and ultra trace determination of most heavy metals. Sensitivity is low because of the reasons given in section 1.3.3. Sensitivity improvement could be provided by introduction of sample solution with effective nebulization or making the atomic vapor to stay longer in pathway of source and by using a special atomizer.

1.4.2.1 Long-Path Absorption Tube Method

In this type of tube, absorption medium is restricted in cylindrical form along the longitudinal axis which absorbed light passes. There are two types of long-path absorption tube; open ended and T-shaped shown in Figure 1.1. Silica, alumina and ceramic tubes with the length of 1 m have been used. The success of this device depends on the life time of free atoms and life time changes with element, temperature and composition of flame gases [21].

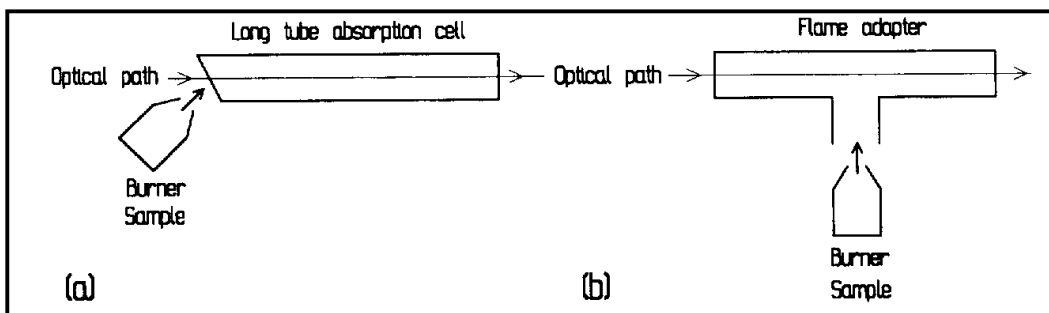


Figure 1.1 Schematic representation of a long-tube absorption cell. (a) Open ended, (b) T-shaped [21].

Also, by using this type of absorption tube and propane-butane-air flame, 5-13 fold sensitivity improvement for the determination of copper, silver, gold and cadmium was observed [30].

Since the length of this absorption tube is very long, about 1 m, it does not fit in burner head of a standard atomic absorption spectrometer. Therefore it has not been utilized commercially [21].

1.4.2.2 Delves' Microsampling Cup Method

Delves' microsampling atomic absorption method [13] is defined as a method in which a nickel cup and an absorption tube in flame are used; it is shown schematically in Figure 1.2. Absorption tube made from a nickel foil positioned in a flame, and is placed 20 mm above the burner and parallel to the burner slots. Sample is placed in a nickel cup, then sample is vaporized into an open-ended absorption tube, and atomized. This device provides high sensitivity, because, sample transfer efficiency to the flame is high as compared pneumatic nebulization; in addition, residence time of the analyte atoms in long cylindrical cell is improved [21].

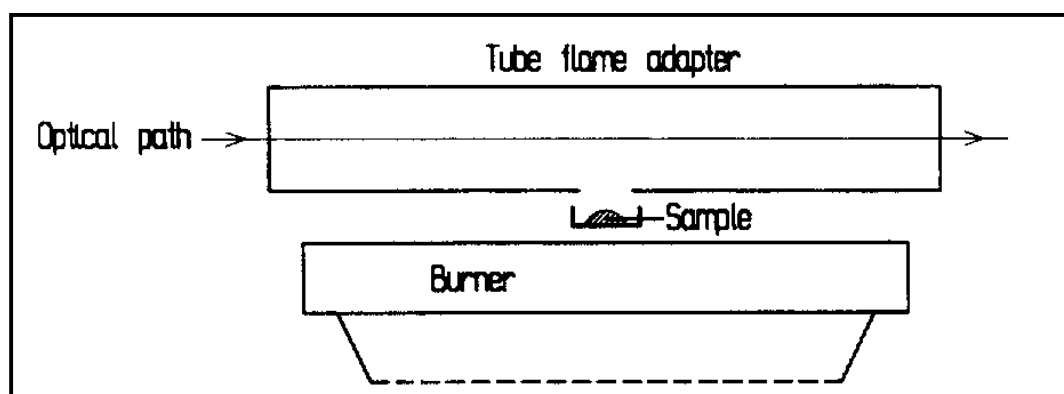


Figure 1.2 Schematic representation of Delves' microsampling cup system [21].

Determination of lead in blood by AAS requires solvent extraction and protein precipitation in most procedures; however in these procedures a large volume of sample (5 mL) is needed and the time required is fairly long (90 min); so Delves used this microsampling method for the determination of lead in children blood, he used only 10 μ L of sample for accurate determination [13].

Since Delves' Cup Technique requires very small volume of sample, it is used for investigation of clinical, industrial and environmental samples. It is very effective for determination of volatile elements like, lead and cadmium. However operating the system with ideal conditions requires extreme care. Due to this reason system is not commercially available any more [21].

1.4.2.3 Slotted Quartz Tube FAAS Method

In 1977 Watling [31] used SQT for the first time for increasing the analytical sensitivity in atomic absorption analysis for elements like Pb, Zn, Cd, Co, Ag, Bi, Mn, Hg, As, Se and Sb. As a result of his study, precision improvement was observed for some elements even at very low concentration; however, for copper, nickel and iron the signal was not improved.

The device is a hollow quartz tube with two slots, the angle between the lower slot and upper slot is 120° or 180° . The tube is positioned on the burner head where laminar flame is aligned with the lower slot. Working principle of SQT is given in Figure 1.3 [20]

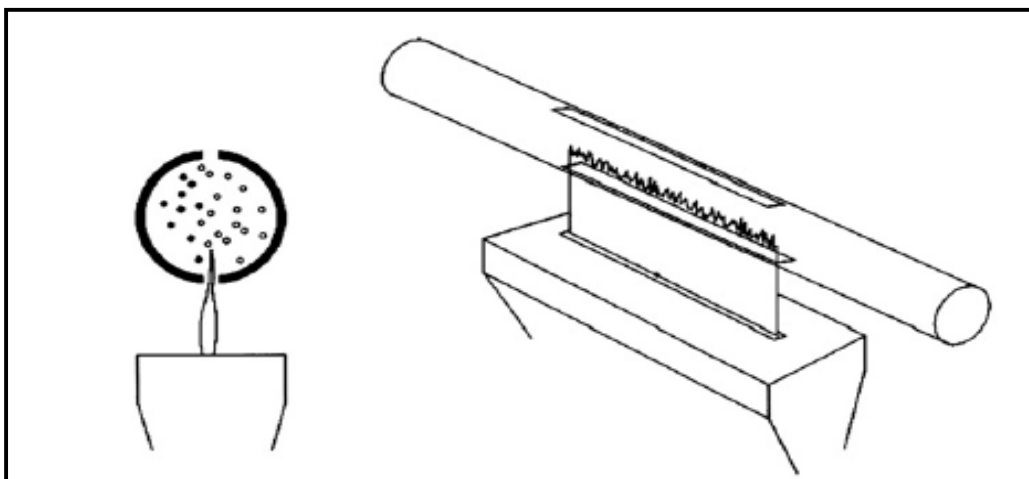


Figure 1.3 Schematic representation of 180° angled slotted quartz tube, SQT [20].

Because of slower flame conditions and length of optical path through which atoms pass, residence time of analyte atoms in measurement zone increases and this causes the sensitivity improvement in FAAS. Since this tube partly isolates the flame from air, chemical environment inside tube will be more stable; consequently the sensitivity is improved.

This technique can also be used with hydride generation methods. Determination of bismuth in copper based alloys was studied with this integration. It was concluded that use of SQT with nebulized solutions or coupled with hydride generation decreased the characteristic concentration and improved precisions by factors of two as compared with obtained without SQT [32].

SQT provides increased sensitivity and precision as compared to conventional flame method; potential interferences are also reduced because of the dilution of the sample. Method is simple and provides rapid analysis; it is inexpensive, and SQT is easily manufactured. One disadvantage of SQT is that it is limited to only volatile element determination.

1.4.2.4 Water-Cooled Silica Atom Trap Method

In this technique; a silica U-tube, cooled by flow of cold water passing through, is positioned just below the optical path of the spectrometer, atoms are nebulized into the flame and condensed onto the outer surface of cooled silica tube. After collection of analyte atoms on the surface of quartz tube, flow of water is switched off and replaced with an air stream; silica surface is thus heated rapidly then condensed analyte atoms are released. By absorbing light from the source, a transient signal is obtained [20]. In Figure 1.4, a water-cooled silica atom trap system is shown.

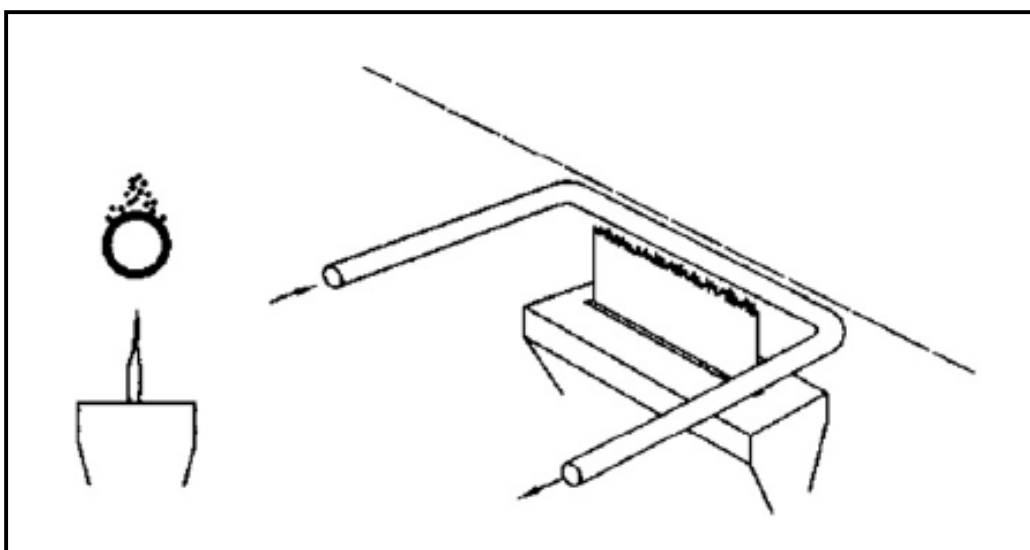


Figure 1.4 Schematic representation of water-cooled U-tube atom trap [20]

With this method; elements with high melting point are trapped but they are not re-atomized. Alkali and alkaline earth elements are also trapped but engrave the silica surface, so they could not be detected [21].

Mechanism of trapping of lead has been studied on water-cooled atom trap; it was found that lead was collected as lead silicate and using a lean flame gave the best enhancement [33].

One of the main advantages of water-cooled trap is that it is comparatively inexpensive, simple to use and permits the analysis of various materials. However, it is slower because of the atom trapping period. It is only used for the analysis of samples with sufficiently high volume, because trapping requires a rather large volume of sample at least in the order of few milliliters. Additionally, due to the thermal shock of silica trap caused by rapid heating and cooling cycles, the life time of the silica trap decreased drastically [34].

1.4.2.5 Integrated Atom Trap Method

In this method, water-cooled silica tube is combined with a double slotted quartz tube, IAT [21]. Working principle of the system is shown in Figure 1.5. So, integration of atom traps results in the further in both sensitivity and detection limit.

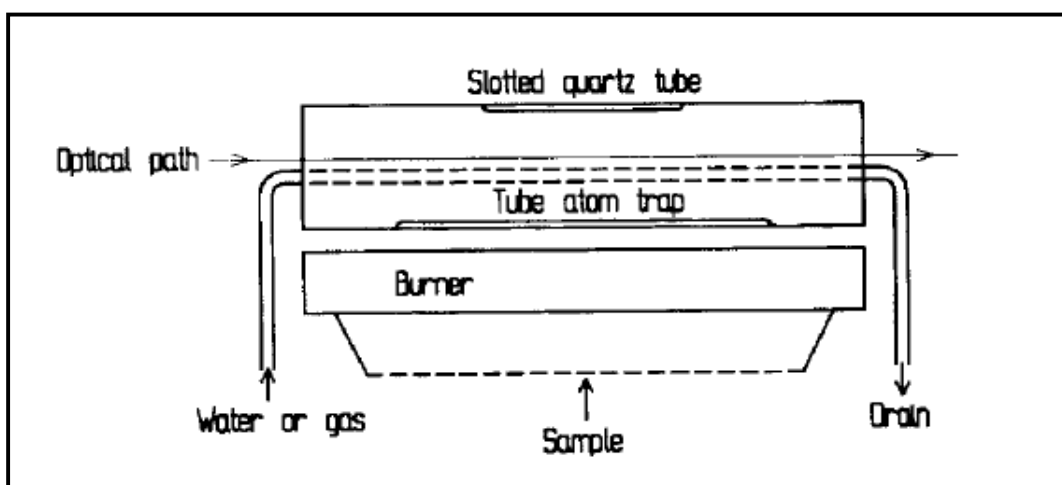


Figure 1.5 Schematic representation of integrated atom trap system [21]

IAT was used for the determination of Pb and Cd. In this study sensitivity was improved 50-200 times for both elements, depending on preconcentration time, by using a double

slotted quartz tube through which the light beam of hollow cathode lamp was passed [35].

By this method, analysis of samples with aqueous medium and the volume of 5-10 mL are possible. Determinations of elements which are volatile such as Cd, Pb and Zn, and atomized in air-acetylene flame are performed. This system is readily decoupled, simple, and has low cost; however, a rather high volume of sample is needed because of the trapping and it is limited to only few elements [34].

In this method, there is a significant light obscuration due to placing a silica trap in the SQT. This obscuration decreases the sensitivity. In addition, water is condensed on the cold silica trap surface causing occasional water drops onto SQT which causes elevated background signal [36]. In addition, because of condensed solvent drops onto hot surface of SQT, the device may crack easily.

1.4.2.6 Slotted Quartz Tube Atom Trap Method

Slotted quartz tube atom trap (SQT-AT) provides preconcentration of analyte atoms on the inner surface of slotted quartz tube [37], the main stages of method are as follows;

- i) **Collection;*** using an optimized lean flame, sample solution is introduced into the flame. Analyte atoms are trapped in the inner surface of SQT. This step takes a few minutes.
- ii) **Revolatilization;*** 10-50 μL of an organic solvent, such as Methyl isobutyl ketone or Methyl ethyl ketone, is introduced into the flame. This introduction alters the flame composition for a very short period of time, it makes the

flame momentarily reducing in nature and analyte atoms are released from the inner surface of SQT.

- iii) **Atomization;** revolatilization is followed by rapid atomization and a transient signal is obtained.

During revolatilization, flame products and trapped species are involved in a fast reaction that causes removal of analyte species from the silica surface. This suggestion was obtained from a study in which SQT was rotated 90° after the collection stage [38].

The most important advantage of using SQT-AT is increased sensitivity, and because of the sensitivity improvement, samples could be diluted to decrease the possible interferences. In addition, few milliliters of sample are sufficient for analysis. Besides, this system has the advantage of increased sample throughput, low cost and it is simple to use. The main disadvantage of the system is the application is limited only volatile elements. Volatile elements easily decompose thermally in the primary reaction zone of air-acetylene flame [39].

Kumser has studied the determination of Bi, Au and Mn by using uncoated FAAS-SQT-AT. Sensitivity improvements for Bi, Au and Mn as compared to FAAS were 94, 180 and 6.6 folds respectively [40]. Ari has investigated Tl determination by Os coated SQT-AT and she obtained 3.5 fold enhancement in sensitivity as compared to uncoated SQT-AT, total sensitivity enhancement with respect to FAAS was 319 fold, using a sample of 25 mL collecting in 5.0 minutes [41].

1.5 Atomization in FAAS-SQT-AT

There are two kinds of atomization used in FAAS-SQT-AT namely; flame alteration technique and organic solvent aspiration technique.

1.5.1 Flame Alteration Technique

Atomization by *flame alteration* system refers to changing the composition of flame by altering the ratio of air to acetylene ratio by introducing an extra flow of acetylene; after this change flame will be momentarily hotter and reducing. When this reducing flame comes into contact with silica surface, revolatilization and rapid atomization takes place.

During a study which is which based on the determination of lead and cadmium using SQT-AT with flame alteration and organic solvent aspiration technique; it has been shown that there is no significant difference between these two techniques [35].

1.5.2 Organic Solvent Aspiration Technique

Atomization by *organic solvent aspiration* consists of the changing the flame composition for a very short period by aspirating a few microliters of an organic solvent into the flame following the collection period. For this reason various kinds of organic solvent can be used such as, methylisobutylketone (MIBK), acetonitrile, methylethylketone, iso-octane, n-hexane and acetone. MIBK was the most effective one among them, because it gives a complete atomization that is, there is no memory effect. In addition, MIBK gave the largest linear range for calibration [35].

Revolatilization by organic solvent aspiration, like flame alteration technique, is not thermal. It makes the flame, momentarily reducing which is more effective for

atomization process. Volume of organic solvent is very low, 10-50 μL ; when uptake rate is about 6.0 mL/min, only about 500 ms are needed for introduction of 50 μL MIBK; therefore, so even if there is any rise in flame temperature this would be for a very short period of time [20].

1.6 Surface Studies

To enhance the sensitivity, surface of SQT may be coated with some elements, such as W, Ta, Mo, Os, Ir, Au and Pd. The most important point here is that the melting point of the coating material should be significantly higher than the element interested. In other words, it is desired that the coating material will not be lost from the surface as the analyte element volatilizes.

Nature of analyte species on surface of SQT investigated by X-ray photoelectron spectroscopy (XPS) [42, 43]. When sample is exposed to X-rays for a long time, there are several kinds of radiation damage. The most important possible damage is the reduction of metal ions to lower oxidation states [42]. Each element produces a characteristic set of XPS peaks at characteristic binding energies, which are related with the identification of the element and its oxidation states on the surface. These characteristic peaks correspond to the electron configuration of the analyte species.

Deposition of Au on silica surface has been investigated by XPS-spectroscopy, and it is found that Au $4f_{7/2}$ peak with binding energy of 84.8 (± 0.2) eV, corresponds to Au (0) [43].

1.7 Aim of the Study

Developing a sensitive analytical method for determination of lead by using FAAS-SQT-AT is the main purpose of this study. An uncoated SQT device with two slots with an angle of either 120° or 180° with respect to each other will be used for sensitivity improvement in the initial stages of research. Then, several coating materials will be used to modify the surface of SQT and sensitivity comparisons will be made. In addition, SQT devices with different inner and outer diameters will be tested in order to investigate on possible differences in analytical behavior depending on the wall thickness of the tube. All the parameters for uncoated and coated FAAS-SQT-AT will be optimized. Characterization of analyte species on quartz surface, on coating material and the coating material on quartz surface will be made using XPS and vibrational spectroscopy. In addition, interference studies will be carried out.

CHAPTER 2

EXPERIMENTAL

2.1 Apparatus and Materials

A 15 cm long slotted quartz tube with two slots positioned at 120° and 180° with respect to each other was used; length of the lower slot was 100 mm and the upper slot was 80 mm; inner diameter of the tube was 13 mm and the outer diameter was 17 mm. The slotted quartz tubes were prepared by Çalışkan Cam in OSTİM (Ortadoğu Sanayi ve Ticaret Merkezi), Ankara.

Standard solutions were prepared by 100-1000 µL and 500-5000 µL Eppendorf micropipettes in glass containers with using a volume of 100 mL. Polyethylene containers with the capacity of 100 mL were used to store the solutions which were kept in refrigerator. For the aspiration of organic solvent into flame, 1.0 mL plastic cups and adjustable micro pipettes were used.

2.2 Chemicals and Reagents

Standard solution of 1000 mg/L lead standard ICP solution (Fisher Scientific International Company) was used for the preparation of working solutions. Intermediate standard solutions of lead were prepared by diluting necessary volumes of 1000 mg/L standard solution with deionized water. Dilutions were made using 18 MΩ·cm deionized water obtained from a Millipore (Molsheim, France) Milli-Q water purification system which was fed using the water produced by Millipore Elix 5 electro deionization system. All standard solutions were prepared in 1.0 M HNO₃, for this purpose analytical grade 65% (v/v) HNO₃ (Merck) was used.

All the glass and polyethylene containers were cleaned in 10% (v/v) HNO₃ solution in a cleaning tank by immersing them for at least over night. Cleaned materials were then washed with deionized water before use.

For the interference study, 4 different solutions were prepared in which concentration of Pb was kept constant, 2.0 ng/mL, and the concentrations of interferent were 1, 10, 100 and 1000 folds in mass of the analyte concentration. Na (High Purity Standards), Mg (Merck), K (Merck), Fe (Merck), Co (High Purity Standards), Ni (High Purity Standards), Cu (Merck), Cd (High Purity Standards), Se (High Purity Standards), Sb (Ultra Scientific), Zn (High Purity), Sn (Merck), Al (Merck) were prepared from 1000 mg/L stock solution in 1.0 M HNO₃.

CRM, SCP SCIENCE EnviroMAT Waste Water Low (EU-L-2) was used as a reference material; its content is given in Table 2.1.

Table 2.1 Certified values for SCP SCIENCE EnviroMAT Waste Water, Low (EU-L-2)

Parameter	Unit	Consensus Value	Confidence Interval	Tolerance Interval
Al	ppm	0.052	0.048 – 0.056	0.028 – 0.075
As	ppm	0.080	0.078 – 0.083	0.065 – 0.095
B	ppm	0.113	0.100 – 0.125	0.046 – 0.180
Ba	ppm	0.124	0.122 – 0.126	0.112 – 0.135
Be	ppm	0.012	0.0117 – 0.0125	0.010 – 0.014
Ca	ppm	1.74	1.70 – 1.78	1.53 – 1.95
Cd	ppm	0.023	0.022 – 0.024	0.017 – 0.029
Co	ppm	0.081	0.080 – 0.082	0.075 – 0.088
Cr	ppm	0.060	0.059 – 0.061	0.054 – 0.067
Cu	ppm	0.105	0.101 – 0.109	0.078 – 0.132
Fe	ppm	0.051	0.048 – 0.054	0.034 – 0.069
K	ppm	2.04	1.95 – 2.13	1.52 – 2.56
Mg	ppm	0.86	0.83 – 0.90	0.68 – 1.05
Mn	ppm	0.12	0.117 – 0.122	0.10 – 0.13
Mo	ppm	0.040	0.037 – 0.042	0.027 – 0.052
Na	ppm	4.46	4.32 – 4.60	3.70 – 5.22
Ni	ppm	0.082	0.080 – 0.084	0.068 – 0.096
P	ppm	1.05	1.03 – 1.07	0.93 – 1.16
Pb	ppm	0.041	0.040 – 0.043	0.032 – 0.051
Sb	ppm	0.019	0.018 – 0.020	0.014 – 0.025
Se	ppm	0.027	0.026 – 0.028	0.023 – 0.032
Sr	ppm	0.14	0.139 – 0.147	0.12 – 0.16
Tl	ppm	0.080	0.076 – 0.084	0.059 – 0.100
V	ppm	0.049	0.047 – 0.051	0.038 – 0.059
Zn	ppm	0.023	0.021 – 0.026	0.011 – 0.036

Notes: Results after dilution 1 : 100

2.3 Atomic Absorption Spectrometer

Varian AA140 single beam atomic absorption spectrometer equipped with a Deuterium (D₂) background corrector was used. The results were saved using the SpectrAA software of the AA instrument. Air-acetylene type flame was used with a burner head of 100 mm. Photron Pb hollow cathode lamp with an operating current of 4 mA was used as a radiation source. All the analyses were done at the wavelength of 217.0 nm and a spectral band pass of 1.0 nm. The operating conditions for the FAAS are shown in Table 2.2.

Table 2.2 Operating Conditions for FAAS

Flame Type	Air-Acetylene
Wavelength of Pb, nm	217.0
Hollow Cathode Lamp Current, mA	4.0
Spectral Band Pass, nm	1.0
Air Flow Rate, L/min	3.5
Acetylene Flow Rate, L/min	0.5 - 2.4

2.4 Coating Procedure for Slotted Quartz Tube

Coated SQT tube is the one that have the slots positioned 180° with respect to each other. For the coating of SQT, 100 mL of 100 mg/L solutions of Pd, Ta, Zr, W, and Mo were prepared from their solids, $K_2[PdCl_6]$, Ta_2O_5 , $Zr(NO_3)_4 \cdot 5H_2O$, W metal and Mo metal; Ir solution was prepared from its 1000 mg/L standard solution (Ultra Scientific Standards). All coatings except Os were obtained by aspirating of coating solution using a suction rate of 3.4 mL/min, in the presence of a lean flame. Os coated SQT was already available in the laboratory, it was prepared by aspirating 100 mL of 1000 mg/L Os solution using a suction rate of 2.0 mL/min, in the presence of a lean flame. During interference studies, some elements damaged the coated surface, so damaged SQT was kept in 60% (v/v) of HF solution for an hour, then recoated with the same procedure of coating.

Procedures for the metal coating solutions are as follows:

- i. $K_2[PdCl_6]$ was dissolved in water.
- ii. Ta_2O_5 was dissolved in 2.79 M HF solution.
- iii. $Zr(NO_3)_4 \cdot 5H_2O$ was dissolved in water.

- iv. W metal was dissolved in a mixture of 1.72 M HF and 1.43 M HNO₃.
- v. Mo metal was dissolved in 1.43 M hot HNO₃ solution.

All the solids were dissolved by using an ultrasonic bath (Elma S 40 H).

2.5 Surface Studies

The chemical nature of Pb on quartz surface and Ta coating, also chemical nature of Ta on quartz surface were investigated with the use of X-ray photoelectron spectroscopy (XPS). For this purpose 1.0 mm thick quartz pieces with the length of 2.0 cm and width of 1.0 cm were used. These pieces were coated with desired analytes by placing the quartz piece into the SQT. Again in the presence of a lean flame, the first piece was coated by 100 mL of 1000 mg/L Pb solution. Second and third pieces were coated by 100 mL of 1000 mg/L Ta solution; then one of Ta coated quartz piece was coated by 100 mL of 1000 mg/L Pb solution. All the coatings were made using a suction rate of 3.9 mL/min.

SPECS ESCA system, at Middle East Technical University, Central Laboratory, with Mg/Al dual mode was used for the analysis of the surface materials. Analyzer of spectrometer was EA 200 hemispherical electrostatic energy analyzer equipped with multichannel detector (MCD) with 18 discrete channels, operation in the constant pass energy mode. Unmonochromatized Mg K α radiation was used as the X-ray source, X-ray gun operated at 10.0 kV, 20.0 mA and for excitation of Pb on quartz 176.0 W, for excitation of Ta on quartz 5.0 W, for excitation of Pb on Ta 1.0 W energy were used. Spectrometer was operated in CAE (constant analyzer energy) mode. Pressure of analyzer chamber was kept in between 10⁻⁸ to 10⁻⁹ torr. Atomic compositions were estimated using SpecsLab software.

C 1s was used as an internal energy calibrant at 284.5 eV binding energy.

Vibrational spectroscopy measurement was performed with Jobin Yvon LabRam confocal microscopy Raman spectrometer with a charge-coupled device (CCD) detector and a holographic notch filter. The spectrograph was equipped with a 1800-grooves/mm grating and all measurements were performed with a 200- μm entrance slit. Excitation was provided by 632.8-nm radiation from a He-Ne laser with a total power of 20 mW.

CHAPTER 3

RESULTS AND DISCUSSION

In this study, development of a sensitive method for lead determination consists of four stages;

- i. The determination of lead by simple FAAS.
- ii. Use of a slotted quartz tube (SQT) to improve sensitivity by increasing the residence time of analyte atoms in measurement zone. SQT provides more stable chemical environment because of the elimination of air diffusion to flame. Efficiency of both 120° and 180° angled tubes were examined. No trapping was involved. SQT-FAAS was used as an acronym for this stage of study.
- iii. The atom trap studies with uncoated SQT, both types of tubes (120° and 180° angled) were used. In addition, effect of wall thickness and inner diameter of SQT on Pb signal were examined. This approach involves preconcentration by atom trapping. The acronym used for this reason is SQT-AT-FAAS.
- iv. The last step is the further improvement of sensitivity by coating of SQT device using a metal, 180° angled tube configuration was used. Variety of coating materials was used for this aim. This method is called coated SQT-AT-FAAS.

In the study, the main interest is focused on the improvement of the trapping methods. Trap techniques depend on the total mass of analyte and also trapping period. As the trapping period increases total mass of trapped analyte increases. Then it seems that there is a sensitivity improvement, but this should be evaluated together with the time

involved. Sensitivity enhancement, E, can be used at this point. Ataman [20] introduced two new terms, enhancement factors in term of unit time, E_t , and unit volume, E_v . First, characteristic concentration, C_0 , concentration that corresponds to 0.00436 absorbance (1% absorption); has to be calculated;

$$C_0 = 0.00436 \times (\text{analyte concentration/absorbance}).$$

Then, comparing the C_0 values of two methods, sensitivity enhancement is found. Sensitivity enhancement also means ratio of calibration sensitivities (slopes). E_t is obtained by dividing E value by total time spent in terms of minutes, and E_v is obtained by dividing E value by total volume spent in terms of milliliters. Therefore, it would be possible to make a fair comparison of two methods using the terms of the trapping period and the total amount trapped. In order to evaluate the trapping efficiency another term is used; characteristic mass, m_0 , is the mass of analyte which produces a defined peak that has an absorbance value of 0.00436 (or 1 % absorption). It is calculated as the *(volume of trapped analyte) x (C_0)*. In addition to sensitivity enhancement limit of detection (LOD) is found as $3s/m$, limit of quantitation (LOQ) is found as $10s/m$ for each method.

3.1 FAAS Study

In this step determination of lead was performed by simple FAAS technique without any SQT device. In order to obtain high S/N ratio, acetylene flow rate and sample flow rate were optimized. For optimizations, 5.0 mg/L Pb standard solution was used.

3.1.1 Optimization of Fuel Flow Rate

Fuel flow rate was optimized by keeping the air flow rate constant at 3.5 L/min and sample flow rate at 8.01 mL/min, only acetylene flow rate was varied. Lead determination by FAAS requires a stoichiometric flame, and as seen from Figure 3.1 increasing fuel flow rate does not cause an important change in absorbance; therefore 2.5 L/min was selected as the acetylene flow rate.

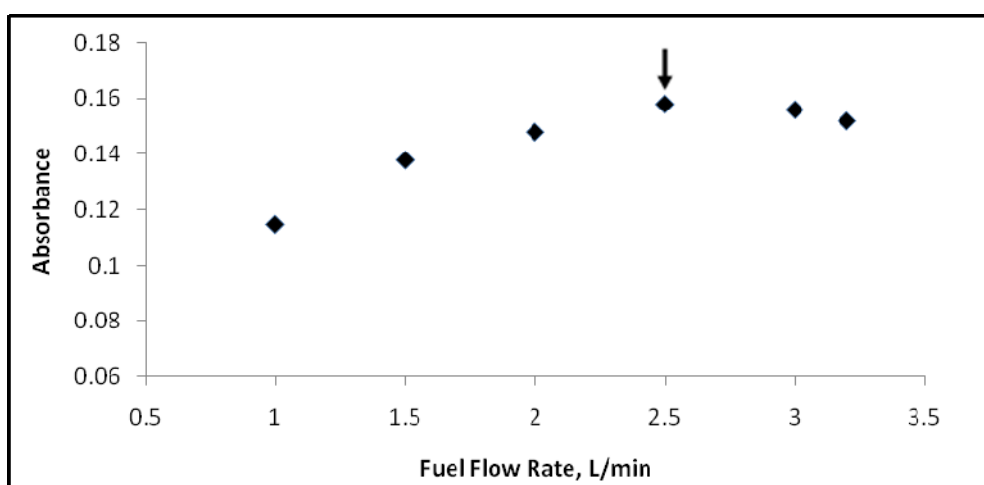


Figure 3.1 Optimization of fuel flow rate with use of 5.0 mg/L Pb in FAAS.

Flow rate of air: 3.5 L/min, Sample suction rate: 8.01 mL/min

3.1.2 Optimization of Suction Rate of Sample Solution

In order to change the sample flow rate, suction rate of nebulizer was altered. The optimization of sample suction rate was done by using 5.0 mg/L Pb solution at a 3.5 L/min air and 2.5 L/min acetylene flow rates. Result of the optimization of suction rate of sample was shown in Figure 3.2. It is clear that at high suction rate, better signal was obtained. It is due to the increasing population of analyte atoms per unit time in flame at

higher suction rates, so at lower suction rates signals of Pb are decreasing. Therefore, 8.01 mL/min was chosen as optimum sample suction rate for Pb.

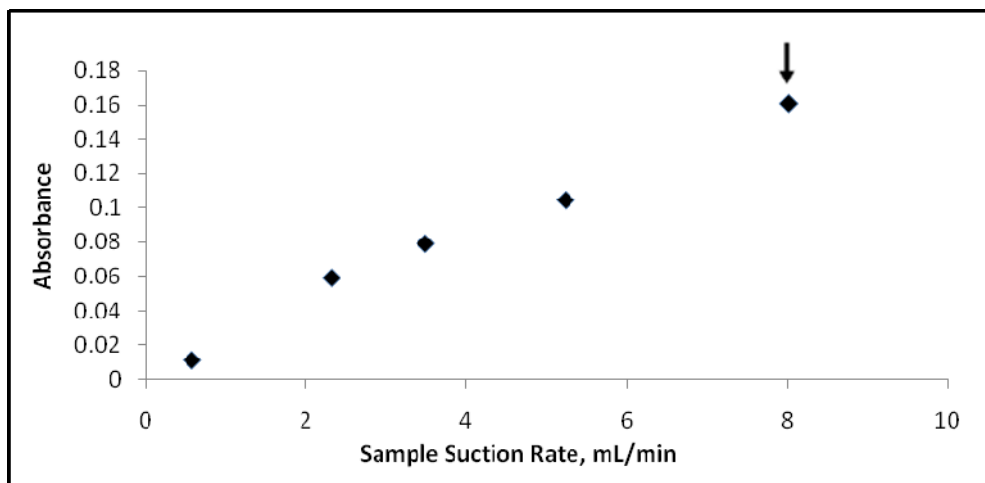


Figure 3.2 Optimization of suction rate with use of 5.0 mg/L Pb in FAAS.

Acetylene flow rate: 2.5 L/min, Flow rate of air: 3.5 L/min,

3.1.3 Calibration Plot for FAAS Method

Using the parameters optimized, absorbance values of lead solutions in concentrations between 0.5-20.0 mg/L were measured (Figure 3.3). Calibration plot was linear between 0.5-5.0 mg/L (Figure 3.4). The best line equation and correlation coefficient were, $y = 0.0315x + 0.0037$ and 0.9987 respectively.

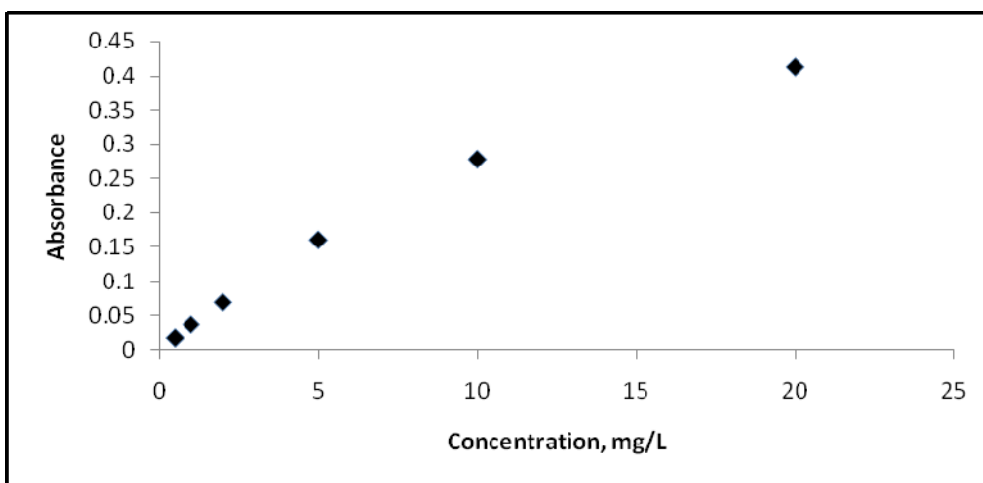


Figure 3.3 Calibration plot for FAAS method

Acetylene flow rate: 2.5 L/min, Flow rate of air: 3.5 L/min

Sample suction rate: 8.01 mL/min

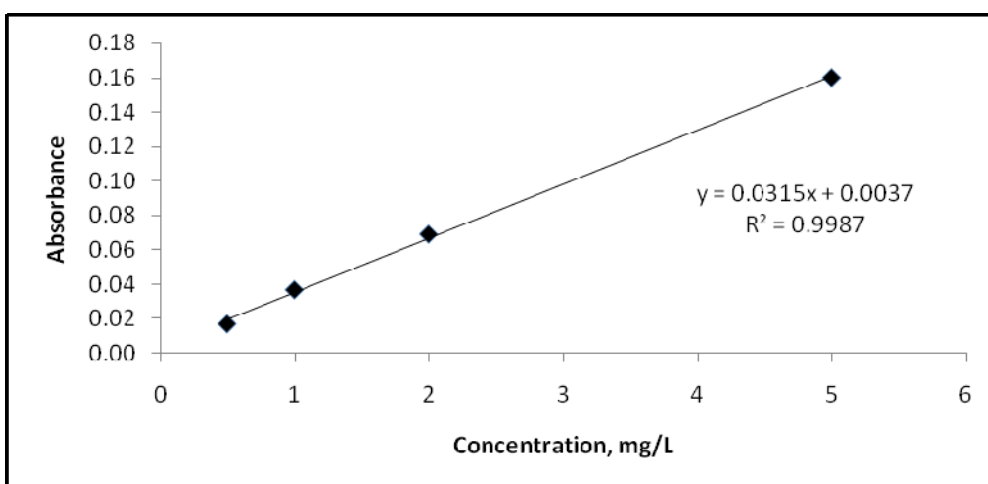


Figure 3.4 Linear calibration plot for FAAS method

Acetylene flow rate: 2.5 L/min, Flow rate of air: 3.5 L/min

Sample suction rate: 8.01 mL/min

As seen from the Table 3.1 LOD and LOQ were calculated as 54 ng/mL and 181 ng/mL respectively. Characteristic concentration was estimated as 132 ng/mL. For LOD and LOQ determination 11 measurements of 0.5 mg/L solution were used.

Table 3.1 Analytical Performance of FAAS

Limit of Detection (LOD), <i>ng/mL</i>	54
Limit of Quantitation (LOQ), <i>ng/mL</i>	181
Characteristic Concentration (C_0), <i>ng/mL</i>	132

3.2 Optimizations of Slotted Quartz Tube Flame AAS Method

This step contains the study which depends on the sensitivity enhancement by increasing the residence time of analyte atoms in measurement zone. SQT is positioned on the burner head; this position allows the entire light beam pass through the tube. Flame is allowed to pass through the lower slot into the tube and sample solution is aspirated continuously. Fuel flow rate, suction rate of sample and height of SQT with respect to burner head was optimized to find the best sensitivity. Conditions were optimized SQT devices with an angle of 120° and 180° between two slots; 5.0 mg/L Pb solution was used throughout the optimizations.

3.2.1 Optimization of Fuel Flow Rate

The optimum acetylene flow rate was found as 1.4 L/min for 120° angled SQT as seen in Figure 3.5 and 1.5 L/min for 180° angled SQT in Figure 3.6. As acetylene flow rate decreasing signal of Pb is increasing; it is probably due to the trapping of analyte atoms on the inner surface of SQT at lower temperatures.

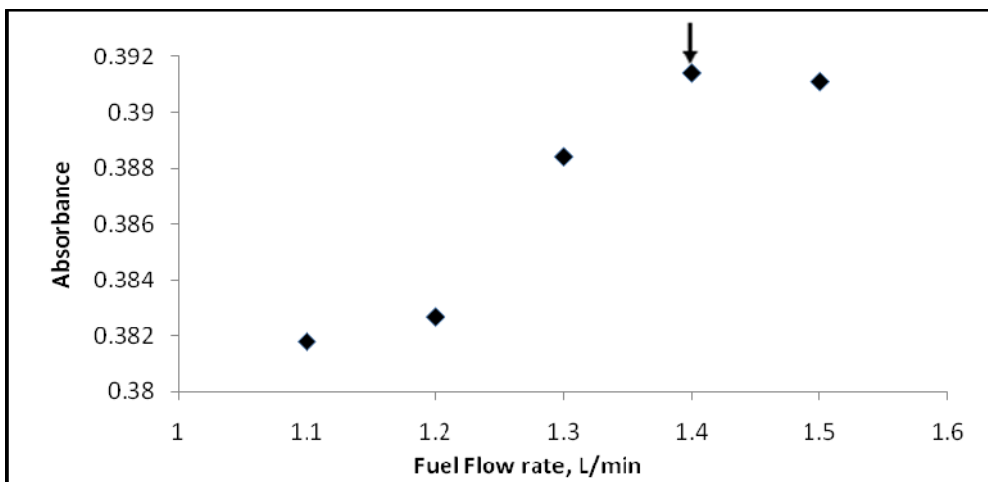


Figure 3.5 Optimization of fuel flow rate using 5.0 mg/L Pb in 120° angled SQT-FAAS.
 Sample suction rate: 8.3 mL/min, Flow rate of air: 3.5 L/min,
 Height of SQT from the burner head: 1.0 mm

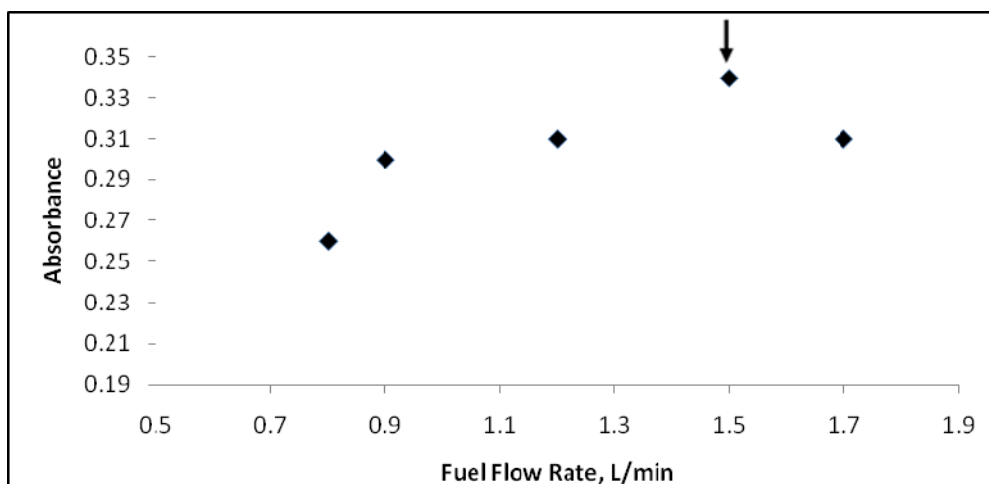


Figure 3.6 Optimization of fuel flow rate using 5 mg/L Pb in 180° angled SQT-FAAS.
 Sample suction rate: 8.3 mL/min, Flow rate of air: 3.5 L/min,
 Height of SQT from the burner head: 1.0 mm

3.2.2 Optimization of Sample Suction Rate

As seen in Figure 3.7 and Figure 3.8 increasing suction rate of sample causes analyte signal to rise, the reason is same as FAAS study, increasing population of analyte atoms per unit time in flame. Optimum suction rate for Pb solution was determined as 8.3 mL/min and 8.1 mL/min in 120° and 180° angled SQT-FAAS method.

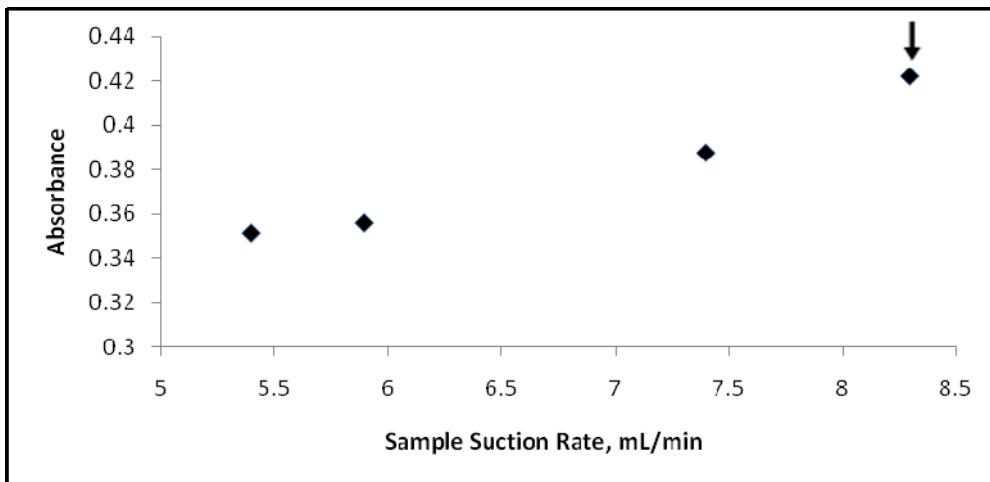


Figure 3.7 Optimization of sample suction rate using 5.0 mg/L Pb in 120°angled SQT-FAAS.

Fuel flow rate: 1.4 L/min, Flow rate of air: 3.5 L/min,

Height of SQT from the burner head: 1.0 mm

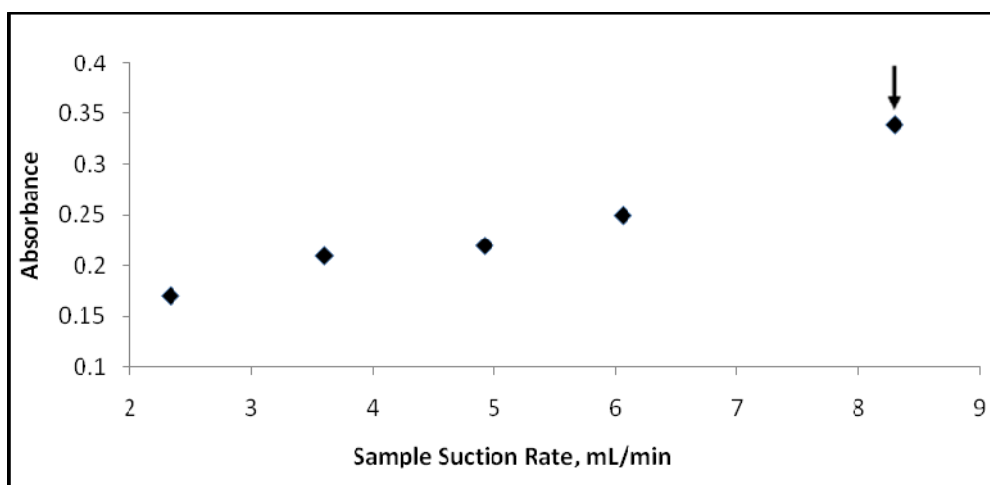


Figure 3.8 Optimization of sample suction rate using 5 mg/L Pb in 180° angled SQT-FAAS.

Fuel flow rate: 1.5 L/min, Flow rate of air: 3.5 L/min,

Height of SQT from the burner head: 1.0 mm

3.2.3 Optimization of Height of the SQT from the Burner Head

Height of the SQT from the burner head is another important parameter to be optimized. It was varied between 1.0 mm and 4.0 mm, and as shown in Figure 3.9 and Figure 3.10, 1.0 mm was found as the optimum height for 120° and 180° angled SQT-FAAS method. Height should be as short as possible for entering of analyte atoms into the tube.

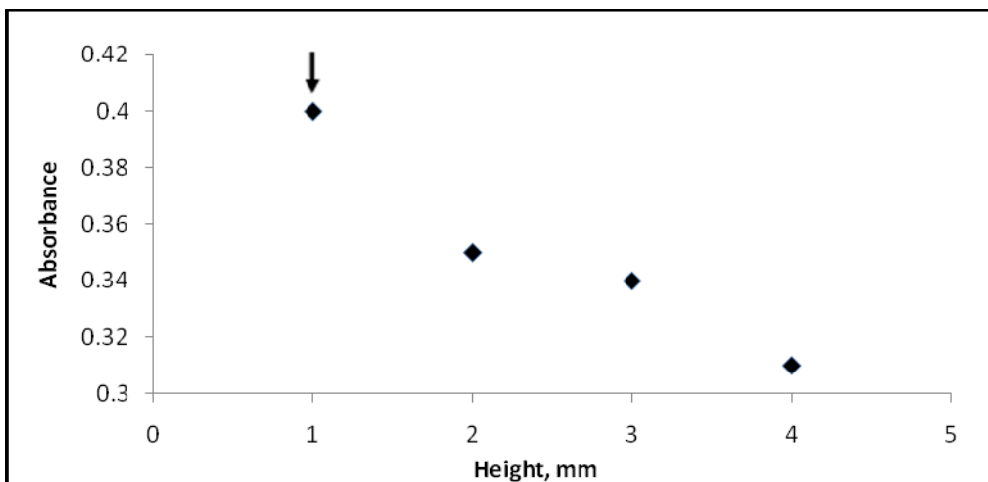


Figure 3.9 Optimization of height of SQT from the burner using 5 mg/L Pb in 120° angled SQT-FAAS.

Fuel flow rate: 1.4 L/min, Flow rate of air: 3.5 L/min,

Sample suction rate: 8.3 mL/min

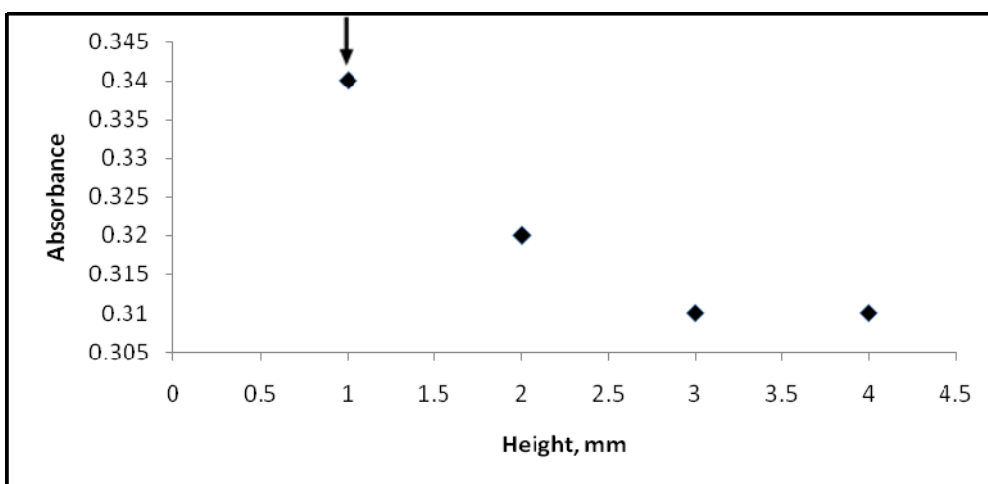


Figure 3.10 Optimization of height of SQT from the burner using 5 mg/L Pb in 180° angled SQT-FAAS

Fuel flow rate: 1.4 L/min, Flow rate of air: 3.5 L/min,

Sample suction rate: 8.1 mL/min

3.2.4 Calibration Plots for SQT-FAAS Method

For the calibration plot, obtained with 120° angled SQT, Pb solutions between 0.1-20 mg/L were used (Figure 3.11). Calibration plot is linear between 0.1-2.0 mg/L. The best line equation and correlation coefficient were, $y = 0.1029x + 0.0054$ and 0.9986, respectively (Figure 3.12).

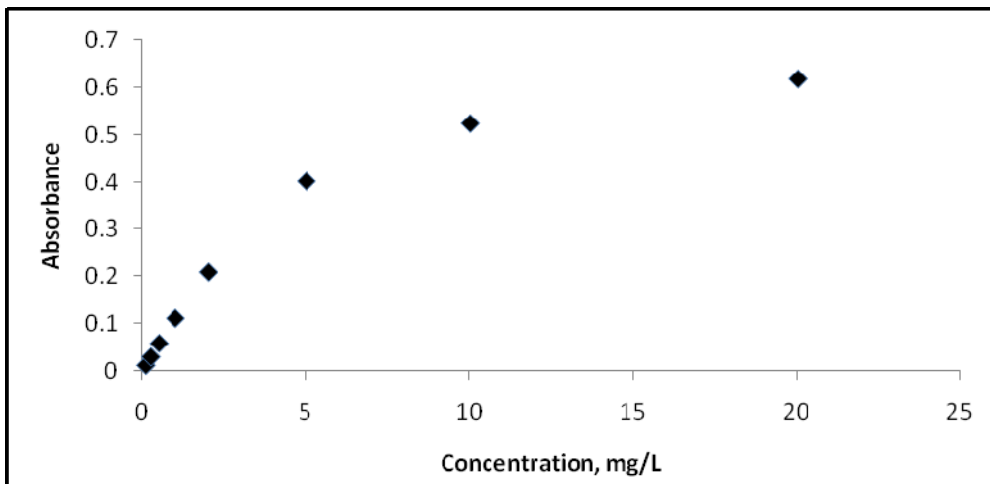


Figure 3.11 Calibration plot for 120° angled SQT-FAAS method

Fuel flow rate: 1.5 L/min, Flow rate of air: 3.5 L/min,

Sample suction rate: 8.3 mL/min, Height of SQT from the burner head: 1.0 mm

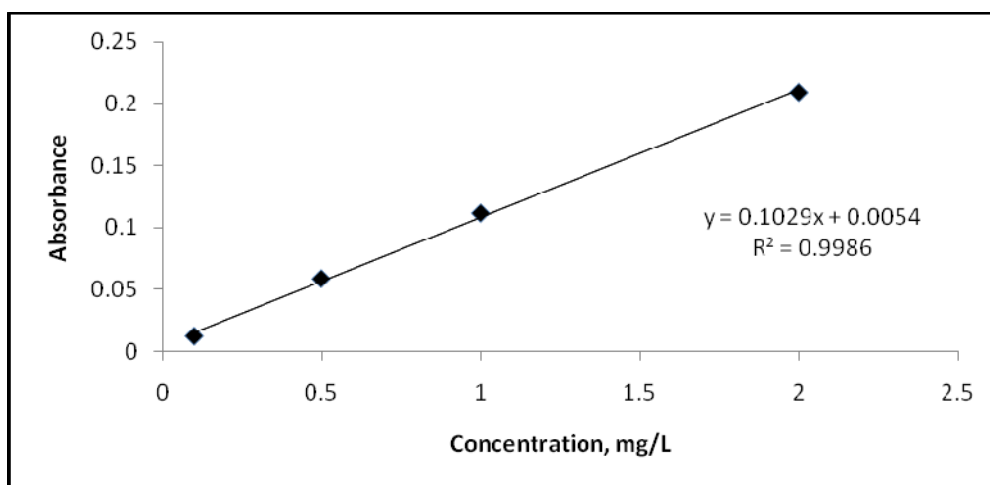


Figure 3.12 Linear calibration plot for 120° angled SQT-FAAS method

Fuel flow rate: 1.5 L/min, Flow rate of air: 3.5 L/min,

Sample suction rate: 8.3 mL/min, Height of SQT from the burner head: 1.0 mm

For calibration plot obtained from 180° angled SQT, Pb solutions between 0.1-20.0 mg/L solutions were used (Figure 3.13), calibration plot is linear between 0.1-2.0 mg/L. The best line equation and correlation coefficient were, $y = 0.1019x + 0.0067$ and 0.9981, respectively (Figure 3.14).

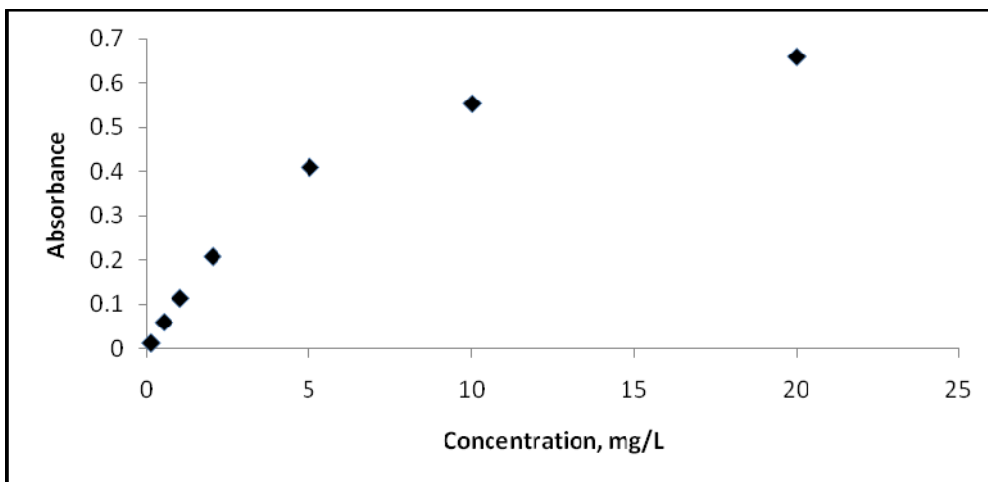


Figure 3.13 Calibration plot for 180° angled SQT-FAAS method

Fuel flow rate: 1.5 L/min, Flow rate of air: 3.5 L/min,

Sample suction rate: 8.1 mL/min, Height of SQT from the burner head: 1.0 mm

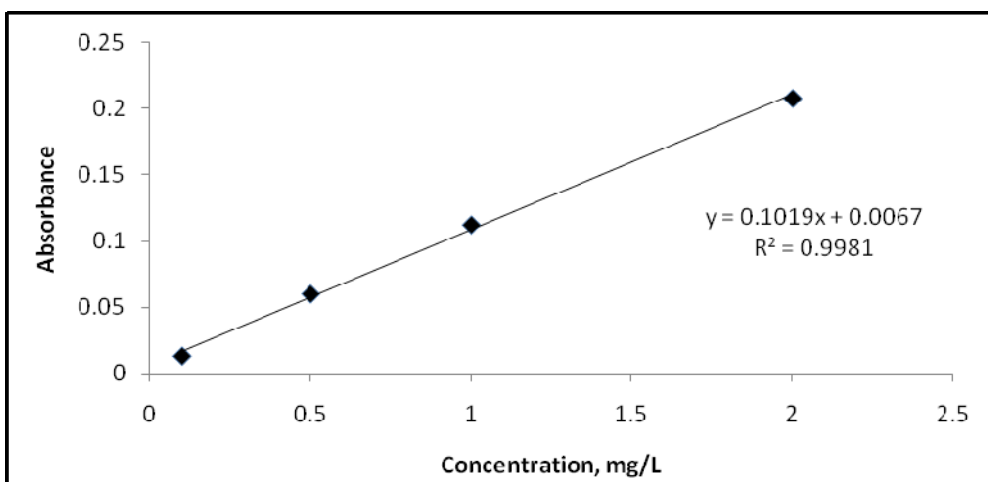


Figure 3.14 Linear calibration plot for 180° angled SQT-FAAS method

Fuel flow rate: 1.5 L/min, Flow rate of air: 3.5 L/min,

Sample suction rate: 8.1 mL/min, Height of SQT from the burner head: 1.0 mm

For 120° angled SQT, as seen from Table 3.2 LOD and LOQ were calculated as 8.2 ng/mL and 28 ng/mL respectively. Characteristic concentration was estimated as 40 ng/mL. On the other hand, for 180° angled SQT, as seen from Table 3.2 LOD and LOQ

were calculated as 9.4 ng/mL and 31 ng/mL respectively. Characteristic concentration was estimated as 40 ng/mL. Enhancement factor obtained with respect to FAAS was 3 for both SQT configurations. For LOD and LOQ determination 11 measurements of 0.1 mg/L solution were taken. There is not a significant difference between the performances of the two tubes with 120° and 180° slot configurations.

Table 3.2 Analytical Performance of 120° and 180° Angled SQT-FAAS

	120° Angled SQT	180° Angled SQT
Limit of Detection (LOD), ng/mL	8.2	9.4
Limit of Quantitation (LOQ), ng/mL	28	31
Characteristic Concentration (C₀), ng/mL	40	40
Enhancement (E) (with respect to FAAS)	3	3

3.3 Optimizations of Slotted Quartz Tube Atom Trap Flame AAS Method (SQT-AT-FAAS) Conditions for Determination of Lead

In this part SQT was used as an atom trap device, it was placed on the burner head as in the previous study (SQT-FAAS). By using a lean flame, lead solution was aspirated for a certain time into the flame. Analyte atoms were collected on the inner surface of SQT. After collection, by aspiration of a low amount of organic solvent, atoms were released from the surface and a transient signal was obtained.

Effect of trapping efficiency of both 120° and 180° angled SQTs were investigated. Important optimization parameters such as flame conditions, suction rate of sample, height of the SQT from burner head were optimized. Also a proper organic solvent and volume of organic solvent and trapping period were selected.

3.3.1 Effect of Organic Solvent

Revolatilization of trapped atoms by organic solvent aspiration was preferred in this study. For rapid revolatilization of analyte atoms, a highly flammable organic solvent is needed. In order to find the optimum revolatilization conditions, several types of organic solvents were used, such as methyl isobutyl ketone (MIBK), methyl ethyl ketone (MEK), acetonitrile, isopropyl alcohol, methyl alcohol, ethyl alcohol, cyclopentanol and N-butanol. Performance of each solvent was shown in Table 3.3. Lead signals obtained by using MIBK and MEK are nearly the same, but the signal obtained by MEK was not stable. Isopropyl alcohol, methyl alcohol, ethyl alcohol, cyclopentanol and N-butanol did not change the flame composition and no result was obtained after introduction of these solvents.

Table 3.3 Effect of Organic Solvents on Pb Signals for SQT-AT-FAAS Method

Type of organic solvent	Absorbance* (120° angled SQT)	Absorbance** (180° angled SQT)
→ MIBK	0.200	0.185
MEK	0.191	0.136
Acetonitrile	0.07	0.07
Isopropyl alcohol	No signal	No signal
Methanol	No signal	No signal
Ethanol	No signal	No signal
Cyclopentanol	No signal	No signal
N-butanol	No signal	No signal

*Concentration of Pb: 5.0 ng/mL, Fuel flow rate: 0.5 L/min, Flow rate of air: 3.5 L/min,
Sample suction rate: 8.1 mL/min, Height of SQT from burner head: 1.0 mm,
Volume of organic solvent: 40 µL, Trapping period: 5.0 min

** Concentration of Pb: 5.0 ng/mL, Fuel flow rate: 0.5 L/min, Flow rate of air: 3.5 L/min,
Sample suction rate: 7.4 mL/min, Height of SQT from burner head: 1.0 mm,
Volume of organic solvent: 40 µL, Trapping period: 5.0 min

In Table 3.4 chemical formulas and flash points of organics used for revolatilization step of Pb are given. It could be expected that the performance of organics with low flash points would be high. However, as seen in Table 3.3 this factor was not found to be important. It could be related with carbon order structure of the molecule.

Table 3.4 Molecular Formulas and Flash Points of Organics used for Revolatilization Step of Pb

Type of Organic solvent	Molecular Formula	Flash Point [44]
MEK	C ₄ H ₈ O	-9°C
Acetonitrile	C ₂ H ₃ N	2°C
Methanol	CH ₄ O	11°C
Isopropyl alcohol	C ₃ H ₈ O	12°C
Ethanol	C ₂ H ₆ O	13°C
MIBK	C ₆ H ₁₂ O	14°C
N-butanol	C ₄ H ₁₀ O	37°C
Cyclopentanol	C ₅ H ₁₀ O	93°C

3.3.2 Optimization of Volume of Organic Solvent

After choosing of proper organic solvent for revolatilization, volume of organic solvent was selected. Small volume of organic (10-50 μ L) is sufficient to revolatilize the trapped atoms; signals from different amounts of MIBK were obtained. It was concluded that 40 μ L gave complete revolatilization of 5.0 ng/mL Pb solution (Figure 3.15, Figure 3.16). Higher amount of organic did not have a significant effect on the signal of lead. In addition, higher volume of organic solvent can damage the windows of instrument; because, after introduction of organic solvent, flame formed momentarily may extend outside through the ends of SQT and approaches to the windows on both sides. Therefore, 40 μ L of MIBK was used for the whole study.

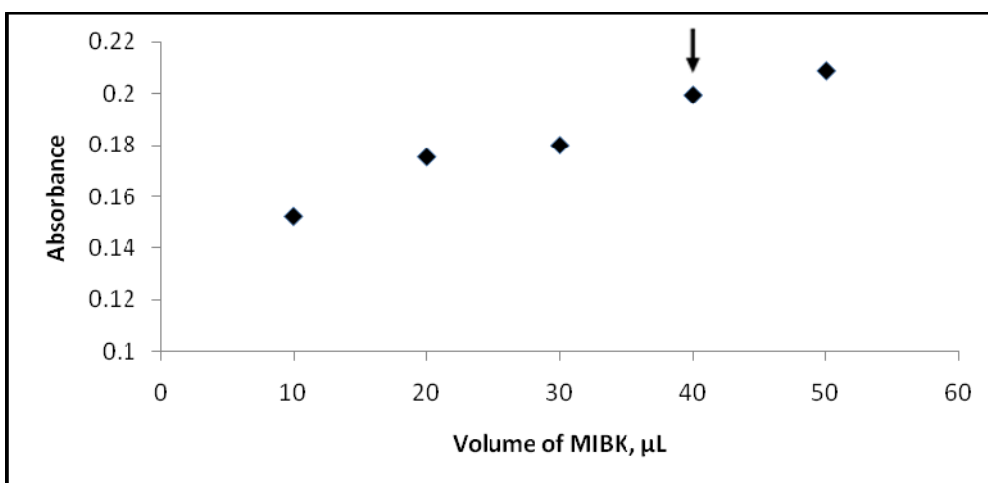


Figure 3.15 Optimization of volume of organic solvent using 5.0 ng/mL Pb in 120° angled SQT-AT-FAAS

Fuel flow rate: 0.5 L/min, Flow rate of air: 3.5 L/min,

Sample suction rate: 8.1 mL/min, Height of SQT from burner head: 1.0 mm,

Organic solvent: MIBK, Trapping period: 5.0 min

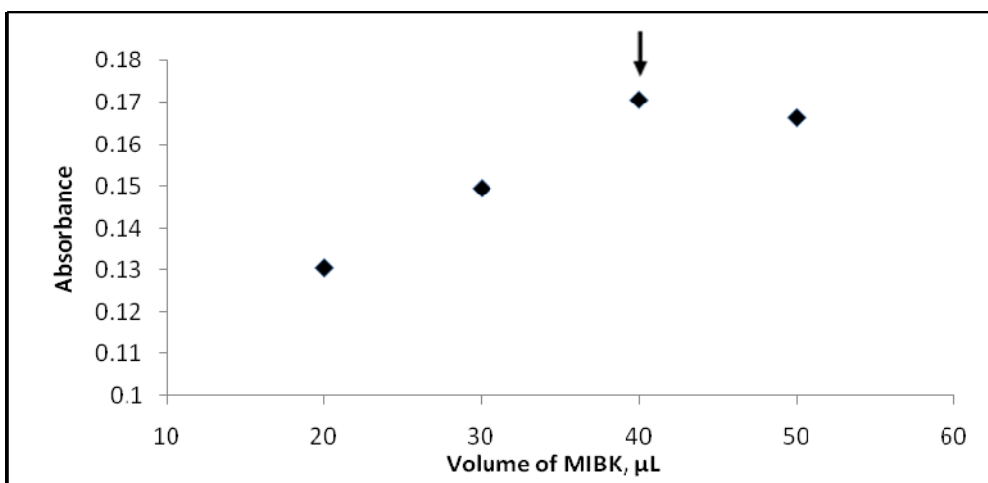


Figure 3.16 Optimization of volume of organic solvent using 5.0 ng/mL Pb in 180° angled SQT-AT-FAAS

Acetylene flow rate: 0.5 L/min, Flow rate of air: 3.5 L/min,

Sample suction rate: 7.4 mL/min, Height of SQT from burner head: 1.0 mm,

Organic solvent: MIBK, Trapping period: 5.0 min

3.3.3 Optimization of Sample Suction Rate

Suction rate of the sample is one of the crucial parameter to be optimized. It is important for two reasons;

- Suction rate affects the nebulization efficiency, the amount of analyte collected for unit time is directly related with the nebulization efficiency. At low suction rates, amount of analyte species aspirated into the flame decreases but nebulization efficiency increases. Higher nebulization efficiency means higher trapping efficiency.
- Since same nebulizer is used also for the organic solvent aspiration, same suction rate is used during the collection and the atomization. So, suction rate affects also the flame conditions during the atomization.

For optimizing the sample suction rate, 5.0 ng/mL, 30 mL of Pb solutions were used. It is clear from Figure 3.17 and Figure 3.18 at lower sample flow rates, Pb signal is high. But for the rest of the optimizations high flow rates were used. Because at lower rates, volume of trapping analyte is low in a limited time, so signal is also low. But calibration curves were obtained at low and high sample suction rates and compared.

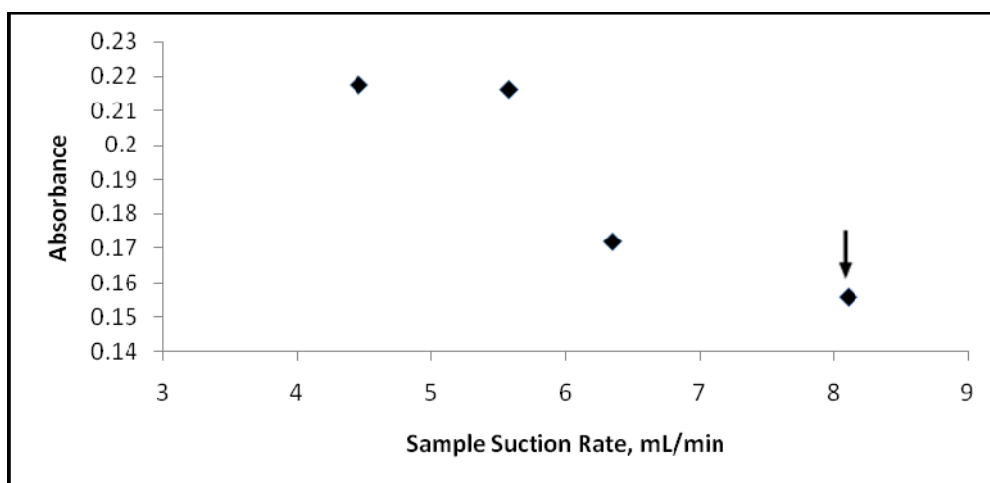


Figure 3.17 Optimization of suction rate of 5.0 ng/mL 30.0 mL analyte solution in 120° angled SQT-AT-FAAS

Fuel flow rate: 0.5 L/min, Flow rate of air: 3.5 L/min,

Height of SQT from burner head: 1.0 mm,

Volume of organic solvent: 40 μ L, Organic solvent: MIBK

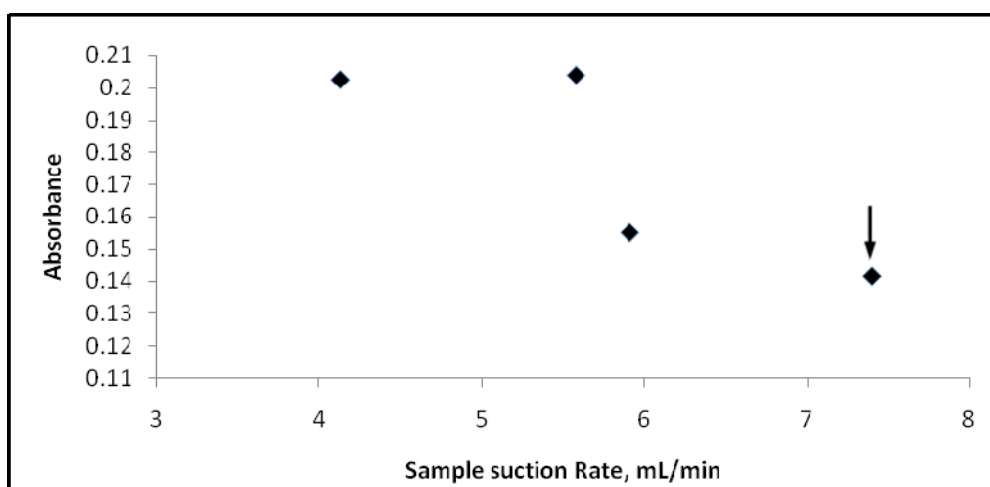


Figure 3.18 Optimization of suction rate of 5.0 ng/mL 30.0 mL analyte solution in 180° angled SQT-AT-FAAS

Fuel flow rate: 0.5 L/min, Flow rate of air: 3.5 L/min,

Height of SQT from burner head: 1.0 mm,

Volume of organic solvent: 40 μ L, Organic solvent: MIBK

3.3.4 Optimization of Fuel Flow Rate

Flow rate of acetylene is another important parameter to be optimized. At stoichiometric or fuel rich flame, analyte species are atomized and removed out of measurement zone instead of trapping. Therefore, a lean, fuel low flame should be used to trap the analyte species on the inner surface of SQT. Acetylene flow rate was optimized as 0.5 L/min (Figure 3.19, Figure 3.20).

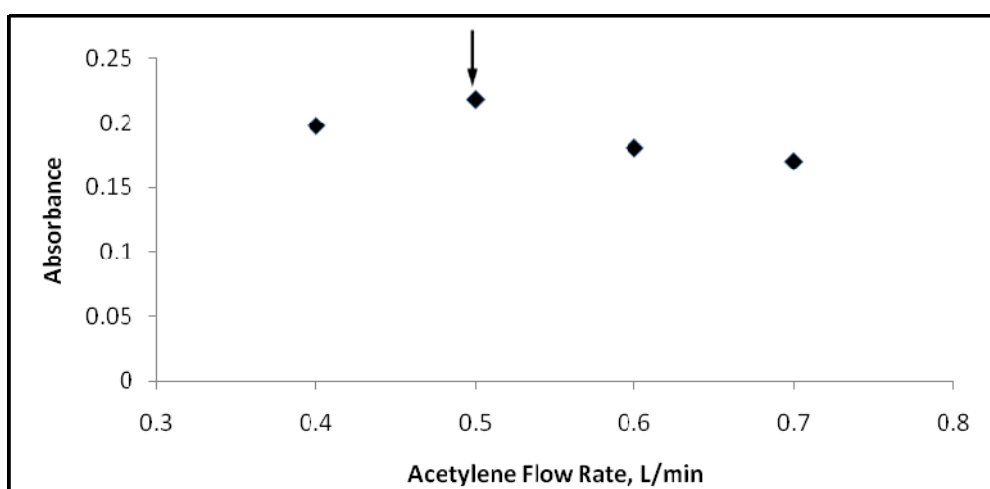


Figure 3.19 Optimization of flow rate of acetylene using 5.0 ng/L Pb in 120° angled SQT-AT-FAAS

Flow rate of air: 3.5 L/min, Sample flow rate: 8.1 mL/min

Height of SQT from burner head: 1.0 mm, Organic solvent: MIBK,

Volume of organic solvent: 40 μ L, Trapping period: 5.0 min

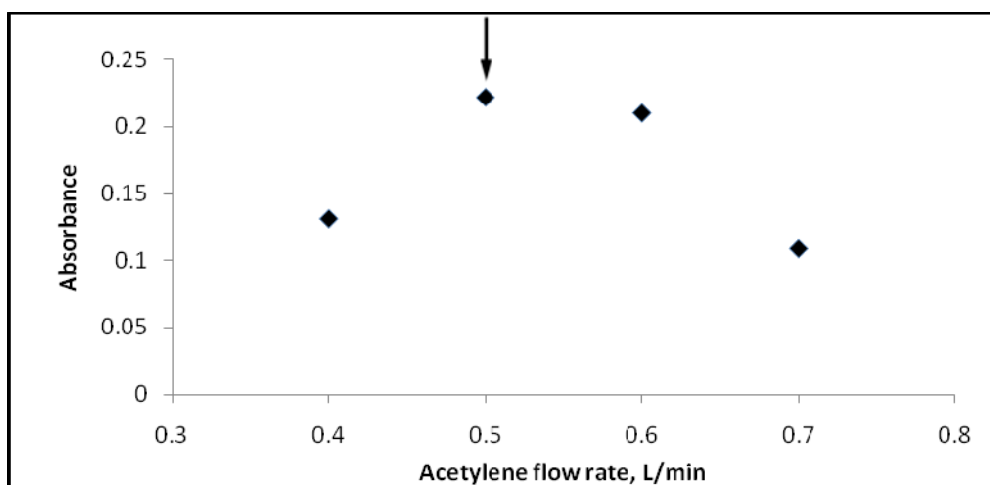


Figure 3.20 Optimization of flow rate of acetylene using 5.0 ng/L Pb in 180° angled SQT-AT-FAAS

Flow rate of air: 3.5 L/min, Sample flow rate: 7.4 mL/min

Height of SQT from burner head: 1.0 mm, Organic solvent: MIBK,

Volume of organic solvent: 40 μ L, Trapping period: 5.0 min

3.3.5 Optimization of Height of the SQT from the Burner Head

In the previous study (SQT-FAAS) rise in the height causes the signal to be lower; because Pb atoms can not be efficiently transported into SQT. This is also valid in SQT-AT-FAAS. As seen in Figure 3.21 and Figure 3.22 the optimum height is 1.0 mm.

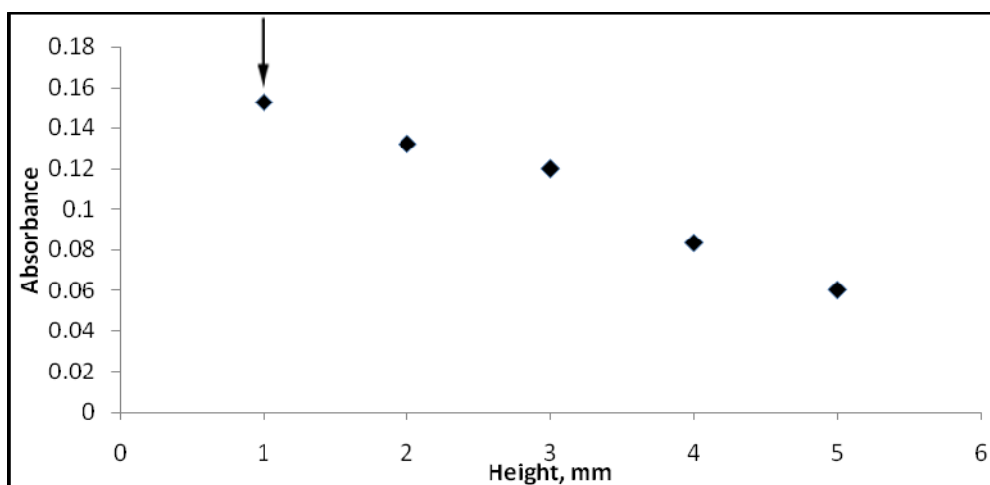


Figure 3.21 Optimization of height of SQT from the burner using 5.0 ng/L Pb in 120° angled SQT-AT-FAAS

Fuel flow rate: 0.5 L/min, Flow rate of air: 3.5 L/min,

Sample flow rate: 3.9 mL/min, Volume of organic solvent: 40 μ L,

Organic solvent: MIBK, Trapping period: 5.0 min

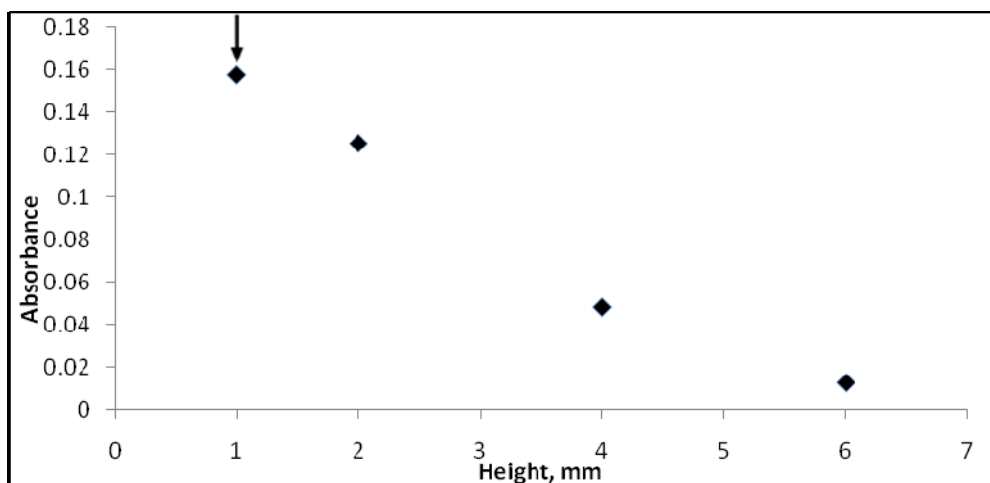


Figure 3.22 Optimization of height of SQT from the burner using 5.0 ng/mL Pb in 180° angled SQT-AT-FAAS

Fuel flow rate: 0.5 L/min, Flow rate of air: 3.5 L/min,

Sample flow rate: 7.4 mL/min, Trapping period: 5.0 min

Volume of organic solvent: 40 μ L, Organic solvent: MIBK

3.3.6 Investigation of Trapping Period

Sensitivity is improved if analyte atoms are trapped for a longer period of time (Figure 3.23 and Figure 3.24). However; this procedure is competing with ETAAS; therefore time required for analysis should be only a few minutes. Results of collection for 1- 7 min were obtained, and then collection period was selected as 5 min.

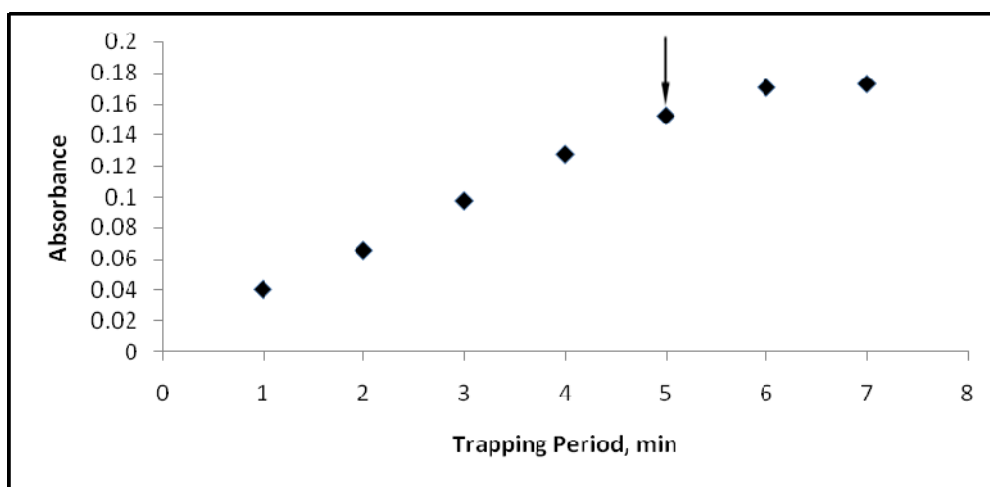


Figure 3.23 Effect of trapping period using 5.0 ng/mL Pb in 120°angled SQT-AT-FAAS

Acetylene flow rate: 0.5 L/min, Flow rate of air: 3.5 L/min,

Sample flow rate: 8.1 mL/min, Height of SQT from burner head: 1.0 mm,

Volume of organic solvent: 40 μ L, Organic solvent: MIBK

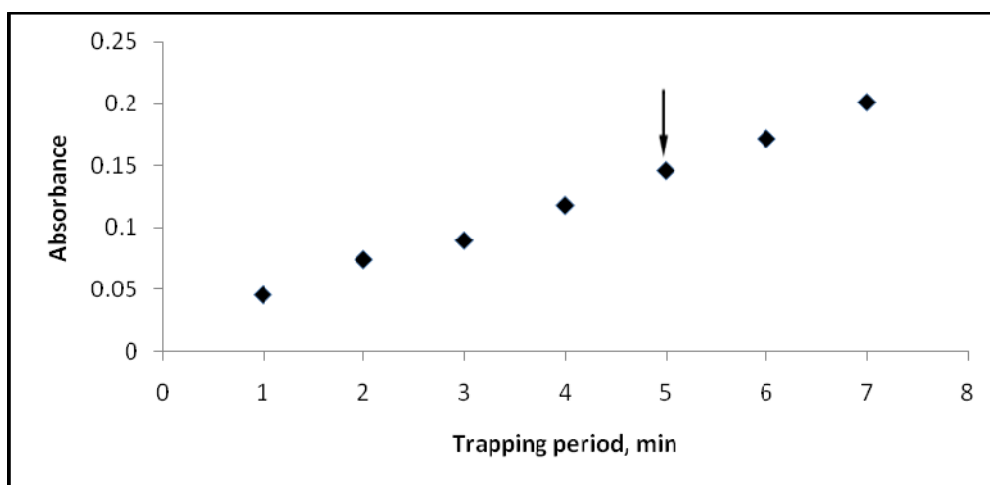


Figure 3.24 Effect of trapping period using 5.0 ng/mL Pb in 180°angled SQT-AT-FAAS

Acetylene flow rate: 0.5 L/min, Flow rate of air: 3.5 L/min,

Sample flow rate: 7.4 mL/min, Height of SQT from burner head: 1.0 mm,

Volume of organic solvent: 40 μ L, Organic solvent: MIBK

The signal for 5.0 ng/mL Pb solution obtained with 180° angled SQT is given in Figure 3.25; the optimized conditions given in Table 3.5 were used. The half bandwidth of this signal was found to be 0.23 s.

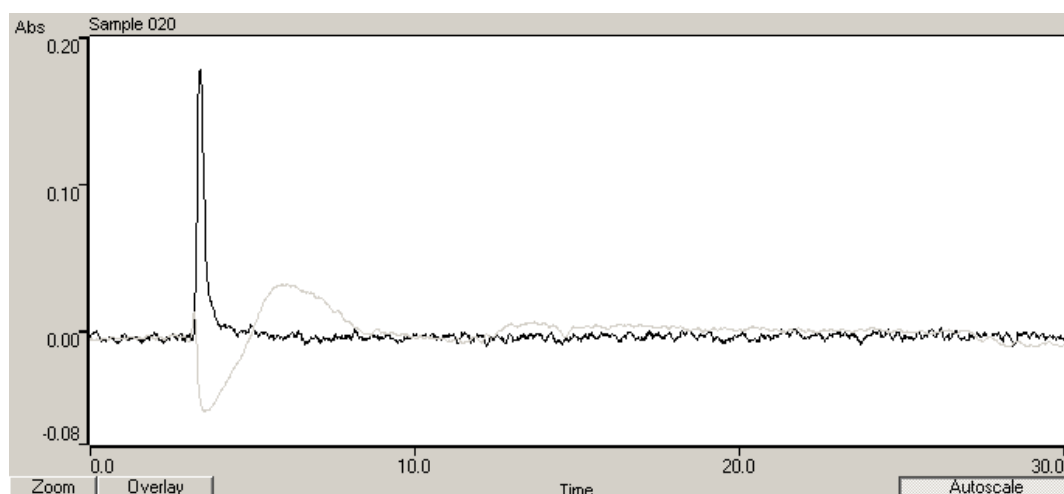


Figure 3.25 The signal of SQT-AT-FAAS for 5.0 ng/mL Pb solution

Table 3.5 Conditions for SQT-AT-FAAS Method

Parameter	Condition (120° angled SQT)	Condition (180° angled SQT)
Type of Organic Solvent	MIBK	MIBK
Sample Suction Rate	8.1 mL/min	7.4 mL/min
Volume of Organic Solvent	40 µL	40 µL
Trapping Period	5.0 min	5.0 min
Height of The SQT from the Head of the Burner	1.0 mm	1.0 mm
Acetylene Flow Rate	0.5 L/min	0.5 L/min

3.3.7 Calibration Plots for SQT-AT-FAAS Method

Calibration plots at low sample flow rate and high flow rate were obtained at this section. For the calibration plot of 120° angled SQT, at a flow rate of 8.1 mL/min, Pb solutions between 0.5-20.0 ng/mL solutions were used (Figure 3.26). Calibration plot is linear between 0.5-5.0 ng/mL. The best line equation and correlation coefficient were, $y = 0.0368x + 0.0084$ and 0.998, respectively (Figure 3.27). Conditions in Table 3.4 were used.

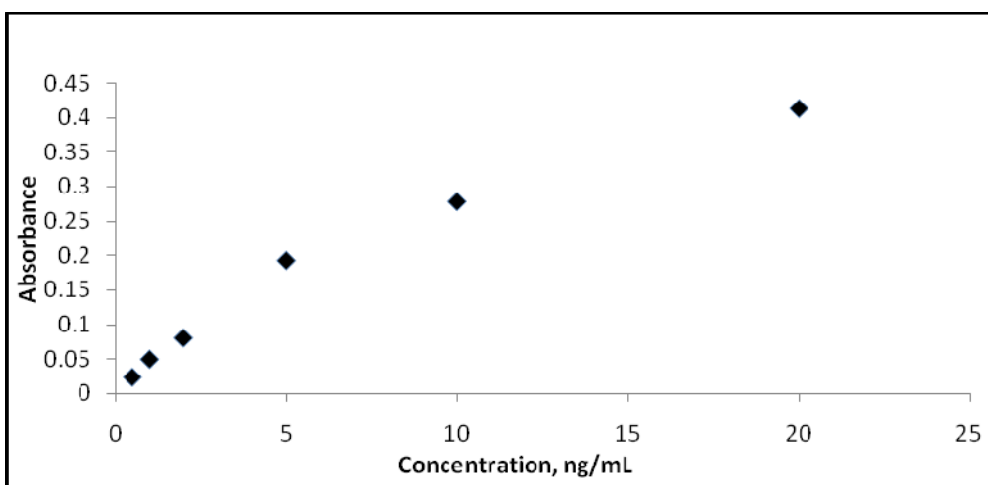


Figure 3.26 Calibration plot for SQT-AT-FAAS 120° angled SQT-AT-FAAS method at 8.1 mL/min flow rate and using the conditions in Table 3.5

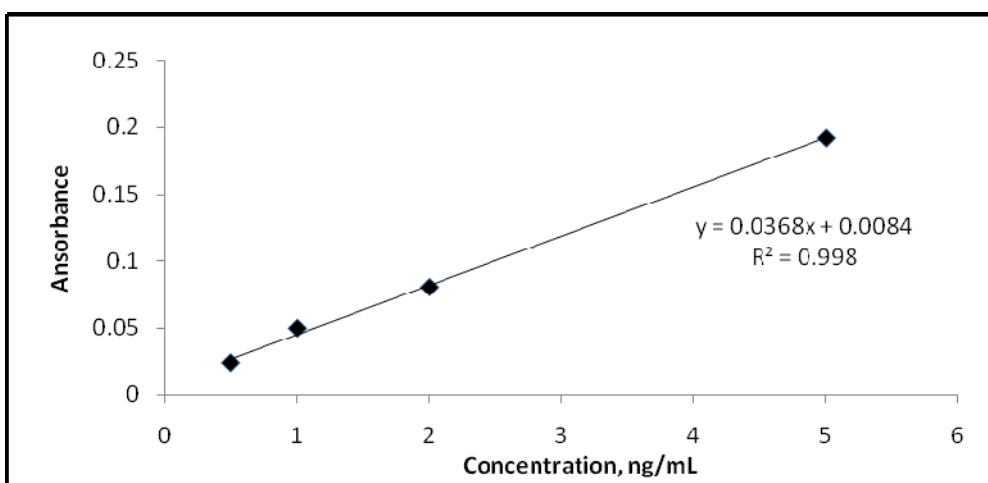


Figure 3.27 Linear calibration plot for 120° angled SQT-AT-FAAS method at 8.1 mL/min flow rate and using the conditions in Table 3.5

Before obtaining a calibration curve at the sample flow rate of 3.9 mL/min, the signal of 5.0 ng/mL Pb was examined if the signal is stable, % RSD was found as 2.20 (N=7). Then signal of Pb solutions between 2.0-50.0 ng/mL were obtained in order to form a calibration curve (Figure 3.28). Calibration plot is linear between 2.0-15.0 ng/mL. The best line equation and correlation coefficient were, $y = 0.0117x + 0.0098$ and 0.9994,

respectively (Figure 3.29). Conditions in Table 3.4, except sample suction rate, were used.

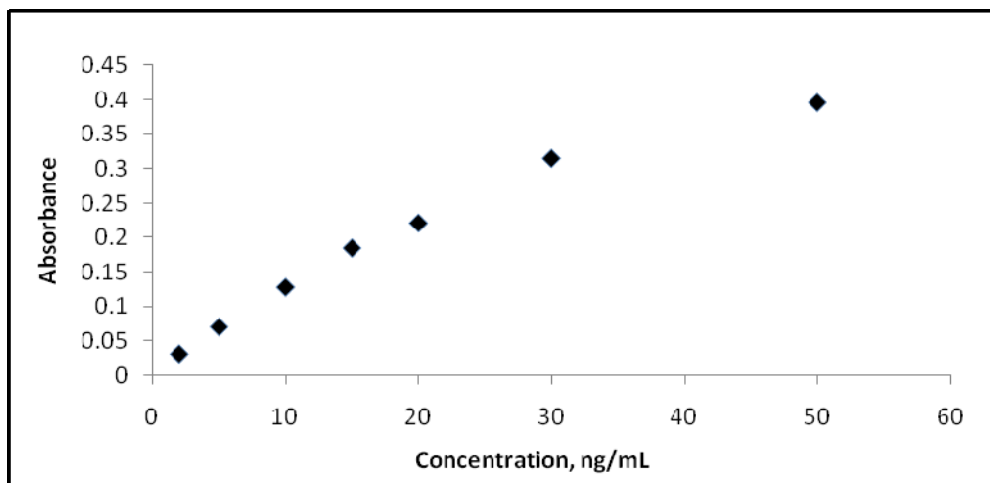


Figure 3.28 Calibration plot for SQT-AT-FAAS 120° angled SQT-AT-FAAS method at 3.9 mL/min flow rate and using the other conditions in Table 3.5

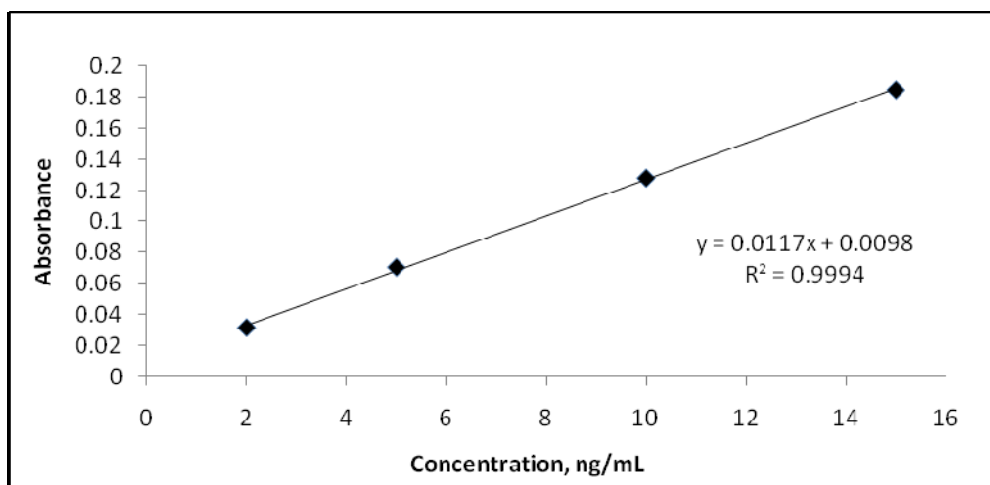


Figure 3.29 Linear calibration plot for 120° angled SQT-AT-FAAS method at 3.9 mL/min flow rate and using the other conditions in Table 3.5

Figure 3.30 simply illustrates the difference between the sensitivities of 120° angled SQT-AT-FAAS at two different sample flow rates, and also the importance of sample

flow rate. As seen from the ratio of calibration sensitivities 3.15 times sensitivity enhancement was achieved at high sample flow rate (8.1 mL/min). Volume of analyte solution is 19.5 mL at 3.9 mL/min and 40.5 mL at 8.1 mL/min sample flow rate.

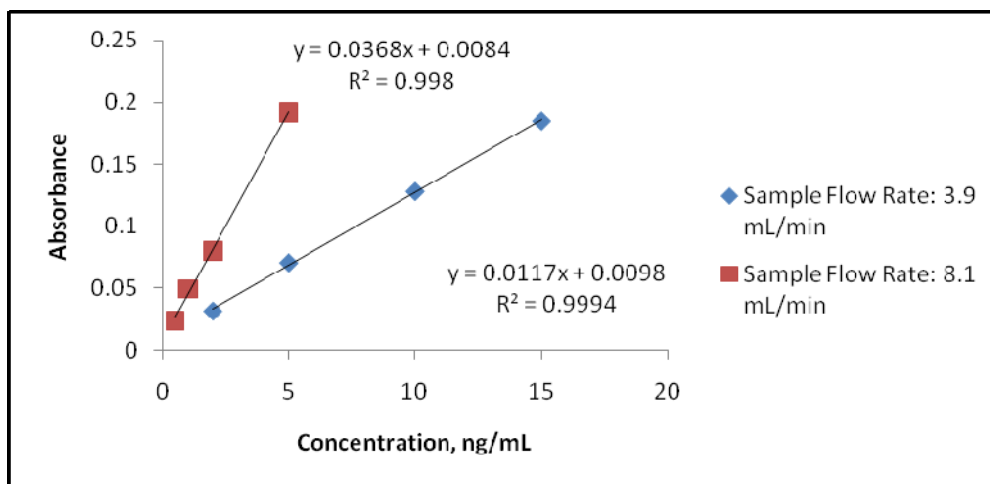


Figure 3.30 Linear calibration plot for 120° angled SQT-AT-FAAS method at different sample suction rates and using the other conditions in Table 3.5

For calibration plot of 180° angled SQT, at a flow rate of 7.4 mL/min, Pb solutions between 0.5-20.0 ng/mL solutions were used (Figure 3.31). Calibration plot is linear between 0.5-5.0 ng/mL. The best line equation and correlation coefficient were, $y = 0.0359x + 0.0216$ and 0.9989, respectively (Figure 3.32). Conditions in Table 3.5 were used.

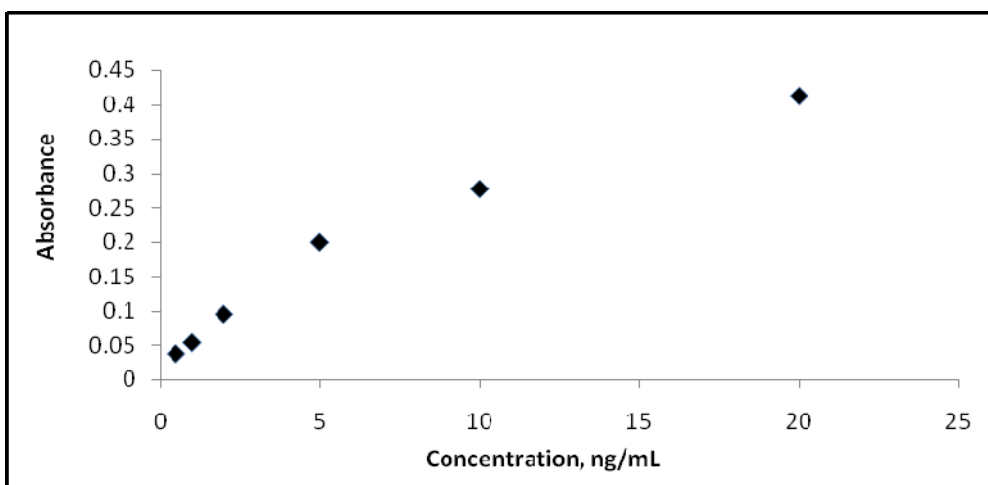


Figure 3.31 Calibration plot for SQT-AT-FAAS 180° angled SQT-AT-FAAS method at 7.4 mL/min flow rate and using the conditions in Table 3.5

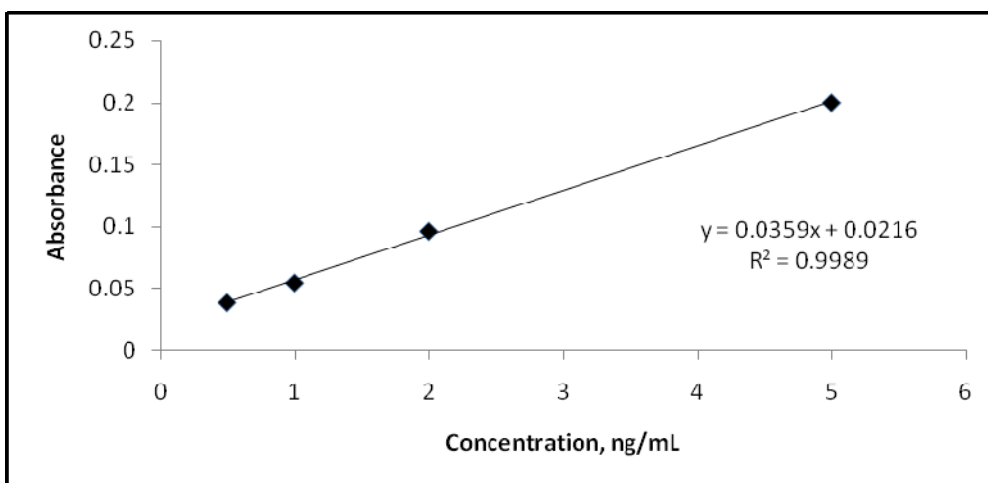


Figure 3.32 Linear calibration plot for 180° angled SQT-AT-FAAS method at 7.4 mL/min flow rate and using the conditions in Table 3.5

Before obtain a calibration curve at sample flow rate of 3.9 mL/min, the signal of 5.0 ng/mL Pb was examined, as previous, if the signal is stable, % RSD was found as 2.44 (N=7). Then signal of Pb solutions between 1.0-30.0 ng/mL were obtained in order to form a calibration curve (Figure 3.33). Calibration plot is linear between 1.0-8.0 ng/mL. The best line equation and correlation coefficient were, $y = 0.0164x + 0.0094$ and

0.9991, respectively (Figure 3.34). Conditions in Table 3.4, except sample suction rate, were used.

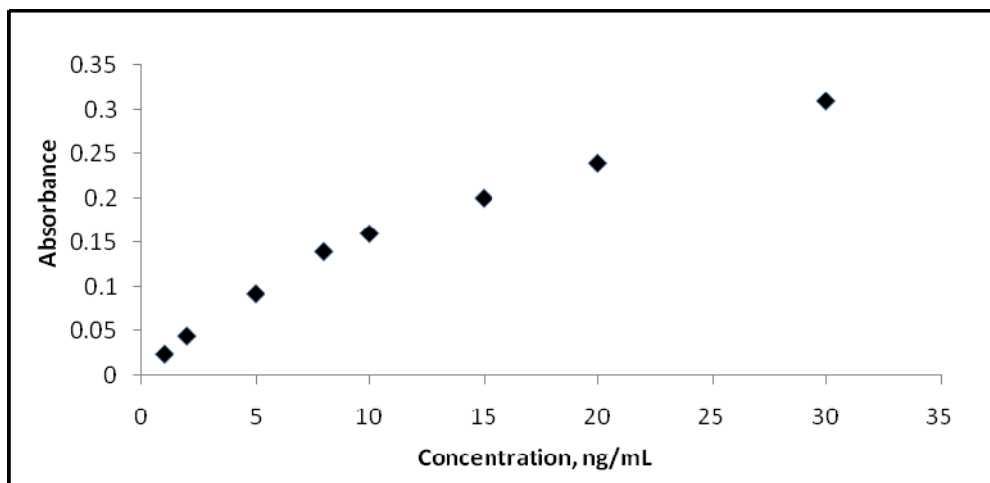


Figure 3.33 Calibration plot for SQT-AT-FAAS 180° angled SQT-AT-FAAS method at 3.9 mL/min flow rate and using the other conditions in Table 3.5

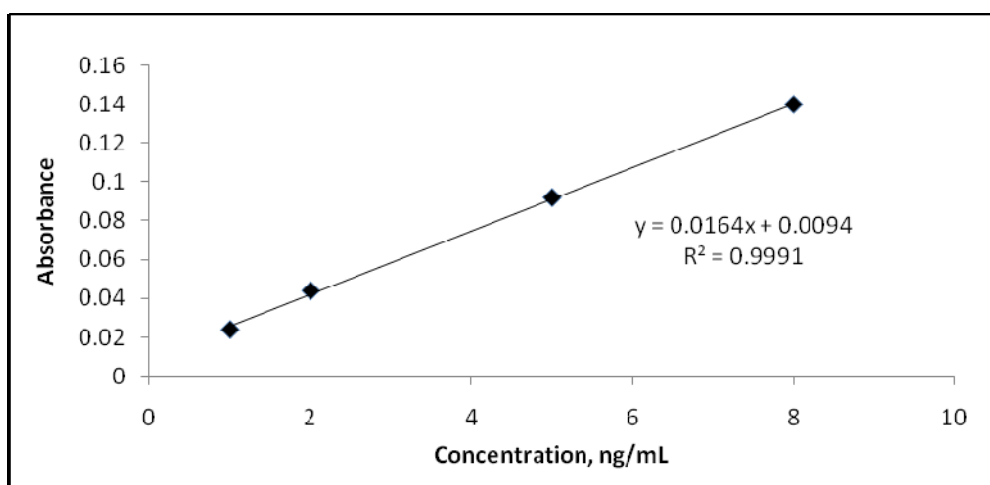


Figure 3.34 Linear calibration plot for 180° angled SQT-AT-FAAS method at 3.9 mL/min flow rate and using the other conditions in Table 3.5

Figure 3.35 simply illustrates the difference between the sensitivities of 180° angled SQT-AT-FAAS at two different sample flow rates, and also the importance of sample

flow rate. As seen from the ratio of calibration sensitivities, 3.12 times sensitivity enhancement was achieved at high sample flow rate (7.4 mL/min). Volume of analyte solution is 19.5 mL at 3.9 mL/min and 37.0 mL at 7.4 mL/min sample flow rate.

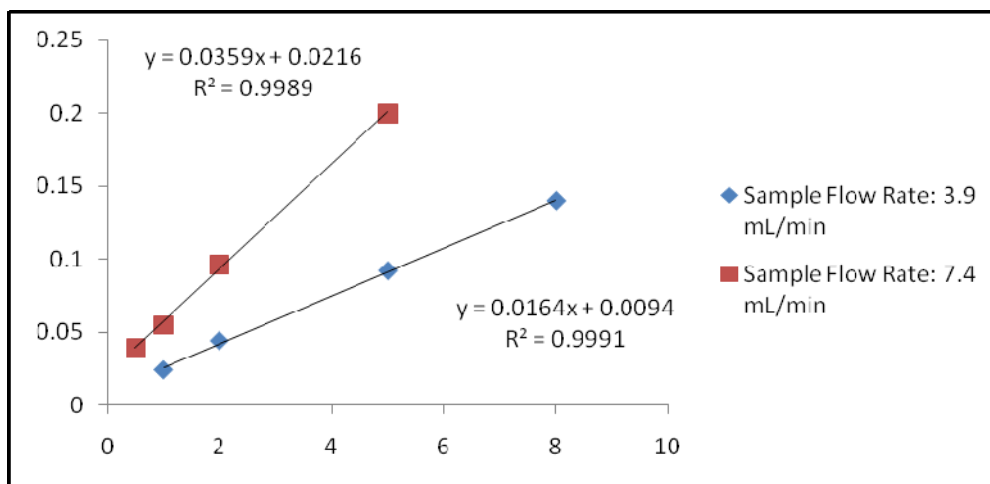


Figure 3.35 Linear calibration plot for 180° angled SQT-AT-FAAS method at different sample suction rates and using the other conditions in Table 3.5

In this study, 120° angled and 180° angled SQT were used, in Figure 3.36 linear calibration plots obtained by both type of tubes were given, it is understood from their calibration sensitivities there is not a significant difference from results of these tubes.

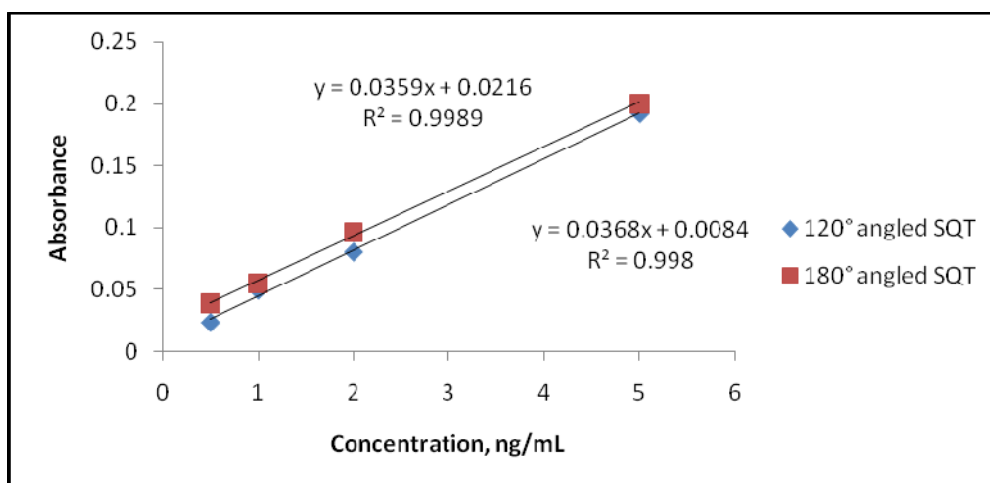


Figure 3.36 Linear calibration plot for SQT-AT-FAAS method with different types of tubes and using the conditions in Table 3.5

3.3.8 Analytical Figures of Merit of SQT-AT-FAAS

Limit of detection as 3s/m, limit of quantitation as 10s/m and characteristic concentration were calculated. For 120° angled SQT, at a sample flow rate of 8.1 mL/min, as seen from Table 3.6 LOD and LOQ were calculated as 0.11 ng/mL and 0.38 ng/mL respectively. Characteristic concentration was 0.11 ng/mL and characteristic mass is 4.50 ng/mL and 1200 fold sensitivity enhancements was obtained with respect to FAAS. On the other hand, at sample flow rate of 3.9, LOD and LOQ were calculated as 0.22 ng/mL and 0.73 ng/mL respectively. Characteristic concentration was 0.33 ng/mL and characteristic mass 6.44 ng/mL; 400 fold sensitivity enhancements in terms of characteristic concentration were obtained with respect to FAAS. With 180° angled SQT, at a sample flow rate of 7.4 mL/min as seen from Table 3.5 LOD and LOQ were calculated as 0.13 ng/mL and 0.43 ng/mL respectively. Characteristic concentration was estimated as 0.1 ng/mL and characteristic mass is 3.70 ng/mL and 1320 fold sensitivity enhancements was get with respect to FAAS. On the other hand, at sample flow rate of 3.9, LOD and LOQ were calculated as 0.26 ng/mL and 0.87 ng/mL respectively.

Characteristic concentration was 0.23 ng/mL and characteristic mass 4.49 ng/mL; 574 fold sensitivity enhancement in terms of characteristic concentration was obtained with respect to FAAS. For LOD and LOQ determination 7 measurements of 0.5 ng/mL solution were taken.

Table 3.6 Analytical Performance of Pb Using SQT-AT-FAAS, 5.0 min Collection

Type of Tube <i>Sample flow rate</i>	120° Angled SQT <i>(8.1 mL/min)</i>	120° Angled SQT <i>(3.9 mL/min)</i>	180° Angled SQT <i>(7.4 mL/min)</i>	180° Angled SQT <i>(3.9 mL/min)</i>
Limit of Detection (LOD), ng/mL	0.11	0.22	0.13	0.26
Limit of Quantitation (LOQ), ng/mL	0.38	0.73	0.43	0.87
Characteristic Concentration (C₀), ng/mL	0.11	0.33	0.10	0.23
Characteristic mass (m₀), ng	4.50	6.44	3.70	4.49
Enhancement (E) <i>(with respect to FAAS)</i>	1200	400	1320	574

3.3.9 Accuracy Check for SQT-AT-FAAS Method

The CRM, SCP SCIENCE, EnviroMAT-Waste Water, Low (EU-L-2), was used for the accuracy check of SQT-AT-FAAS method. The direct calibration was employed and three replicate measurements were done under optimum conditions. The results were in good agreement with the certified value as shown in the Table 3.7.

Table 3.7 The Result of the Accuracy Test for 180° Angled SQT-AT-FAAS Method

SCP SCIENCE, EnviroMAT	Certified Pb Result, ng/L	*Found Result, ng/mL	**Found Result, ng/mL
Waste Water EU-L-2	40.0-43.0	41.0 ± 1.1	40.2 ± 0.4

* Sample suction rate: 7.4 mL/min

**Sample suction rate: 3.9 mL/min

3.4 SQT-AT-FAAS Study with Different Inner and Outer Diameters Tubes

In addition to the tubes used for the rest of the study, also the efficiency of tube with smaller inner diameter and effect of the thickness were investigated.

Three basic types of tubes could be used for SQT studies [31]:

- i)* The tube with smaller internal diameter than that of the incident light beam,
- ii)* The tube has equal or nearly equal internal diameter of incident light beam,
- iii)* The tube with greater internal diameter than that of the incident light beam.

The most appropriate design is the one where incident light beam has a diameter equal or nearly equal to internal diameter of the tube. This design does not cause incident light

beam to touch the walls of the tube. In the case of first type of tube, there is obscuration of source light but since the area is small, the interaction of analyte atoms and the source will be high. In the case of third type, there is increasing flame turbulence inside the tube, in addition air easily enters into the flame at the ends of the tube, and then the signal will be noisy [31].

First, for investigation of the effect of internal diameter, signals for the tube that was used for the whole study, with inner diameter of 14 mm and outer diameter of 17 mm, and the thinner tube, with inner diameter of 10 mm and outer diameter of 13 mm, were compared. Both types of tubes are 180° angled, and 10.0 ng/mL Pb solution was used. As seen in Table 3.8, the signal obtained by smaller internal diameter SQT is higher than the usual one, but RSD is higher. The conventional tube and the tube with smaller inner and outer diameter have S/N values of 47.6 and 32.3, respectively.

Table 3.8 Effect of Diameter of SQT on 10.0 ng/mL Pb Signal for SQT-AT-FAAS Method

SQT	Absorbance	%RSD (N=3)	S/N (N=3)
Inner diameter: 14 mm Outer diameter: 17 mm	0.330	2.1	47.6
Inner diameter: 10 mm Outer diameter: 13 mm	0.360	3.1	32.3

Concentration of Pb solution: 10 ng/mL, Acetylene flow rate: 0.5 L/min,

Flow rate of air: 3.5 L/min, Sample flow rate: 7.4 mL/min, Organic solvent: MIBK,

Volume of organic solvent: 40 µL, Height of SQT from burner head: 1.0 mm,

Trapping period: 5.0 min

Then a study for the effect of wall thickness was performed. For this aim, three tubes with the same internal diameters (10 mm) and different outer diameters were used. Wall thickness and signal values obtained by using of 10.0 ng/mL were given in Table 3.9. The most intense peak was obtained with the SQT had wall thickness of 1.5 mm.

However; it can be seen from the data in Table 3.8, the SQT device with 0.5 mm wall thickness gave the best S/N value. It may be because of penetration of Pb into the pores of thin SQT easily; deeper penetration would render the process more difficult during reatomization.

Table 3.9 Effect of Wall Thickness on 10.0 ng/mL Pb Signal for SQT-AT-FAAS Method

Wall thickness of SQT	Absorbance	%RSD (N=3)	S/N (N=3)
0.5 mm	0.344	1.9	52.6
1.5 mm	0.360	3.1	32.3
2.0 mm	0.329	5.95	16.8

Concentration of Pb solution: 10 ng/mL, Acetylene flow rate: 0.5 L/min,
 Flow rate of air: 3.5 L/min, Sample flow rate: 7.4 mL/min, Organic solvent: MIBK,
 Volume of organic solvent: 40 μ L, Height of SQT from burner head: 1.0 mm,
 Trapping period: 5.0 min

3.5 Optimizations of Coated Slotted Quartz Tube Atom Trap Flame AAS (Coated-SQT-AT-FAAS) and Conditions for Determination of Lead

The aim of this step is modification of the inner surface of the SQT to obtain a better surface than quartz and obtain better detection limit. As well as the efficient trapping of the analyte on the new surface, successful releasing is also important. After finding the best coating material, all parameters were optimized because of the difference behavior of surface coating element. Optimizations were done by 5.0 ng/mL and 2.5 ng/mL Pb standard solutions as indicated.

3.5.1 Investigation of Coating Material on SQT-AT-FAAS Method

The most important point here is that the melting point of the coating material should be higher than the analyte element. Coating material should not be significantly lost from the surface when element volatilizes from the SQT. Effect of Ta, Zr, Ir, W, Mo, Os and Pd were investigated. Coating procedure was described in the section 2.4.

As seen in the Table 3.10, use of Pd coated and Os coated SQT devices gave the smallest signal with high RSD. Signals of Ir, W and Mo are nearly the same. Results of uncoated and Ta-coated-SQT-AT-FAAS seem to be close to each other; but these results were obtained by using optimized conditions of SQT-AT-FAAS method without optimizing the parameters of Ta-coated-SQT-AT-FAAS. In addition, concentration of Pb was kept relatively high to observe the differences between different coating materials. The best signal was obtained using Ta among the coating elements. The melting point of Ta, 3017°C, is higher than the boiling point of Pb, 1755°C. Therefore, it is unlikely for Ta to melt or boil during the atomization process of trapped lead.

Table 3.10 Effect of Coating Material on 10.0 ng/mL Pb Signal for SQT-AT-FAAS Method

	Absorbance	%RSD (N=3)
None	0.359	2.4
→ Ta	0.368	1.1
Zr	0.178	1.1
Ir	0.140	6.7
W	0.136	4.5
Mo	0.130	1.4

Table 3.10 (continued)

Os	0.093	5.7
Pd	0.026	8.7

Acetylene flow rate: 0.5 L/min, Flow rate of air: 3.5 L/min, Concentration of Pb solution: 10.0 ng/mL, Sample flow rate: 7.4 mL/min, Height of SQT from burner head: 1.0 mm, Volume of organic solvent: 40 μ L, Organic solvent: MIBK, Trapping period: 5.0 min

3.5.2 Effect of Organic Solvent

For this step, again effect of organic solvents, available in laboratory, was investigated and MIBK was the best organic solvent for complete revolatilization (Table 3.11).

Table 3.11 Effect of Organic Solvents on 5.0 ng/mL Pb Signal for Ta coated-SQT-AT-FAAS Method

Type of organic solvent	Absorbance
→ MIBK	0.244
MEK	0.214
Acetonitrile	0.139
Isopropyl alcohol	No signal
Methanol	No signal
Ethanol	No signal
Cyclopentanol	No signal
N-butanol	No signal

Acetylene flow rate: 0.5 L/min, Flow rate of air: 3.5 L/min, Sample flow rate: 7.4 mL/min, Height of SQT from burner head: 1.0 mm, Volume of organic solvent: 40 μ L, Trapping period: 5.0 min

3.5.3 Optimization of Volume of Organic Solvent

As seen in the Figure 3.37, 40 μL of MIBK was sufficient for the complete revolatilization step. After 40 μL , signal of Pb was constant.

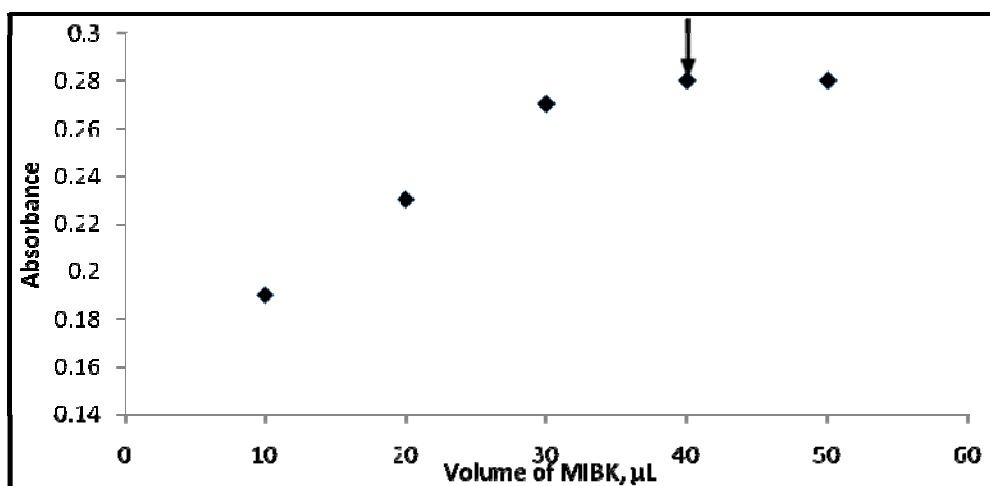


Figure 3.37 Optimization of amount of organic solvent using 5.0 ng/mL Pb in Ta Coated-SQT-AT-FAAS

Acetylene flow rate: 0.5 L/min, Flow rate of air: 3.5 L/min,

Sample flow rate: 7.4 mL/min, Height of SQT from burner head: 1.0 mm,

Organic solvent: MIBK, Trapping period: 5.0 min

3.5.4 Optimization of Sample Suction Rate

Sample suction rate was investigated between 3.4 mL/min and 8.4 mL/min (Figure 3.38). To observe the effect of Pb signal, 30 mL of 2.5 ng/mL Pb solution was used. Again at lower sample flow rates trapping efficiency is high because of increasing nebulization efficiency.

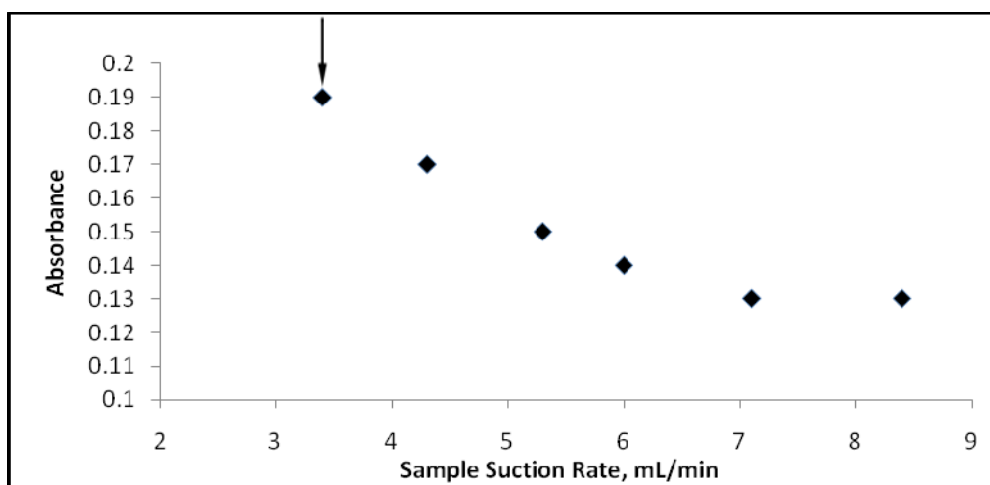


Figure 3.38 Optimization of sample suction rate using 30 mL of 2.5 ng/mL Pb in Ta Coated-SQT-AT-FAAS

Acetylene flow rate: 0.5 L/min, Flow rate of air: 3.5 L/min,

Height of SQT from burner head: 1.0 mm, Organic solvent: MIBK,

Volume of organic solvent: 40 μ L

3.5.5 Optimization of Fuel Flow Rate

As seen in the Figure 3.39, leanest possible flame gives the best result for collection step. Therefore, 0.5 L/min was chosen as the optimum acetylene flow rate for the technique. Flame at acetylene flow rate of 0.4 L/min was not stable for the values lower than 0.4 L/min, the flame was extinguished, at 0.6 L/min trapping efficiency is very low, and at higher rates there is no trapping, analyte species are not collected in SQT.

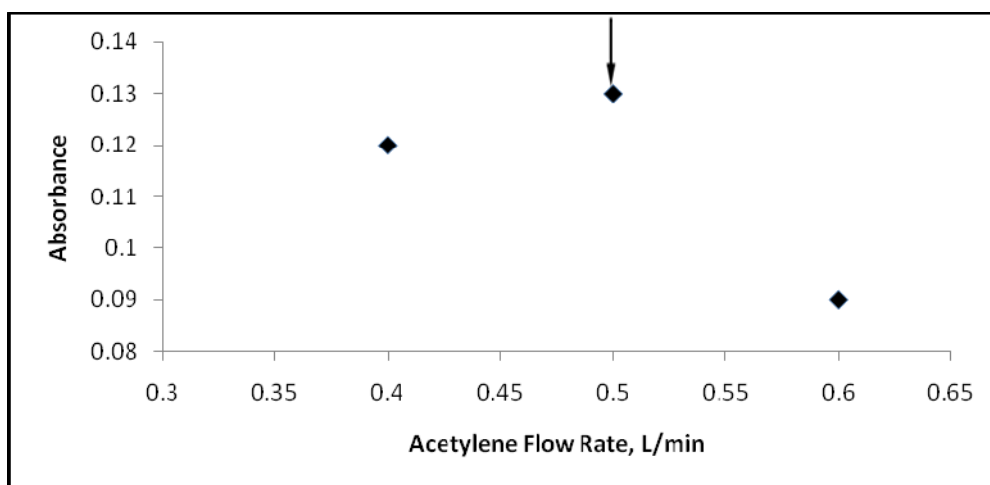


Figure 3.39 Optimization of acetylene flow rate using 2.5 ng/mL Pb in Ta Coated-SQT-AT-FAAS

Flow rate of air: 3.5 L/min, Sample suction rate: 8.4 mL/min,
Height of SQT from burner head: 1.0 mm, Organic solvent: MIBK,
Volume of organic solvent: 40 μ L, Trapping period: 5.0 min

3.5.6 Optimization of Height of the SQT from the Burner Head

The optimum height of the SQT from the burner head of FAAS was defined as 1.0 mm (Figure 3.40), the reason is same as SQT-AT-FAAS, not entering analyte atoms into the flame and variation of flame temperature.

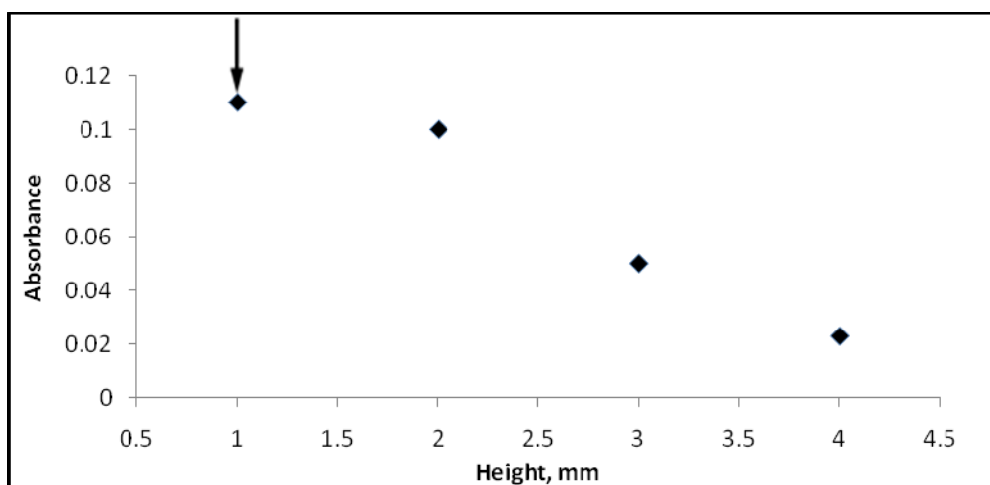


Figure 3.40 Optimization of height of SQT from burner head using 2.5 ng/mL Pb in Ta Coated-SQT-AT-FAAS

Acetylene flow rate: 0.5 L/min, Flow rate of air: 3.5 L/min,

Sample suction rate: 3.9 mL/min, Organic solvent: MIBK,

Volume of organic solvent: 40 μ L, Trapping period: 5.0 min

3.5.7 Investigation of Trapping Period

As the trapping period is increased, signals also increased proportionally. However, due to the same reasons for SQT-AT-FAAS, 5 min was chosen as the optimum trapping period (Figure 3.41).

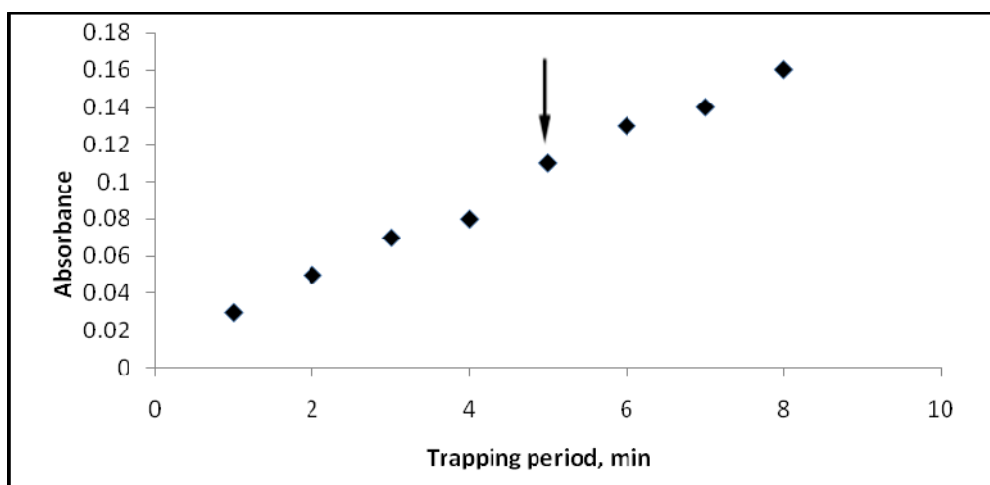


Figure 3.41 Effect of trapping period on Pb signal using 2.5 ng/mL Pb in Ta Coated-SQT-AT-FAAS

Acetylene flow rate: 0.5 L/min, Flow rate of air: 3.5 L/min,

Sample suction rate: 3.9 mL/min, Height of SQT from burner head: 1.0 mm,

Organic solvent: MIBK, Volume of organic solvent: 40 μ L

The signal for 5.0 ng/mL Pb solution is given in Figure 3.42; the optimized conditions given in Table 3.12 were used. The half bandwidth of this signal was found to be 0.16 s.

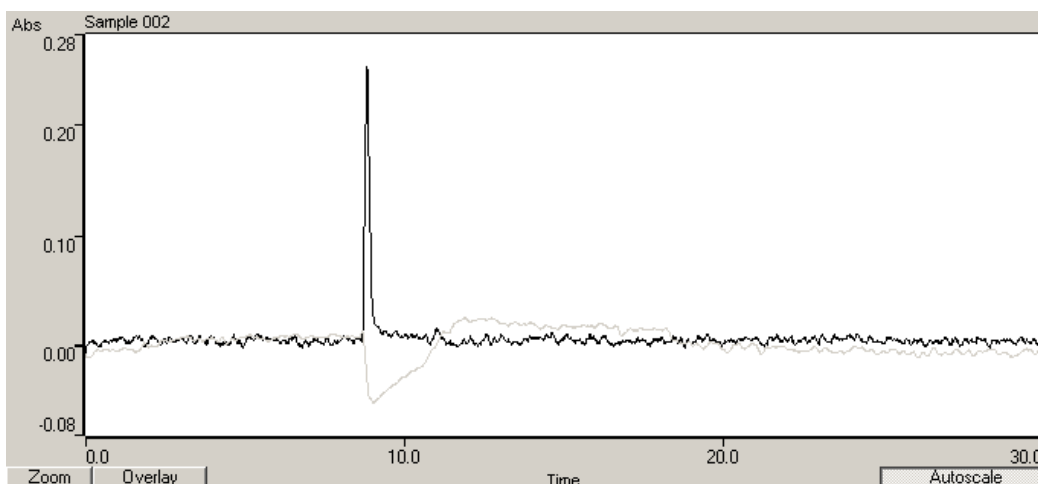


Figure 3.42 The signal of Ta- Coated-SQT-AT-FAAS for 2.5 ng/mL Pb solution, using the conditions in Table 3.11 except for sample suction rate

Table 3.12 Optimized Conditions for Ta-Coated-SQT-AT-FAAS Method

Parameters	Optimized Conditions
Coating Material	Tantalum
Type of Organic Solvent	MIBK
Sample Suction Rate	3.9 mL/min
Volume of Organic Solvent	40 μ L
Trapping Period	5.0 min
Height of The SQT from the head of the burner	1.0 mm
Acetylene Flow Rate	0.5 L/min

3.5.8 Calibration Plots for SQT-FAAS Method

Pb standards between 0.25-20.0 ng/mL were used for calibration plot (Figure 3.43), linearity was obtained between 0.25-3.0 ng/mL (Figure 3.44). The best line equation and correlation coefficient were, $y = 0.0518x + 0.0056$ and 0.9992, respectively. Conditions given in Table 3.12 were used and volume of analyte solution was 19.5 mL.

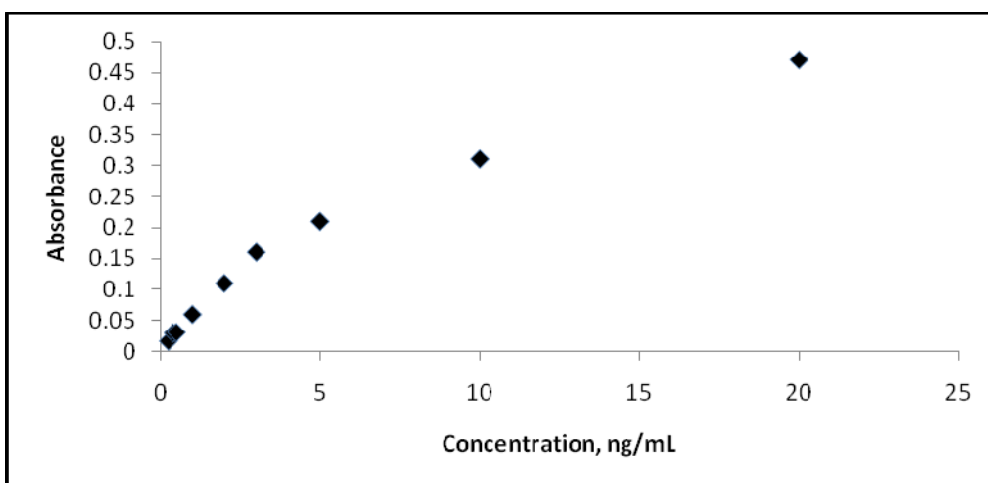


Figure 3.43 Calibration plot for Ta-Coated-SQT-AT-FAAS method, conditions in Table 3.12 were used

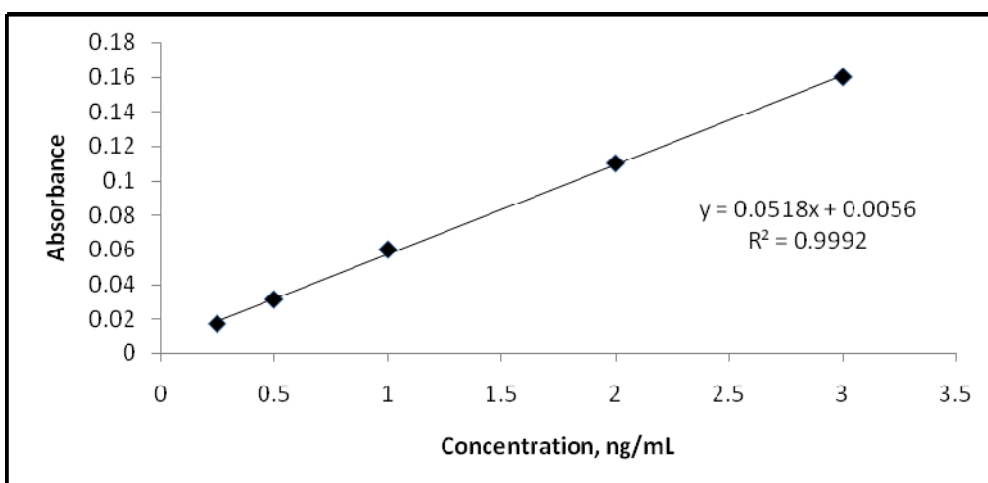


Figure 3.44 Linear calibration plot for Ta-Coated-SQT-AT-FAAS method, conditions in Table 3.12 were used

3.5.9 Analytical Figures of Merit of Ta coated-SQT-AT-FAAS

Limit of detection as 3s/m, limit of quantitation as 10s/m and characteristic concentration were calculated. As seen from Table 3.13 LOD and LOQ were calculated

as 0.15 ng/mL and 0.49 ng/mL respectively. Characteristic concentration was estimated as 0.08 ng/mL and the characteristic mass is 1.56 ng/mL and 1653 fold sensitivity enhancement was obtained with respect to FAAS. Volume of analyte solution was 19.5 mL.

Table 3.13 Analytical Performance of Ta-Coated-SQT-AT-FAAS

	Ta-Coated SQT-AT-FAAS
Limit of Detection (LOD), ng/mL	0.15
Limit of Quantitation (LOQ), ng/mL	0.49
Characteristic Concentration (C₀), ng/mL	0.08
Characteristic mass (m₀), ng	1.56
Enhancement (E) <i>(with respect to FAAS)</i>	1650

3.5.10 Accuracy Check for Ta coated-SQT-AT-FAAS Method

The CRM, SCP SCIENCE, EnviroMAT-Waste Water, Low (EU-L-2), was used for the accuracy check of Ta coated-SQT-AT-FAAS method. The direct calibration was employed and three replicate measurements were done under optimum conditions. The results were in good agreement with the certified value as shown in the Table 3.14.

Table 3.14 Result of the Accuracy Test for SQT-AT-FAAS Method

SCP SCIENCE, EnviroMAT	Certified Value, <i>ng/mL</i>	Experimental Result, <i>ng/mL</i>
Waste Water EU-L-2	40.0-43.0	41.3±1.5

3.6 Evaluation of System Performance

Table 3.15 illustrates the results of different SQT techniques. As seen from the table E_t and E_v values of the method provide a pair comparison with other studies and other techniques used for Pb determination. E_t and E_v values were found as 330, 85 respectively. Ertaş *et al.* [35] used SQT-AT for determination of Pb, they trapped Pb atoms on the inner surface of SQT for 2 min and at 6.0 mL/min sample suction rate and found 92 fold sensitivity enhancement. E_t and E_v values were calculated as 46 and 8 respectively. The most important effect that causes this sensitivity difference is the age of instruments that was used for both analyses. The instrument that was used for previous study is A Perkin-Elmer 305B manufactured in 1974, using a flatbed recorder, whereas the new instrument, Varian AA140 has a more reliable and fast computer based data processing system, manufactured in 2006. In addition, flame conditions that were used for trapping period were different again because of the age of the Perkin Elmer instrument. For the previous study, acetylene flow rate was kept at 1.8 L/min, while it was 0.5 L/min in this study. For the trapping period, acetylene flow rate should be as low as possible. Therefore, it is obvious that the current conditions provided better sensitivity.

The half width of the peak shaped signal obtained by SQT-AT-FAAS (Figure 3.25) is 0.23 s; the same figure obtained by Ta-coated-SQT-AT-FAAS (Figure 3.42) is 0.16 s. This difference indicates that the revolatilization from Ta coating is easier and faster

than the previous method. The areas under the peaks obtained from both methods were measured to see whether the improved sensitivity of Ta coated SQT is based only on the increased trapping efficiency or faster revolatilization of Pb from surface of Ta. It should be remembered that all the signal values in this study are based on peak height values. The area under the peak of SQT-AT-FAAS was found as 0.05241 ± 0.0016 s and the area under the peak of Ta-coated-SQT-FAAS was found as 0.03116 ± 0.00093 s. The higher area obtained by SQT-AT-FAAS indicates that the sensitivity improvement obtained by Ta-coated-SQT-FAAS is based only on the rapid revolatilization of Pb from surface.

As a result of relevant computations, the trapping efficiency of SQT-AT-FAAS is 57.7% and the trapping efficiency of Ta-coated-SQT-AT-FAAS is 34.2% with respect to SQT-FAAS.

SQT device was used for whole optimizations and calibrations and its sensitivity was still the same at the end of the study; this corresponds to at least 400 uses of the same SQT. However; Ta-coated-SQT was used for about 100 measurements. Coated or uncoated SQT device was replaced when its sensitivity was about 50% of the initial or the precision was lower than 10%.

Table 3.15 Comparison of Methods in Terms of E, E_t and E_v Values

Technique, Period, Volume	LOD, ng/mL	LOQ, ng/mL	C ₀ , ng/mL	m ₀ , ng	E	E _t , min ⁻¹	E _v , mL ⁻¹
FAAS	54.44	181.46	132	-	1	-	-
SQT-FAAS	9.39	31.12	40	-	3	-	-
SQT-AT-FAAS <i>5.0 min, 37.0 mL</i>	0.13	0.43	0.10	3.70	1320	264	36
SQT-AT-FAAS <i>5.0 min, 19.5 mL</i>	0.26	0.87	0.23	4.49	574	115	29
Ta-Coated-SQT-AT- FAAS <i>5.0 min, 19.5 mL</i>	0.15	0.49	0.08	1.56	1650	330	85
*Previous SQT-AT- FAAS study <i>2.0 min, 12.0 mL</i>	3.70	12.35	2.4	28.80	92	46	7.7

$$E = C_{0(\text{FAAS})}/C_{0(\text{Selected Method})}, E_t = E/t_{\text{total}}, E_v = E/v_{\text{total}}$$

* Flow rate of air: 25 L/min, Sample flow rate: 6.0 mL/min

Height of SQT from burner head: 6.0 mm, Organic solvent: MIBK,

Volume of organic solvent: 20 µL, Trapping period: 2.0 min

Comparison of SQT-AT-FAAS and Ta-coated-SQT-AT-FAAS with ICPOES, ICPMS, GFAAS and HGAAS was shown in Table 3.16. It is understood from the table, LOD levels of developed methods are at the level of ICPMS and HGAAS, lower than LOD of ICPOES.

Table 3.16 Comparison of Developed Methods with Other Techniques

	LOD Values (ng/mL)
ICPOES	35.9 [45]
ICPMS	0.1 [46]
GFAAS	0.3 [47]
HGAAS	4.5 [48]
SQT-AT-FAAS <i>5.0 min, 19.5 mL</i>	0.3
Ta-coated-SQT-AT-FAAS <i>5.0 min, 19.5 mL</i>	0.2

3.7 Interference Studies for Ta Coated-SQT-AT-FAAS Method

For determination of the effect of other elements and ions to the Pb signal, interference studies were performed. For this aim, 4 different solutions were prepared in which the concentration of Pb was kept constant, 2.0 ng/mL, and concentrations of interferent were 1, 10, 100 and 1000 folds of the analyte concentration, using the mass ratios. Conditions given in Table 3.11 were used.

Figure 3.45 contains the effects of 1A and 2A elements. The most significant effect was from Na; 1, 10, 100 folds of Na suppress the Pb signal by 23.7%, 20.3% and 22.6, respectively. Therefore, Ta-coated-SQT-AT-FAAS could not be used for Pb determination in samples that contain Na at a level of 2.0 mg/L or higher. On the other, hand 1000 folds the signal increase is 41.9%, and then although high amount of MIBK was introduced to remove Na, the attempts were not successful and a new tube was used. 2.0 mg/L K increase the Pb signal by 17.68% while other concentrations did not give significant effects. Mg and Ca did not give a significant suppression on Pb signal.

Korkmaz *et al* [49] investigated the effect of some ions on 75.0 ng/mL Pb signal. They used uncoated SQT atom trap for this aim, optimized condition of sample flow rate was 6.0 mL/min and collection time was 2.0 min. They found that there was a suppressive effect of Mg and Ca at 100 mg/L concentration on Pb signal.

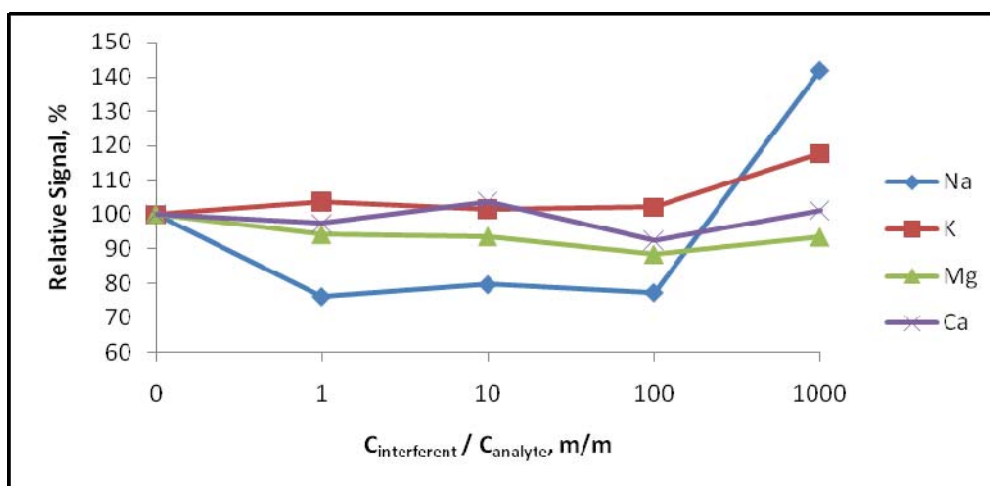


Figure 3.45 Interference effects of Na, K, Mg, Ca 2.0 ng/mL Pb signal in Ta-Coated-SQT-AT-FAAS

Effect of some transition metals (Fe, Mn, Cr) is seen in Figure 3.46. 1, 10 and 100 folds of the elements did not change Pb signal significantly. However, 1000 fold of Fe and Mn suppress the Pb signal, while 1000 fold of Cr increases the signal. After trapping of 2.0 mg/L Cr tube had to be recoated, as trapping efficiency of Pb on surface was decreased.

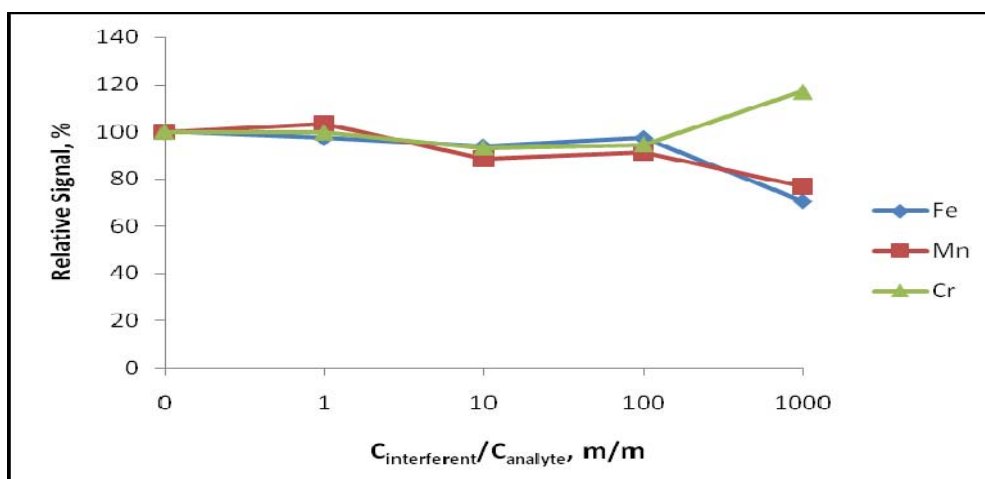


Figure 3.46 Interference effects of Fe, Mn, Cr 2.0 ng/mL Pb signal in Ta-Coated-SQT-AT-FAAS

In Figure 3.47, still effect of transition metals (Co, Ni, Cu) are seen. Although 1 and 10 folds of Co did not affect the Pb signal significantly, 200 ng/mL Co element decreased the Pb signal as 16.61 % and 2 mg/L Co increased the signal by 45.39%. Other most important effects were caused by 1000 fold of Ni and Cu, Pb signal was suppressed as 49.86% and 52.71% by 2.0 mg/L by 2 mg/L Ni and Cu respectively. After trapping of 2.0 mg/L Ni tube had to be recoated, as the normal analyte signal shape became broader and deformed; further analyte trapping was not possible.

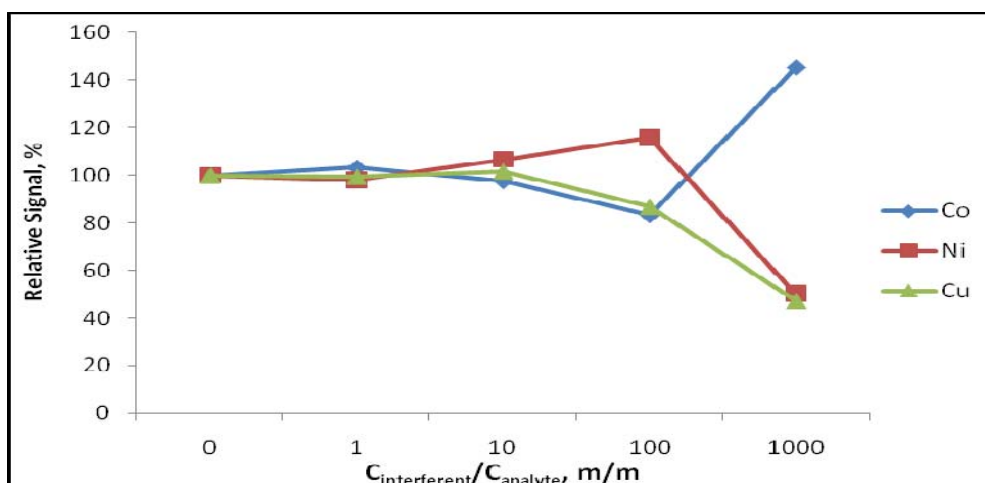


Figure 3.47 Interference effects of Co, Ni, Cu 2.0 ng/mL Pb signal in Ta-Coated-SQT-AT-FAAS

Next group is hydride forming elements, Cd, Se, Sb. Pb is also hydride forming element, so as seen in Figure 3.48 these elements did not give a significant change in 2.0 ng/mL Pb signal.

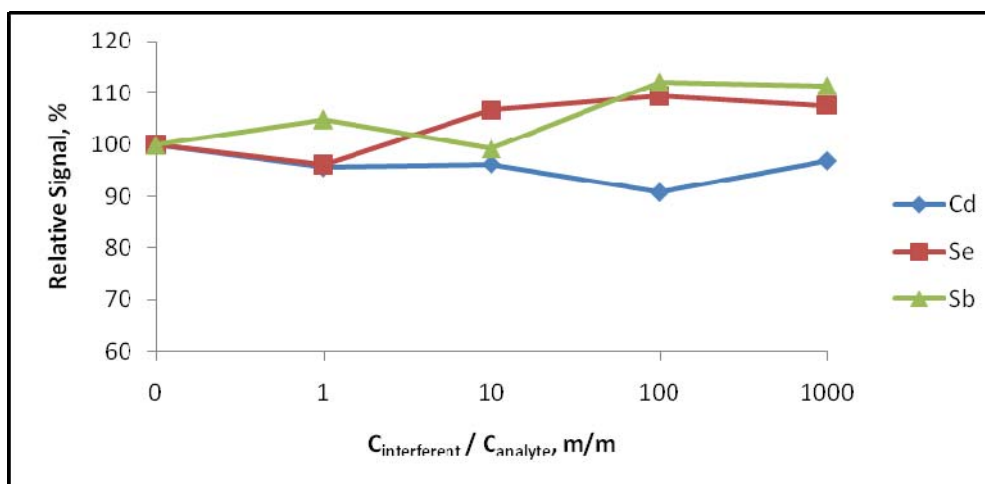


Figure 3.48 Interference effects of Cd, Se, Sb 2.0 ng/mL Pb signal in Ta-Coated-SQT-AT-FAAS

Other hydride forming element is Sn its 1000 fold concentration cause Pb signal to increase (Figure 3.49), also effect of Zn is nearly same as Sn.

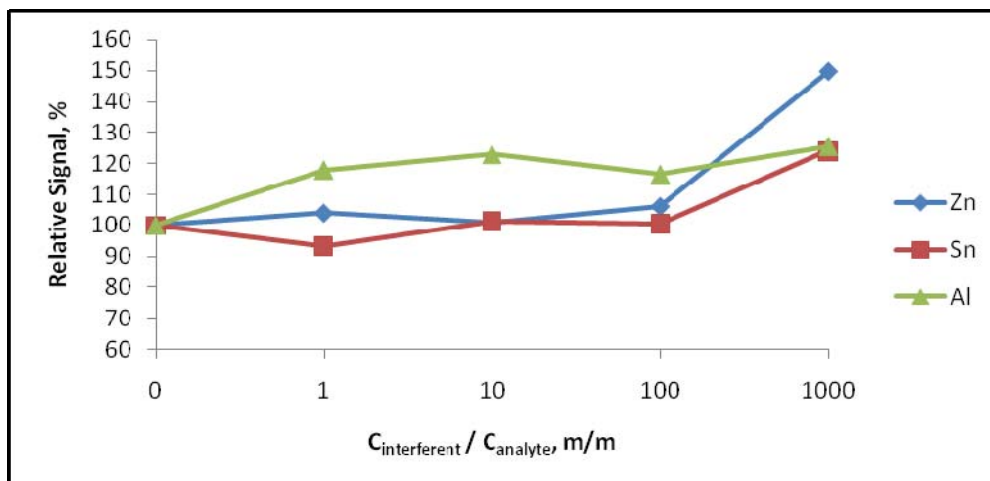


Figure 3.49 Interference effects of Zn, Sn, Al 2.0 ng/mL Pb signal in Ta-Coated-SQT-AT-FAAS

As it is seen in the Figure 3.50, there is no significant interference effect of SO_4^{2-} , F^- and PO_4^{3-} anions on Pb signal. On the contrary, Korkmaz *et al* [49] found a suppressive effect of SO_4^{2-} on Pb signal. Interference effect of NO_3^- on Pb signal was not investigated because all standards were prepared in 1.0 M HNO_3 solution. Signal of blank solution was obtained in each stage of study and no significant difference was seen.

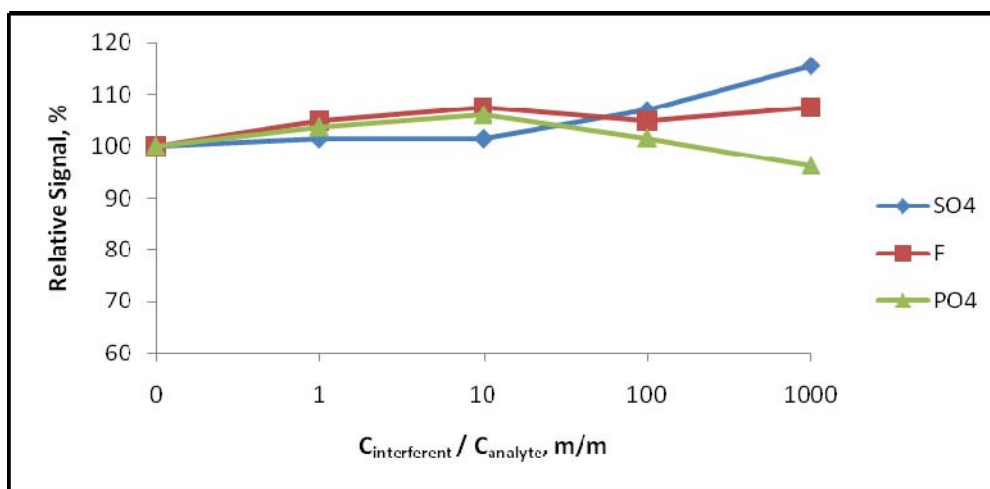


Figure 3.50 Interference effects of SO_4^{2-} , F^- , PO_4^{3-} on 2.0 ng/mL Pb signal in Ta-Coated-SQT-AT-FAAS

3.8 Surface Studies

Chemical state of analyte species and trapped species collected on SQT was investigated using XPS. The peaks obtained by XPS study are well resolved and provides definite identification of the element if concentration of element is greater than about 0.1 % [17]. XPS is used for understanding the roles of constituent, the results obtained could be used to reveal the mechanism during the atom trapping period. For this aim, XPS spectra of Pb on quartz surface, Pb on Ta surface and Ta on quartz surface were obtained. Coating procedures were described in section 2.3.

In XPS, C is always present as a result of hydrocarbon deposits in air or vacuum, and used as an internal energy calibrant at 284.5 or 285.5 eV binding energy. Depending on the chemical or physical environment, binding energies shift. Referencing on C peak and C shift real binding energies of interested elements could be found.

3.8.1 Chemical State of Pb on Quartz Surface

Figure 3.51 is XPS spectrum of Pb on quartz surface. There are O, C, Si and Pb_{4f} peaks. C peak was shown in detail in Figure 3.52, to find the C shift. C 1s was used as an internal energy calibrant at 284.5 eV binding energy. C peak was observed at 287.7 eV, so C shift was found as + 3.2 eV.

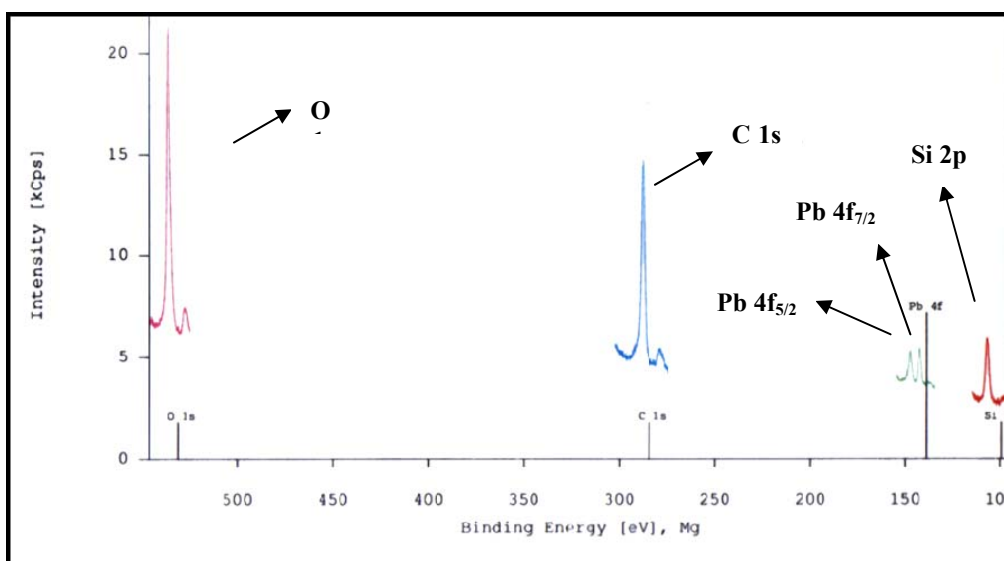


Figure 3.51 XPS spectrum of Pb on quartz surface

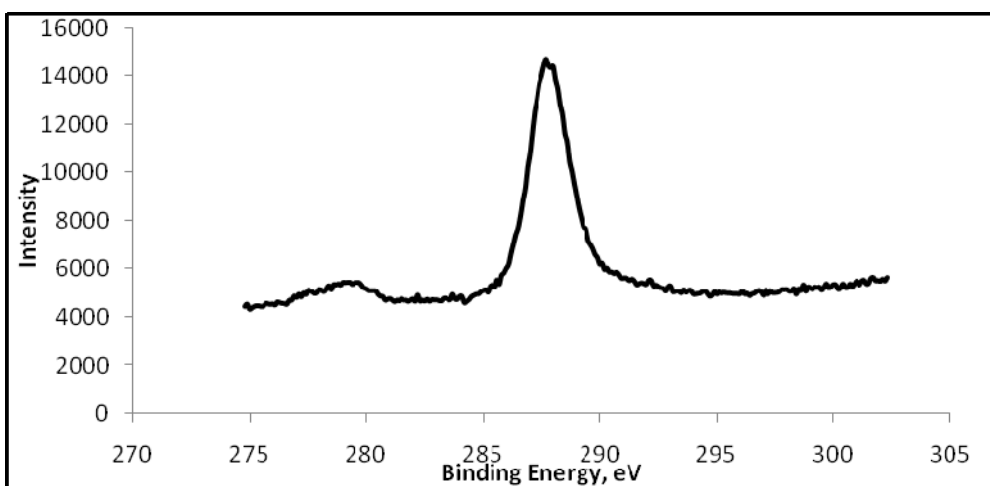


Figure 3.52 XPS spectrum of C in presence of Pb

$Pb_{4f7/2}$ and $Pb_{4f5/2}$ peaks were shown in Figure 3.53, the peaks are at 142.9 eV and 147.8 eV, respectively. By subtracting the C shift from these peaks real $Pb_{4f7/2}$ and $Pb_{4f5/2}$ peaks were found as 139.7 eV and 144.6 eV, respectively. These peaks are assigned to Pb^{2+} [50]. So, oxidation state of Pb on quartz surface during trapping period is +2.

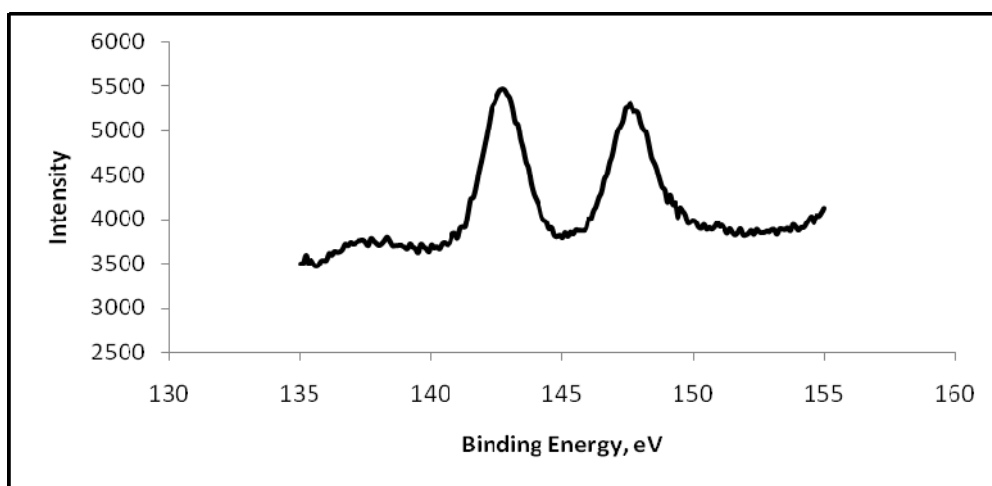


Figure 3.53 XPS spectrum of Pb_{4f} on quartz surface

Table 3.17 shows the percentages of C, O, Si and Pb during analysis of quartz sample which contains Pb, the percentage of Pb in this sample is 0.2 %.

Table 3.17 Percentages and Orbitals of Elements on SQT Trapped with Pb

Element	Atom %	Orbital
C	48.8	1s
O	38.9	1s
Si	12.1	2p
Pb	0.2	4f

3.8.2 Chemical State of Pb on Ta Surface

Chemical behavior of Pb on Ta surface was also investigated. Seen in Figure 3.54 there are O, C, Si and Pb_{4f} and Ta_{4f} peaks. C peak was shown in detail in Figure 3.55, to find the C shift. C peak was observed at 288.9 eV, shift was found as + 4.0 eV. Shift is higher than the previous spectra because of the presence of Ta.

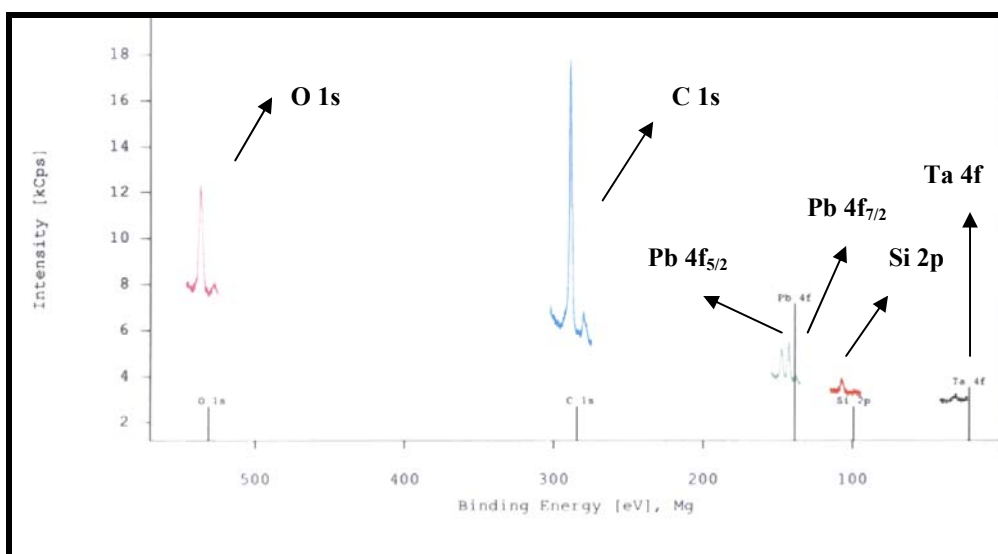


Figure 3.54 XPS spectrum of Pb on Ta surface

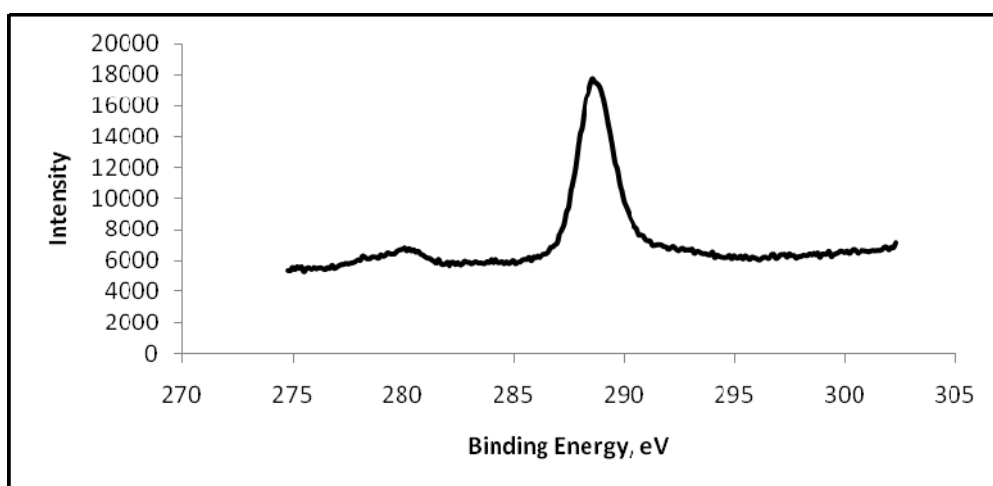


Figure 3.55 XPS spectrum of C in presence of Pb and Ta

$Pb_{4f7/2}$ and $Pb_{4f5/2}$ peaks were shown in Figure 3.56, the peaks are at 143.2 eV and 148.1 eV, respectively. By subtracting the C shift from these peaks real $Pb_{4f7/2}$ and $Pb_{4f5/2}$ peaks were found as 139.2 eV and 144.1eV, respectively. The peaks of Pb on quartz and Pb on Ta are same; therefore the oxidation state of Pb on Ta surface during trapping period is +2 [50].

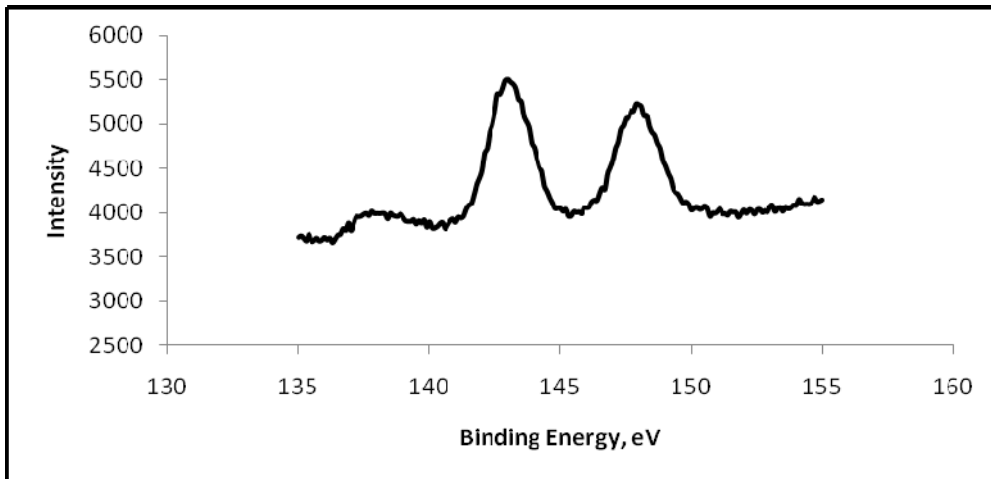


Figure 3.56 XPS spectrum of Pb_{4f} on Ta surface

Table 3.18 shows the percentages of C, O, Si, Pb and Ta during analysis of quartz sample which contains Pb and Ta. Percentage of Pb in this sample is 0.2 % and Ta is 0.2 %. Percentage of Ta is low because of the Pb layer on.

Table 3.18 Percentages and Orbitals of Elements on Ta Coated SQT Trapped with Pb

Element	Atom %	Orbital
C	77.6	1s
O	19.0	1s
Si	3.0	2p
Ta	0.2	4f

Table 3.18 (Continued)

Pb	0.3	4f
----	-----	----

3.8.3 Chemical State of Ta on Quartz Surface

Pb was trapped on both quartz and Ta surface as Pb^{2+} , but if Ta is coated in metallic form on quartz. Seen in Figure 3.57 there are Ta_{4f} peaks with O, C and Si. C peak was shown in detail in Figure 3.58, to find the C shift. C peak was observed at 288.6 eV, shift was found as +4.1 eV.

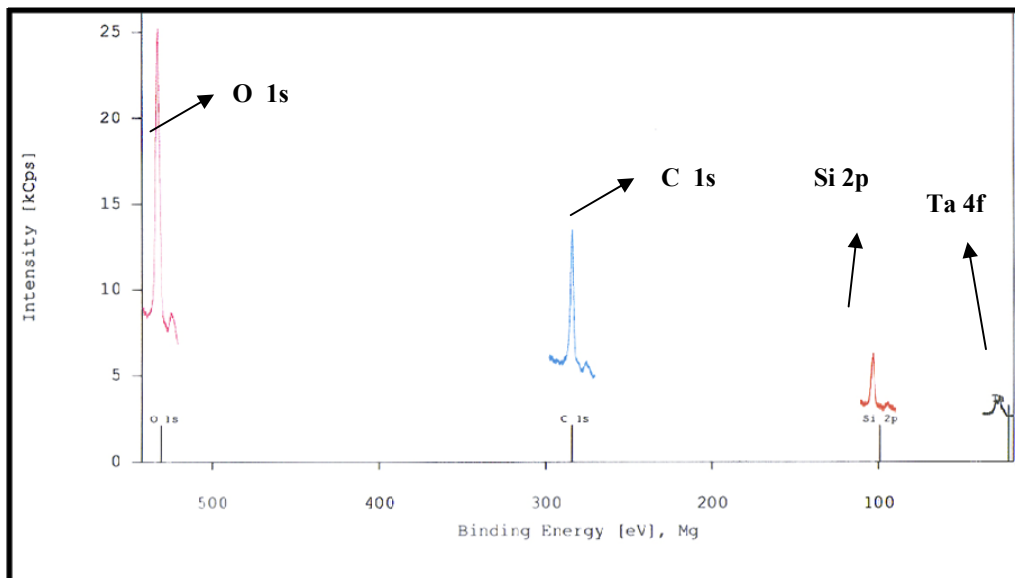


Figure 3.57 XPS spectrum of Ta on quartz surface

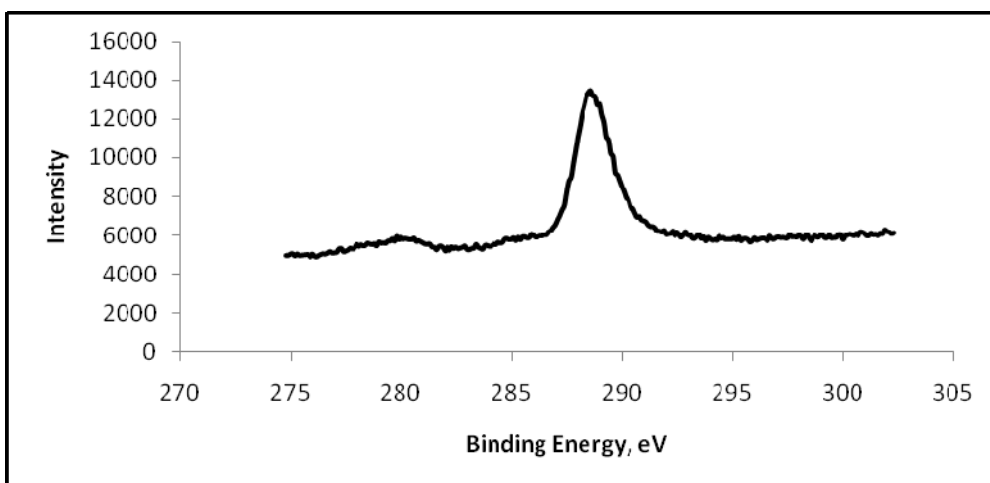


Figure 3.58 XPS spectrum of C in presence of Ta

Ta_{4f7/2} and Ta_{4f5/2} peaks were shown in Figure 3.59, the peaks are at 32.0 eV and 34.0 eV, respectively. By subtracting the C shift from these peaks real Ta_{4f7/2} and Ta_{4f5/2} peaks were found as 27.9 eV and 29.91eV, respectively. The oxidation state of Ta on quartz surface during the coating period could be +5 [51].

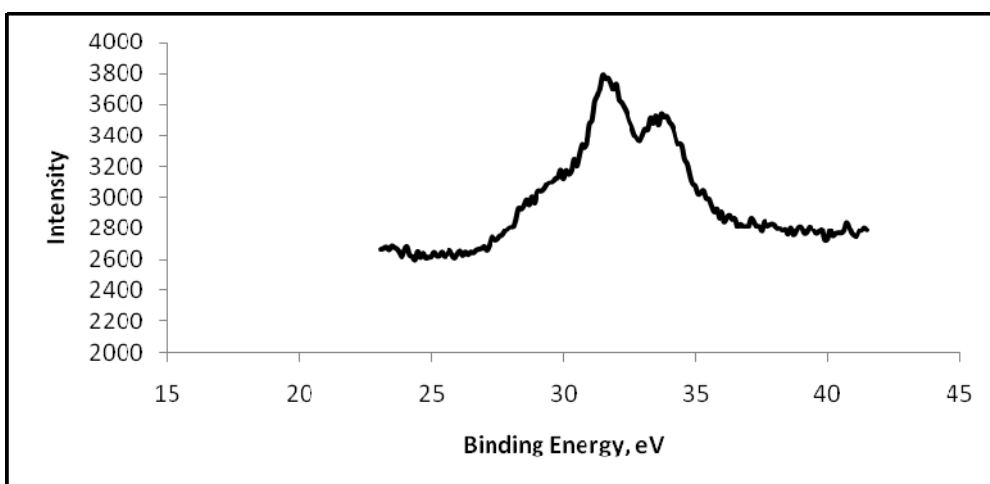


Figure 3.59 XPS spectrum of Ta_{4f} on quartz surface

Table 3.19 shows the percentages of C, O, Si and Ta during analysis of quartz sample which contains Pb and Ta. Percentage of Ta in this sample is 0.8 %.

Table 3.19 Percentages and Orbitals of Elements on Ta Coated SQT Trapped with Pb

Element	Atom %	Orbital
C	38.3	1s
O	48.5	1s
Si	12.4	2p
Ta	0.8	4f

Ta solution was prepared from Ta_2O_5 by dissolving the solid in concentrated HF. Therefore, Ta could be in the form of either Ta_2O_5 or TaF_5 . Melting point of Ta_2O_5 is $1870^\circ C$ and melting point of TaF_5 is $96.8^\circ C$. From these data, it could be estimated that Ta is in the form of Ta_2O_5 because of the significantly higher melting point of this compound. In order to support this suggestion, Raman spectrum of Ta coated SQT was obtained. Figure 3.60 is the reference Raman spectrum of Ta_2O_5 , Figure 3.61 is the Raman spectrum of Ta coated SQT. These two spectra have the same features. Therefore, it has been decided that Ta was coated on SQT in form of Ta_2O_5 .

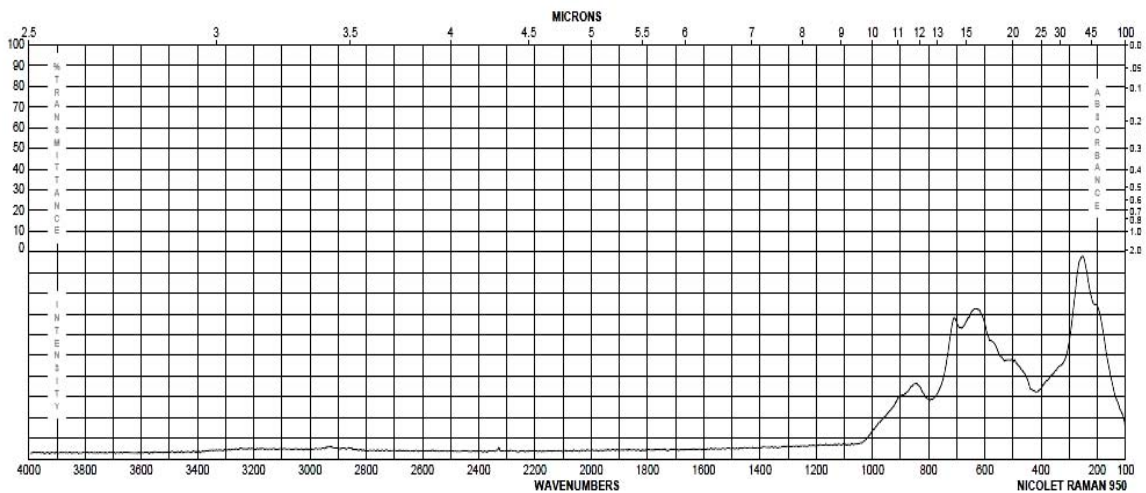


Figure 3.60 Raman Spectrum of Ta_2O_5 [52].

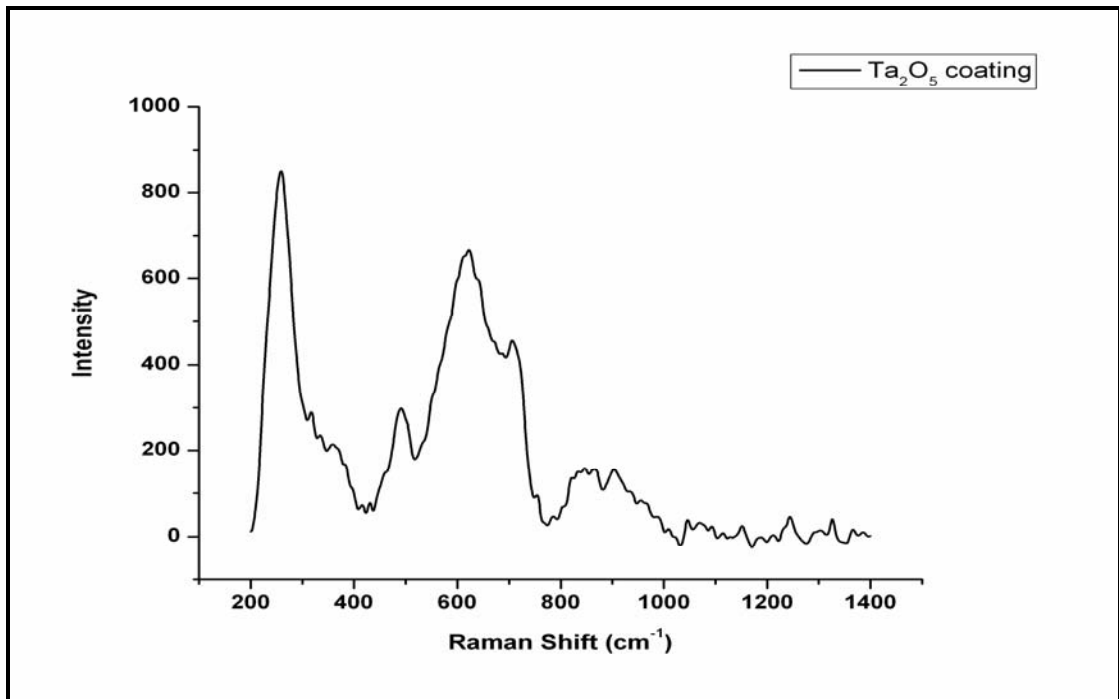


Figure 3.61 Raman Spectrum of Ta coated SQT

CHAPTER 4

CONCLUSIONS

The main purpose of this study was the enhancement of sensitivity of lead determination by flame atomic absorption spectrometry using slotted quartz tube atom trap and metal coatings.

SQT was used for two modes in the study. First, it was only used for increasing the residence time of analyte atoms in measurement zone, 120° angled and 180° angled tubes were used and sensitivity was enhanced as 3 fold with respect to FAAS. No trapping was used at this stage. Second, it was used as an atom trap for on-line preconcentration of analyte atoms. At this stage, bare SQT and metal coated SQT devices were used. Efficiency of 120° angled and 180° angled tubes were compared, and it was concluded that there was no significant difference; the angle between slots is not important for Pb determination. However it was observed that sample suction rate was very important. At low sample flow rates, nebulization efficiency is higher and better analyte collection takes place for a constant sample volume. On the other hand, at high sample suction rates sensitivity increases for a constant collection period.

In addition, the effect of inner diameter and wall thickness of SQT on Pb signal was investigated. It was seen that sensitivity of SQT with smaller diameter was better than the other one which has equal inner diameter as the diameter of incident light beam. But, the former gave better S/N ratio. For the effect of wall thickness, 3 types of tube with wall thickness of 0.5, 1.5 and 2.0 mm were used. Better sensitivity was obtained with 1.5 mm thick tube, but better S/N ratio was obtained by 0.5 mm thick tube.

At the last stage, inner surface of SQT (180° angled) was coated using some transition metals namely Pd, Mo, W, Ir, Ta, Zr, Ir and Os; the best sensitivity enhancement was obtained by Ta; 1650 fold with respect to FAAS was obtained for sensitivity enhancement. This sensitivity enhancement was obtained with the analyte volume of 19.5 mL.

Interference effects on Ta coated-SQT-AT-FAAS was performed, effect of 1A, 2A, 3A, 7A elements, some transition metals, hydride forming metals and some ions were investigated. Effect of hydride forming elements and ions were not significant on Pb signal, but for other type of elements when interferent concentration was 1000 fold higher than Pb concentration, effect was not ignored.

For the accuracy check, the analyses of standard reference material were performed by use of SCP SCIENCE EnviroMAT Low (EU-L 2) and results for Pb was to be in good agreement with the certified value for SQT-AT-FAAS and Ta coated-SQT-AT-FAAS.

Finally, for investigation of chemical state of Pb on quartz, Pb on Ta and Ta on quartz XPS analysis performed. It was concluded that oxidation state of Pb on quartz and Pb on Ta during trapping period were same, 2+; Ta was coated on quartz surface as Ta⁵⁺. In addition, application of Raman Spectroscopy revealed that the form of Ta on quartz surface was Ta₂O₅.

As a summary, SQT-AT-FAAS and Ta coated-SQT-AT-FAAS were sensitive analytical methods for lead determination. The sensitivities are at the level of ETAAS and HGAAS. Methods developed were simple, economical and provides LOD as low as plasma techniques.

REFERENCES

- [1] S. Bakirdere, M. Yaman, "Determination of Lead, Cadmium and Copper in Roadside soil and Plants in Elazığ, Turkey", *Environ. Monit. Asses.* **136** (2008) 401-410.
- [2] M. G. A. Korn, J. B. De Andrade, D. S. De Jesus, V. A. Lemos, M. L.S.F. Bandeira, W. N. Dos Santos, M. A. Bezerra, F. A. C. Amorim, A. S. Souza, S. L. C. Ferreira "Separation and Preconcentration Procedures for the Determination of Lead Using Spectrometric Techniques: A Review", *Talanta* **69** (2006) 16-24.
- [3] J. S. C. Fernandez, J. Sordo, "Lead Chemistry, Analytical Aspects, Environmental Impact and Health Effects", ScienceDirect (online service), Amsterdam, Boston, Elsevier, (2006).
- [4] X. Yu, H. Yuan, T. Grecki, J. Pawliszyn, "Determination of Lead in Blood and Urine by SPME/GC", *Anal. Chem.* **15** (1999) 2998-3002.
- [5] Health Protection Agency, <http://www.hpa.org.uk/web/HPAwebFile/HPAweb>, accessed in 03.05.2009.
- [6] D. Peter, E. Biggins, R. M. Harrison, "Atmospheric Chemistry of Automotive Lead", *Env. Sci. and Tech.* **5** (1979) 558-565.
- [7] Win, D.T, M.M Than, S. Tun, "Lead Removal from Industrial Waters by Water Hyacinth", *AU Journ. of Tech.* **4** (2003) 187-192.
- [8] United Nations Environment Programme, <http://www.unep.org/pcfv/pdf/VSR-FinalDraft.pdf>, accessed in 03.07.2009.
- [9] M. O. Luconi, M. F. Silva, R. A. Olsina, L. P. Fernandez, "Cloud Point Extraction of Lead in Saliva via Use of Nonionic PONPE 7.5 Without Added Chelating Agents", *Talanta* **51** (2000) 123-129.
- [10] I. Ali, H. Y. Aboul-Enein, "Instrumental Methods in Metal Ion Speciation", CRC/Taylor&Francis, Boca Raton, 2006.

- [11] G. Kaya, M. Yaman, "Online Preconcentration for the Determination of Lead, Cadmium and Copper by Slotted Tube Atom Trap (STAT)-Flame Atomic Absorption Spectrometry", *Talanta* **75** (2008) 1127-1133.
- [12] Environmental Protection Agency, <http://www.epa.gov/lead/pubs/leadinfo.html>, accessed in 13.05.2009.
- [13] H. T. Delves, "A Micro-sampling Method for the Rapid Determination of Lead in Blood by Atomic –absorption Spectrophotometry", *Analyst* **95** (1970) 431-438.
- [14] World Health Organization, Fifty-third report of the Joint FAO/WHO Expert Committee on Food Additives, WHO Technical Report Series 896, Geneva, Switzerland, 2000.
- [15] J. P. Vernet, "Impact of Heavy Metals on the Environment", Elsevier, New York, 1992.
- [16] J. F. Tyson, R. I. Ellis, G. Carrick, F. Fernandez, "Flow Injection Hydride Generation Electrothermal Atomic Absorption Spectrometry with In-atomizer Trapping for the Determination of Lead in Calcium Supplements" *Talanta* **52** (2000) 403-410.
- [17] D. A. Skoog, F. J. Holler, T. A. Nieman, "Principles of Instrumental Analysis" Thomson Learning Inc, USA, 4th edition, 1998.
- [18] J. R. Dean, "Atomic Absorption and Plasma Spectroscopy", John Wiley&Sons, England, 1997.
- [19] B. Welz, M. Sperling, "Atomic Absorption Spectrometry", Wiley-VCH, Germany, 1999.
- [20] O. Y. Ataman, "Vapor Generation and Atom Traps: Atomic and Absorption Spectrometry at the ng/L Level", *Spectrochim. Acta Part B* **63** (2008) 825-834.
- [21] H. Matusiewicz, "Atom Trapping in Situ Preconcentration Techniques for Flame Atomic Absorption Spectrometry", *Spectrochim. Acta Part B* **52** (1997) 1711-1736.

- [22] N. Ertaş, Z. Arslan, J. F. Tyson, “Determination of Lead by Hydride Generation Atom Trapping Flame Atomic Absorption Spectrometry”, *J. Anal. At. Spectrom.* **23** (2008) 223-228.
- [23] H. Matusiewicz, R. E. Sturgeon, “Atomic Spectrometric Detection of Hydride Forming Elements Following *in situ* Trapping within a Graphite Furnace”, *Spectrochim. Acta Part B* **51** (1996) 377-397.
- [24] X. Yan, Z. Ni, “Determination of Lead by Hydride Generation Atomic Absorption Spectrometry with *in Situ* Concentration in a Zirconium Coated Graphite Tube”, *J. Anal. At. Spectrom.* **6** (1991) 483-486.
- [25] D. K. Korkmaz, N. Ertaş, O. Y. Ataman, “A Novel Silica Trap for Lead Determination by Hydride Generation Atomic Absorption Spectrometry”, *Spectrochim. Acta Part B* **57** (2002) 571-580.
- [26] O. Cankur, N. Ertaş, O. Y. Ataman, “Determination of bismuth using on-line preconcentration by Trapping on Resistively Heated W Coil and Hydride Generation Atomic Absorption Spectrometry”, *J. Anal. At. Spectrom.* **17** (2002) 603-609.
- [27] F. Barbosa Jr., S. S. de Souza, F. J. Krug, “In Situ Trapping of Selenium Hydride in Rhodium-Coated Tungsten Coil Electrothermal Atomic Absorption Spectrometry” *J. Anal. At. Spectrom.* **17** (2002) 382–388.
- [28] S. Titretir, E. Kendüzler, Y. Arslan, İ. Kula, S. Bakırdere, O. Y. Ataman, “Determination of Antimony by Using Tungsten Trap Atomic Absorption Spectrometry” *Spectrochim. Acta Part B* **63** (2008) 875-879.
- [29] X. Guo, X. Guo, “Determination of Ultra-trace Amounts of Selenium by Continuous Flow Hydride Generation AFS and AAS With Collection on Gold Wire”, *J. Anal. At. Spectrom.* **16** (2001) 1414-1418.
- [30] Y. V. Zeljukova, N.S. Poluektov, “Atomic Absorption Analysis by Means of Exhaust Gases of the Flame”, *Zh. Anal. Khim.* **18** (1963) 435-439.
- [31] R. J. Watling, D. J. De Villers, “A Slotted Quartz Tube for Increasing Sensitivity in Flame Atomic Absorption Analysis”, Special Report, FIS 108, Division of Applied Spectroscopy, National Physical Research Laboratory, Council for Scientific and Industrial Research, Pretoria, South Africa, 1977.

- [32] D. T. Nurns, N. Chimpalee, M. Harriot, “Applications of a Slotted Tube Atom Trap and Flame Atomic Absorption Spectrometry: Determination of Bismuth with and without Hydride Generation, *Anal. Chim. Acta* **311** (1995) 93-97.
- [33] J. Wei, Z. Zhang, Y. Wong, G. He, “Study on Mechanism of Determination of Lead by Atom-Catching Atomic-Absorption Spectrometry”, *Guangpuxue Yu Guangpu Fenxi* **10** (1990) 59-63.
- [34] H Matusiewicz, M. Koprás, “Methods for Improving the Sensitivity in Atom Trapping Flame Atomic Absorption Spectrometry: Analytical Scheme for the Direct Determination of Trace Elements in Beer” *J. Anal. At. Spectrom.* **12** (1997) 1287-1291.
- [35] N. Ertaş, D. K. Korkmaz, S. Kumser, O. Y. Ataman, “Novel Traps and Atomization Techniques for Flame AAS”, *J. Anal. At. Spectrom.* **17** (2002) 1415-1420.
- [36] A.D. Turner, D.J. Roberts, “Metal Determinations with a Novel Slotted-Tube Water Cooled Atom Trap”, *J. Anal. At. Spectrom.* **11** (1996) 231–234.
- [37] O. Y. Ataman, “Economical Alternatives for High Sensitivity in Atomic Spectrometry Laboratory”, *Pak. J. Anal. Chem.* **8** (2007) 64-68.
- [38] D. Korkmaz, S. Kumser, N. Ertaş, M. Mahmut, O. Y. Ataman, “Investigation on Nature of Re-volatilization from Atom Trap Surfaces in Flame AAS”, *J. Anal. At. Spectrom.* **17** (2002) 1610-1614.
- [39] A. A. Brown, B. Milner, A. Taylor, “Use of a Slotted Quartz Tube to Enhance the Sensitivity of Conventional Flame Atomic Absorption Spectrometry”, *Analyst* **110** (1985) 501-505.
- [40] S. Kumser, M.S. thesis, “Atom trapping atomic absorption spectrometry using organic solvent atomization”, Middle East Technical University, Ankara, Turkey, 1995.
- [41] B. Arı, M.S. thesis, “Development of Sensitive Analytical Methods for Thallium Determination by Atomic Absorption Spectrometry”, Middle East Technical University, Ankara, Turkey, 2009.
- [42] Ş. Süzer, “XPS Investigation of X-Ray-Induced Reduction of Metal Ions”, *Appl. Spectrosc.* **54** (2000) 1716-1718.

- [43] Ş. Süzer, N. Ertaş, S. Kumser, O. Y. Ataman, "X-ray Photoelectron Spectroscopic Characterization of Au Collected with Atom Trapping on Silica for Atomic Absorption Spectrometry" *Appl. Spectrosc.* **51** (1997) 1537-1539.
- [44] National Institute for Occupational Safety and Health, Pocket Guide to Chemical Hazards, <http://www.cdc.gov/niosh/npg/npgd0326.html>, accessed in 26.07.2009.
- [45] B. Feist, B. Mikula, K. Pytlakowska, B. Puzio, F. Buhl, "Determination of Heavy Metals by ICP-OES and FAAS after Preconcentration with 2,2'-bipyridyl and erythrosine", *J. Hazard. Mater.* **152** (2008) 1122-1129.
- [46] Z. Zhang, S. Shimbo, N. Ochi, M. Eguchi, T. Watanabe, C. Moon, M. Ikeda, "Determination of Lead and Cadmium in Food and Blood by Inductively Coupled Plasma Mass Spectrometry: a Comparison with Graphite Furnace Atomic Absorption Spectrometry", *Sci. of Tot. Env.* **205** (1997) 179-187.
- [47] J.Y. Cabon, "Determination of Cd and Pb in Seawater by Graphite Furnace Atomic Absorption Spectrometry with the use of Hydrofluoric Acid as a Chemical Modifier", *Spectrochim. Acta Part B* **57** (2002) 513-524.
- [48] N. Maleki, A. Safavi, Z. Ramezani, "Determination of Lead by Hydride Generation Atomic Absorption Spectrometry (HGAAS) using a Solid Medium for Generating Hydride", *J. Anal. At. Spectrom.* **14** (1999) 1227-1230.
- [49] D. Korkmaz, M. Mahmut, R. Helles, N. Ertaş, O. Y. Ataman, "Interference Studies in Slotted Silica Tube Trap Technique", *J. Anal. At. Spectrom.* **18** (2003) 99-104.
- [50] T. Yoshida, T. Yamaguchi, Y. Iida, S. Nakayama, "XPS Study of Pb(II) on γ -Al₂O₃ Surface at High pH Conditions", *Journ. Of Nucl. Sci. and Tech.* **40** (2003) 672-678.
- [51] G. E. McGuire, G. K. Schweitzer, T. A. Carlson, "Core Electron Binding Energies in Some Group IIIA, VB and VIB Compounds", *Inorg. Chem.* **12** (1973) 2450-2453.
- [52] Sigma-Aldrich, <http://www.sigmaaldrich.com/spectra/rair/RAIR003746.PDF>, accessed in 20.07.2009.